Development of a new screening system for the identification of RNF43-related genes and characterisation of other PA-RING family members

Alessandra Merenda

University of Cambridge

Department of Genetics

This dissertation is submitted for the degree of
Doctor of Philosophy

Darwin College

April 2017

This dissertation is dedicated to my exemplary grandfather.

Declaration

I hereby declare that, except where specific reference is made to the work of others, the contents of this dissertation are original and they are the result of my own work. This dissertation contains nothing which is the outcome of work done in collaboration with others, except as specified in the text and under “External contributions”.
It is not substantially the same as any that I have submitted, or, is being concurrently submitted for a degree or diploma or other qualification at the University of Cambridge or any other University or similar institution. This dissertation does not exceed the prescribed word limit of 60,000 words excluding bibliography, figures and appendices.

Alessandra Merenda

April 2017

External contributions

The details about external contributions to the work presented in this thesis are as follows:

Dr. Ingrid Jordens (UMC) and Dr. Cara Jamieson (UMC) performed the pulse chase experiments with SNAP-Frizzled5 (Figure 5.2 and Figure 5.3).

Dr. Jihoon Kim (University of Cambridge) performed FZD5 western blot and FACS analysis, ubiquitination assay and co-immunoprecipitation (Figures 5.4-5.7).

Acknowledgments

As this intense journey comes to an end, many are the people I feel like thanking for making it worth undertaking.
I would firstly like to thank **Bon-Kyoung** for his great supervision and guidance, his support and encouraging words whenever needed during these years and, of course thank you to all the current and past Koo lab members. In particular, thanks to **Jihoon** for intensively collaborating with me on my main project.
In addition, I appreciate the support received from the **Stem Cell Institute core facilities**, especially the Tissue Culture, Flow Cytometry, Histology and Animal facilities.

A special thank goes to **Chris Hindley** and **Luigi Aloia** for patiently reading and proofreading this thesis and giving me plenty of insightful feedbacks.

I am also very grateful to **Meritxell Huch** (Gurdon Institute) and **Joo-Hyeon Lee** (SCI) for their valuable advice and feedbacks on my progress, and to everyone in their labs.
In particular, thanks **Mastrogiova'** for being such an amazing PhD buddy and friend!

Moreover, I would like to thank my advisors **Marisa Segal** and **Alfonso Martinez-Arias** (Department of Genetics) for providing feedback on my first and second year reports and following my progress since I joined the Department.

I would also like to thank the Seventh Framework Program, Marie Curie Actions and the European Union for generous funding of my project and **Madelon Maurice** (University Medical Centre Utrecht) for mentoring me within the Wntsapp network.
In her lab, I am particularly grateful to **Ingrid** for being such a great Wntsapp project manager and for collaborating with me together with **Cara**, and to **Nicola** for his friendship and all the scientific and non-scientific discussions.

Then, many thanks also to all the other **Wntsapp PIs and fellows** for their great inputs and the many fun times shared together. This PhD experience wouldn't have been the same without you!

…And it would not have been the same either without my **friends**, far or near, old and new. Thanks for bringing a smile on my face as well as putting up with me!

Finally, the biggest thank you I for sure owe it to my **family**.
Grazie per essermi stati così vicini anche da lontano durante questo intenso cammino di formazione, ma soprattutto grazie per l'inestimabile bagaglio con cui avete fatto in modo che partissi.

Title: Development of a new screening system for the identification of RNF43-related genes and characterisation of other PA-RING family members.

Candidate: Alessandra Merenda

Abstract

The E3 ubiquitin ligase RNF43 (RING finger protein 43) is an important negative modulator of the WNT signalling pathway that acts at the plasma membrane by targeting Frizzled and its co-receptor LRP for degradation. In the small intestine, this prevents uncontrolled expansion of the stem cell compartment and so it is essential to the maintenance of normal tissue homeostasis. However, despite its crucial role in fine-tuning the WNT pathway and its role as a tumour suppressor, it is unclear whether RNF43 has further binding partners and what their functional relevance is to the modulation of WNT signalling.

Here, I describe the development of a new screening strategy which combines CRISPR/Cas9 technology with 3D-intestinal organoid culture for the identification of novel molecular interactors of RNF43. Overall, this study and the technology developed provide a tool to enable the detailed description of the mechanism of action of RNF43, which is important not only in order to increase our understanding of WNT pathway regulation but also to gain potential new insights into *RNF43* paralogs, by analogy.

The investigation of paralogs is crucial as *RNF43* belongs to a newly identified family of E3 ubiquitin ligases, named the PA-RING family, whose members are still poorly characterised. The majority of PA-RING family members have not been linked to any signalling pathway, most of their targets are still unknown and in many cases their *in vivo* function has not been addressed. In this context, my work has specifically focused on the

investigation of the potential involvement of additional PA-RING family members in WNT pathway modulation and also on target identification for selected members. The results summarised in this dissertation show that no other PA-RING family member plays a prominent role in WNT pathway modulation aside from *Rnf43* and its homologue *Znrf3*, however, different classes of adhesion molecules are likely to be regulated by certain of these E3 ligases.

In conclusion, my work has contributed to unravelling previously unexplored aspects of this protein family, with particular regard to RNF43 and its mechanism of action. Thanks to this original approach, it was possible to identify potential new players involved either in membrane clearance of Frizzled or in RNF43 maturation. In particular, my thesis focuses on the characterisation of the role of DAAM in RNF43-mediated Frizzled internalisation.

Table of contents

List of figures

List of tables

.

Abbreviations

2i	2 inhibitors (CHIRON / PD03)
4-OHT	4-hydroxytamoxifen
BMP	Bone morphogenetic protein
CBCs	Crypt base columnar cells
CHIRON	CHIR99021 GSK3 inhibitor
CMV	Cytomegalovirus
CreERT2	Cre Estrogen Receptor T2
CRISPR	Clustered Regularly Interspaced Short Palindromic Repeats
Dll	Delta-like
DMSO	Dimethyl sulfoxide
Dox	Doxycycline
Dvl	Dishevelled
E3s	E3 Ubiquitin ligases
EGF	Epidermal growth factor
EN	EGF-Noggin
ENR	EGF-Noggin-RSPO
ESC	Embryonic Stem Cells
FZD	Frizzled
GOI	Gene of Interest
gRNA	Single guide RNA
hiPSC	Human induced Pluripotent Stem Cells
IRES	Internal Ribosome Entry Site
KO	Knockout
Lgr5	Leucine-Rich Repeat-Containing G-Protein Coupled Receptor

LIF	Leukaemia inhibitory factor
Mib1	Mind bomb-1
Neo	Neomycin
PA	Protease-associated
PBS	Phosphate Buffered Saline
PD03	PD0325901 MAPK/ERK Kinase inhibitor
pMSCV	Plasmid for Murine Stem Cell Virus
RING	Really Interesting New Gene
RNF43	Ring finger protein 43
RSPO	R-spondin
rtTA	Reverse tetracycline trans-activator
*RZ*DKO	*Rnf43*&*Znrf3* double knock-out
gRNA	Guide RNA
SI	Small Intestine
SPA	Surface proteome analysis
TET	Tetracycline-Responsive Promoter Element
WEN	WNT EGF Noggin
ZNRF3	Zinc/RING finger protein 3

Chapter 1

Introduction

1.1 Maintenance of homeostasis in the adult small intestine

1.1.1 Architecture of the adult small intestine

Adult tissue homeostasis is the basis for functional and structural maintenance of the organs of our body and is the result of a delicate balance between adult stem cell proliferation, quiescence and differentiation. Adult stem cells reside in specialized microenvironments, often called niches, where they receive and integrate multiple signals from neighbouring cells that contribute to the homeostatic regulation of the tissue.
De-regulation of these processes results in either loss or hyperplasia of the stem cells, which may severely impact the physiology of the organ and even the whole organism (Simons & Clevers 2011).

The small intestine is considered to be an instrumental model for studying adult stem cells in health and disease (Clevers 2013), mainly due to the fact that it is the most rapidly self-renewing tissue in adult mammals and has a simple, repetitive architecture. It is comprised of the regular alternation of crypt-villus units and its turnover, allowing continuous cell replacement, is three to five days in the adult mouse. This feature is connected to the dual function of the organ as both a protective barrier against external agents and as a selectively permeable mucosa for the absorption of nutrients (Turner 2009).

The bottom of the intestinal invaginations, termed the crypts of Lieberkühn, is home to the so-called "stem cell zone" where *Lgr5*$^{+}$ stem cells reside and divide approximately once every 24 hours, giving rise to transit-amplifying progenitor cells. Lineage tracing experiments labelling *Lgr5*$^{+}$ cells and their progeny showed that "ribbons" of cells extended from the crypt base to the villus tip, labelling all of the differentiated epithelial cell types of the intestine (Barker et al., 2007): enterocytes, goblet cells, tuft cells, enteroendocrine cells and Paneth cells (**Figure 1.1**). Moreover, it was shown that *Lgr5*$^{+}$ stem cells are characterised by long-term self-renewal potential and by the capacity to divide symmetrically, characteristics which establish neutral competition among the *Lgr5*$^{+}$ population for the limited space at the bottom of the crypts (Snippert et al. 2010). This mechanism represents the basis for cell homeostasis in the small intestine, with a more recent analysis of cell dynamics by intravital imaging demonstrating how *Lgr5*$^{+}$ stem cells residing in the upper border of the stem cell compartment can be passively pushed into the transit-amplifying region, following the division of underlying cells (Ritsma et al. 2014). These daughter cells can then migrate upwards, differentiate to diverse lineages and eventually undergo apoptosis, when they reach the tip of the villus, and be shed into the intestinal lumen (Barker, 2014).

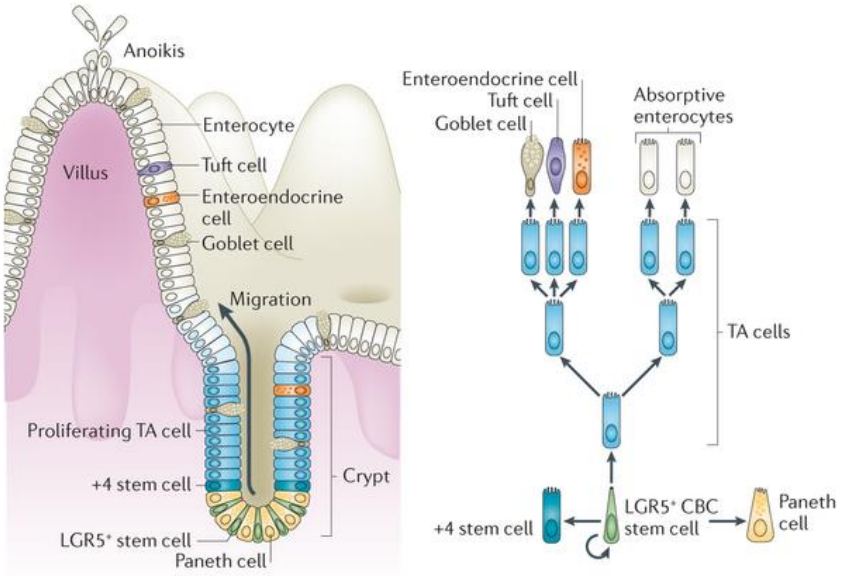

Figure 1.1 The distribution of epithelial cell types in the mammalian small intestine. A villus with one of the crypts that contribute to renewal of its epithelium. Arrows indicate the upwards flow of cells out of the crypts. Stem cells lie near the crypt base, whilst above them there are transit-amplifying (TA) cells. In the neck of the crypt and on the villus lie post-mitotic differentiated cells (absorptive cells, goblet cells, tuft cells and enteroendocrine cells). Paneth cells are intermingled with stem cells at the bottom of the crypt. (Barker, 2014).

If the bottom of the crypt is considered the "stem cell area" in the small intestine, villi, the digit-like protrusions flanking each crypt, constitute the "differentiated cell domain". Intestinal progenitors can differentiate along two different lineages: absorptive and secretory. The former lineage consists of nutrient-absorbing enterocytes, while the latter comprises hormone-secreting enteroendocrine cells, mucin-producing goblet cells and Paneth cells, which produce lysozyme. The Notch signalling pathway has been shown to play a pivotal role in determining lineage specification in the gut and in balancing secretory versus absorptive cell type numbers (Stanger, Datar, Murtaugh, & Melton, 2005; VanDussen et al., 2012). More specifically, Notch inhibition is crucial for inducing secretory cell differentiation, particularly for goblet and Paneth cell formation (VanDussen et al. 2012b), and the expression of its downstream effector, the helix-loop-helix transcription factor *Math1*, is also required, since the loss of *Math1* causes depletion of all secretory cell

types without affecting the enterocyte population (Yang, Bermingham, Finegold & Zoghbi, 2001).

As previously mentioned, the differentiation process of these cells is concomitant with their upward migration, but Paneth cells are an exception to this rule. They are the only differentiated cell type that migrates back to the crypt, because, in addition to Notch inhibition, for their full maturation they also require a high WNT environment, which can be found only at the base of the crypt (van Es, Jay, et al. 2005). Most importantly, in that position Paneth cells come into direct contact with *Lgr5*$^{+}$ stem cells and provide them with trophic support, contributing to a specialized microenvironment that constitutes the stem cell niche (Sato et al. 2011).

1.1.2 The stem cell niche and signalling pathways

The overall homeostasis of the small intestine is dependent upon the maintenance and tight regulation of the stem cell compartment at the bottom of the crypt, which not only harbours the *Lgr5*$^{+}$ stem cells but also a type of granulated cell named after their discoverer, the Paneth cells.

Paneth cells are the only terminally differentiated cells belonging to the secretory lineage that reside at the bottom of intestinal crypts, tightly intermingled with *Lgr5*$^{+}$ stem cells as delineated very clearly in the *Lgr5*-GFP knock-in mouse (Barker et al., 2007). These cells have a very prominent role in maintaining the health and homeostasis of the intestine and their presence at the crypt base is not a coincidence; their major function is to actively secrete antimicrobial peptides for host protection and essential trophic factors for stem cell maintenance (Zasloff, 2002; Sato et al., 2011).

Paneth cells were identified as a cellular component of the niche for *Lgr5*$^{+}$ stem cells, as they produce several ligands and growth factors that are essential for the stem cell microenvironment, such as epidermal growth factor (EGF), Notch ligands, TGFα and WNT-3 (**Figure 1.2**). These factors reinforce stem cell identity and cooperate in driving stem cell proliferation; genetic depletion of Paneth cells following *Sox9* ablation results in the parallel loss of stem cells *in vivo* (Sato et al., 2011; Koo & Clevers, 2014). Similarly, complete

loss of the stem cell compartment can be observed following the genetic ablation of Notch and WNT ligands in Paneth cells *in vivo* (Notch ligands: Dll1 and Dll4) and *in vitro* (WNT ligand: WNT-3), respectively. Curiously, genetic removal of WNT-3 from the epithelium *in vivo* does not seem to affect stem cell maintenance (Pellegrinet et al. 2012; Farin et al. 2012).

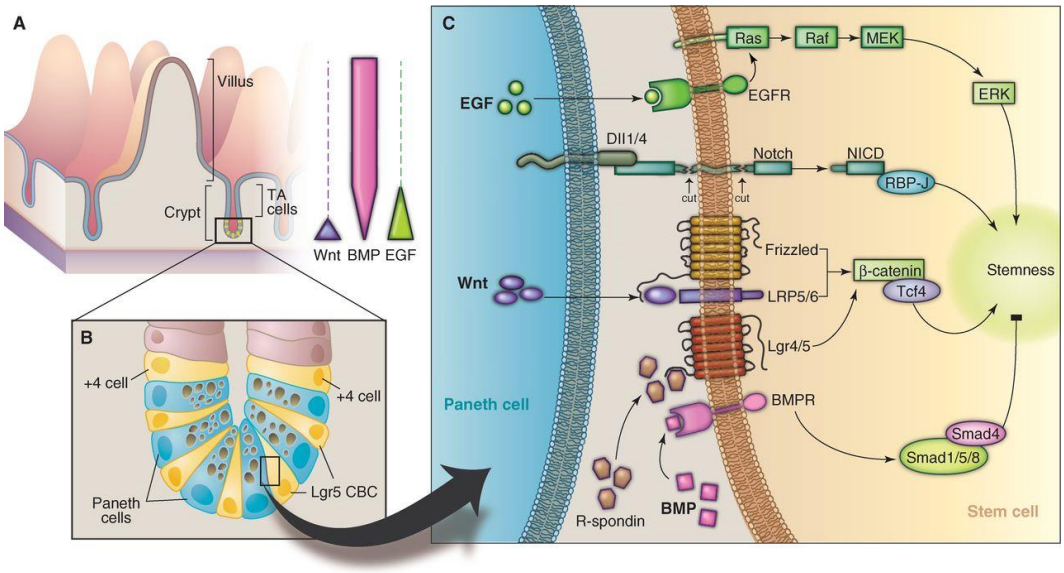

Figure 1.2 The stem cell niche in the adult small intestine. **A)** Schematic of the adult intestinal epithelium showing the spatial gradients of WNT, BMP and EGF signals along the crypt-villus axis. **B)** The stem cell niche at the bottom of the crypts are composed of $Lgr5^{+}$ CBCs (Crypt base columnar cells) intermingled with Paneth cells, which provide them with signals for stem cell maintenance. **C)** EGF, Notch and WNT signalling pathways are essential for intestinal epithelial stemness, whereas BMP signalling acts as a negative regulator of stemness. For full WNT activation in the intestinal epithelium, R-spondin–Lgr4/5 signalling is required (Sato&Clevers, 2013).

On the one hand, these observations confirm that Paneth cells play a crucial role as part of the niche, however they also suggest a certain level of redundancy with other sources of key growth factors *in vivo*. As might be expected, the subepithelial mesenchyme surrounding the crypts is responsible for providing additional niche factors, such as WNT ligands other than WNT-3 (Valenta et al. 2016; Kabiri et al. 2014) and the crucial molecular family of WNT agonists, the R-spondins (Kang et al. 2016)**.** The ligands BMP-2

and -4 are also predominantly produced by stromal cells in the villi, where they suppress WNT proliferative signals and drive cell differentiation (Haramis et al. 2004); at the base of the crypts, the surrounding mesenchyme also has the function of neutralising those differentiation signals by secreting BMP inhibitors (Kosinski et al. 2007).

Taken together, all the observations so far point to the canonical WNT signalling pathway as a major driver of crypt proliferation and stem cell maintenance in the adult intestinal epithelium. Many of the molecular players involved in this signalling pathway have been shown to have a key role in the maintenance of stem/progenitor cells. For example, WNT ligands themselves were identified as strong mitogens in the context of the intestinal epithelium (Korinek et al. 1998; van de Wetering et al. 2002). Moreover, genetic deletion of the WNT receptor Frizzled7 (Flanagan et al. 2015), β-catenin (Ireland et al. 2004) or the transcription factor TCF4 (van Es et al. 2012) leads to the loss of proliferating intestinal stem/progenitor cells. By contrast, *Apc* mutation or β-catenin activation causes the constitutive activation of WNT signalling and the subsequent formation of intestinal adenomas (Sansom et al. 2004; 2007).

Therefore, the activity of the WNT signalling pathway in regulating intestinal stem cells is a double-edged sword, requiring robust control to maintain a delicate homeostatic balance, and indeed one of the main focuses of this thesis is the investigation of the regulatory mechanisms operating to ensure appropriate levels of WNT activity.

In conclusion, the orchestration of these different signalling pathways ultimately determines the balance of proliferation, quiescence and differentiation in the adult intestine, and it was the recreation of this special microenvironment *in vitro* that was the key component that allowed Sato and colleagues to establish a self-sustaining and self-organising three-dimensional intestinal culture system (Sato et al. 2009).

1.2 Modelling the small intestine *in vitro*

1.2.1 Establishment of intestinal organoid culture

For decades, the technical difficulty of expanding somatic cells derived from adult primary tissues *in vitro* has hampered our understanding of fundamental physiological processes; the vast majority of primary cells could not be propagated in culture for long periods due to the onset of replicative senescence. The lack of appropriate culture conditions for the maintenance of progenitor cell populations prevented the expansion of primary tissues *in vitro*.

Thanks to the knowledge acquired from *in vivo* studies regarding the growth factor requirements and signalling pathway crosstalk within the intestinal stem cell niche, in 2009 it was finally possible to establish a murine, long-term, 3D culture system starting from a single *Lgr5*$^{+}$ stem cell and using Matrigel as an ECM substitute (Sato et al. 2009). These multicellular structures were termed “organoids” or “mini-guts” because of their resemblance to the tissue of origin and, most importantly, they could be maintened for over a year without the cells undergoing senescence or suffering genetic instability (Huch & Koo 2015).

It is noteworthy that analogous cultures were later established from a different source by directing the differentiation of human and mouse embryonic stem cells (ESCs) and induced pluripotent stem cells (iPSCs) towards an intestinal tissue identity (Spence et al. 2011).

As mentioned above, indispensable growth factors for the expansion and maintenance of the stem cell pool in the small intestine include WNT, EGF and BMP inhibitors (Sato & Clevers 2013); similarly, the WNT agonist R-spondin1, EGF and the BMP inhibitor Noggin were identified as essential constituents of organoid culture medium.

Gene expression analysis conducted on Paneth cells has confirmed that the spectrum of growth factor components secreted by these cells *in vivo* (*e.g.* EGF, WNT-3) is mirrored in the composition of organoid culture medium (Sato et al. 2011). In particular, WNT-3 was

observed to be an essential factor *in vitro*, since WNT-3-depleted Paneth cells cannot support organoid growth and maintenance over time (Farin et al. 2012).

Another fundamental pecularity of this novel culture system is that it consists of 3D, self-organising structures which recapitulate the architecture of the adult small intestine and contain all of the cell types found there (Ootani et al. 2009; Sato et al. 2009); for instance, it is possible to identify the presence of crypt and transit-amplifying regions in the organoid bud regions, at the end of which *Lgr5*$^{+}$ stem cells and Paneth cells are located, and the lumen of the organoid is lined by a villus domain containing all differentiated cell types (**Figure 1.3**). Analogous to the intestine, cells are shed into the lumen of the organoid after completion of their life cycle approximately every 5 days, after which the organoids will need passaging.

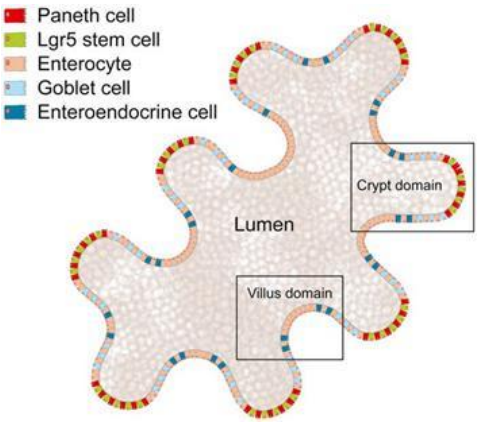

Figure 1.3 Schematic structure of a small intestinal organoid. These "mini-guts" preserve the original *in vivo* architecture of the small intestine by segregating into crypt domains, containing Lg5^{+} stem cells and Paneth cells, and villus domains, containing several differentiated cell types such as goblet cells, enteroendocrine cells and enterocytes. Organoids have a central lumen which accumulates the debris from differentiated cells when they undergo apoptosis. (Picture adapted by Academilib.com from Roeselers et al, 2013).

In addition, the organoid cultures recapitulate not only the structural organisation of the intestine but also its physiology. To demonstrate that organoids retain a high degree of fuctional similarity to their tissue of origin, Yui and collegues transplanted fluorescently-labelled intestinal organoids into a mouse model of enterocolitis and showed that they could engraft and functionally replace the damaged tissue (Yui et al. 2012).

For all of these reasons, organoid cultures can be considered an unprecedented tool to bridge the gap between *in vivo* models and 2D *in vitro* culture systems. Given their physiological accuracy and robustness, organoids allow the prediction of the *in vivo* role of

a gene, representing a much faster and more affordable approach than traditional mouse genetic studies. Despite being slightly more labour-intensive and time-consuming than conventional 2D cell culture, organoid culture systems have rapidly been applied globally to various problems and fields of study.

1.2.2 Applications of organoid technology

The arrival of organoid technology has represented a major breakthrough for many different fields due to its versatility and physiological relevance; from the study of adult stem cells and tissue development to the screening of new compounds for cancer treatment, intestinal organoids have turned out to be an excellent model system for a wide range of applications.

An exemplary case is the application of organoid culture to the investigation of cell lineage decisions *in vitro*; Yin and co-workers exploited *Lgr5*$^{+}$ stem cell plasticity *in vitro* to shift organoid cell composition to either mainly enterocytes or secretory cells simply by modulating WNT and Notch signalling pathways using small molecule inhibitors (Yin et al. 2014). In addition to the study of stem cell lineage selection, organoids have also been fruitfully employed in the investigation of the tissue microenvironment in terms of interactions between the intestinal epithelium and the intraepithelial immune cells, such as T lymphocytes (Nozaki et al. 2016).

Given the remarkable physiological relevance of organoids, in recent years there has also been a growing interest in applying these 3D culture systems to the study of pathophysiology of host-microbe interactions; for instance, many groups have modelled bacterial infectious diseases, such as Salmonella infection (Zhang et al. 2014), as well as enterovirus replication (Finkbeiner et al. 2012).

In terms of disease modelling *in vitro*, most efforts have been directed towards the establishment of more accurate and reliable cancer models than traditional cancer cell lines. This goal has been pursued from two main directions: firstly, advanced genetic engineering tools have allowed the introduction of a combination of mutations to mimic

the process of carcinogenesis (Drost et al. 2015; Matano et al. 2015), and secondly, the possibility of deriving human organoid cultures directly from patient tumour biopsies has opened the way towards a better characterisation of cancer subtypes and potential treatments. In this respect, the generation of a colorectal cancer organoid "biobank" gave van de Wetering and colleagues the opportunity to characterise different types of mutational landscapes, potentially associate those to a particular drug sensitivity via high-throughput drug screens, and thus address the problem of tumour heterogeneity (van de Wetering et al. 2015). The same approach for drug validation and discovery using human organoid cultures has been applied to other tissues as well, such as the liver (Sampaziotis et al. 2015; Meng 2010), and it holds great promise for providing a new frontier in personalised medicine.

To conclude, it is clear that organoid technology has rapidly revolutionised multiple aspects of basic and translational research, and it is no coincidence that some of its major accomplishments were possible thanks to a series of tools for genome engineering that will be the next major topic of consideration.

1.2.3 Genetic manipulation of organoids

The ability to combine intestinal organoids as a model system with the latest technological advances in genetic engineering is enabling researchers to modulate the expression of genes of interest and explore the function of unknown genes under near physiological conditions. Such powerful approaches based on the genetic manipulation of organoids can be exploited for various purposes: to generate stable transgenic organoid lines, to model cancer or other pathologies *in vitro* by disrupting or altering a certain gene(s) or even to restore the wild-type sequence of a mutated gene.

The need to investigate gene function *in vitro* has led to the development of a series of protocols based on retroviruses (Koo, Stange, et al. 2012; Koo et al. 2013) or lentiviruses (Miyoshi & Stappenbeck 2013) to perform inducible overexpression or knock down of a gene of interest. In this way, transgenes are provided by viral transduction and those cells with the modification randomly integrated in their genome are selected by the addition of

antibiotics. One alternative to virus-based methods for stable genome integration is the piggyBac transposon system, which was utilised by Fujii et al. in 2015 in combination with electroporation as a delivery system.

Besides the generation of stable transgenic lines, efforts have also been directed towards developing efficient strategies for gene knock-out in organoids, and the introduction in 2012 of CRISPR/Cas9 technology for genome editing represented a significant breakthrough in the field. CRISPR/Cas9 gene editing is a simple and rapid methodology for the disruption of a specific gene, as well as its precise editing (Ran et al. 2013), and it will be discussed in greater detail in the next sections. The present section focuses instead on notable examples of the pioneering application of this cutting-edge technology to intestinal organoid culture by Schwank and colleagues. As a proof of principle, they first knocked out *Apc*, a component of the β-catenin destruction complex and negative regulator of the WNT pathway, and showed that mutated organoids overcame their dependency upon both WNT and R-spondin for their growth (Schwank et al. 2013). This highlighted a major advantage of the organoid system, namely the possibility to easily screen for genetic modifications by phenotypic analysis. Following this proof of principle, the authors utilized CRISPR/Cas9 technology for site-specific gene modification by providing a DNA template to correct the mutant CFTR locus by homologous recombination in intestinal organoids derived from cystic fibrosis patients. More recently, a similar approach for knock-in purposes was exploited to introduce driver colorectal cancer mutations into human intestinal organoids in order to model *ex vivo* the adenoma-carcinoma sequence (Matano et al. 2015).

Lastly, our group has also contributed to the diversity of tools available for genetic studies in organoids with the development of a CRISPR-concatemer vector for simultaneous multiple gene knockout (Andersson-Rolf et al. 2016); this system is particularly useful in simultaneously targeting a gene together with its paralogues, as well as increasing the chances of single gene knockout by using multiple gRNAs targeting the same gene.

Taken together, these examples of tools for the genetic manipulation of organoids point out the great utility of combining novel technologies, especially when conducting loss-of-

function studies whose speed and feasibility have recently been boosted by the introduction of the CRISPR/Cas9 system.

1.3 CRISPR/Cas9 technology for genome editing

1.3.1 CRISPR/Cas9 for knockout and precise gene editing

Reverse genetics is a widely used approach in the investigation of gene function, enabling scientists to assess how genotype influences phenotype. Loss-of-function studies in particular can provide conclusive information on the role of a gene and greatly contribute to our knowledge of diverse biological processes. For this reason, in the past decade, a number of powerful methods for specific gene inactivation or modification began to be widely available and have been used in a wide range of applications and model systems.

Prior to the development of CRISPR/Cas9-mediated gene editing, zinc-finger nucleases (ZFNs) and transcription activator-like effector nucleases (TALENs) were the most efficient and versatile strategies for genome engineering. As a common feature, both of these technologies rely on protein/DNA recognition and are centred on site-specific designer nucleases consisting of sequence-specific DNA-binding domains fused to a generic DNA cleavage domain (Mussolino et al. 2011; Carroll 2011). Similar to the CRISPR/Cas9 system, ZFNs and TALENs can induce targeted double-strand breaks (DSBs) in the genome that can activate the DNA damage response and be repaired either via error-prone non-homologous end joining (NHEJ) or via homology-directed repair (HDR), where a suitable DNA template is available (Wyman & Kanaar 2006).

In recent years the introduction of CRISPR/Cas9 technology has revolutionised the genome-editing field by emerging as the latest and fastest advance for introducing site-specific genetic alterations (Mali et al. 2013). In contrast to ZFNs and TALENs, the

CRISPR/Cas9 system is based on the formation of a ribonucleotide complex between an RNA molecule and the target DNA, which greatly simplifies the target design.

CRISPR is an acronym that stands for 'clustered, regularly interspaced, short, palindromic repeats' and Cas9 is the CRISPR-associated endonuclease that is targeted to a specific genomic region by a single guide RNA (sgRNA) which is complementary to the target DNA sequence. This technology was developed by exploiting key components of the acquired immune system that protects prokaryotic cells against foreign DNA. In bacteria, short exogenous DNA fragments, termed "spacers", are integrated into the genome at the CRISPR locus to produce CRISPR RNAs (crRNA). These molecules anneal to the transactivating crRNAs (tracrRNAs) that are bound to Cas9 and the Cas9-crRNA-tracrRNA complex is then responsible for site recognition, DNA binding and cleavage. It has been observed that Cas9 requires a "seed" sequence in the crRNA for DNA recognition as well as a conserved protospacer adjacent motif (PAM) upstream of the crRNA binding region (Jinek et al. 2012). Our understanding of the system has been exploited to adapt the type II CRISPR system from S. *pyogenes* into a flexible and efficient universal platform for RNA-programmable genome editing. In the absence of a DNA template for homologous recombination, the Cas9 endonuclease generates double-strand breaks that are then ligated back together by the DNA repair machinery via NHEJ; since this process is inherently error-prone, the insertion or deletion of a nucleotide(s) frequently occurs, resulting in frameshift mutations (Ran et al. 2013).

Alternatively, when a donor vector is co-delivered together with gRNAs and Cas9, it is possible for repair to occur via homologous recombination, which therefore allows precise gene editing through knock-in (**Figure 1.4**).

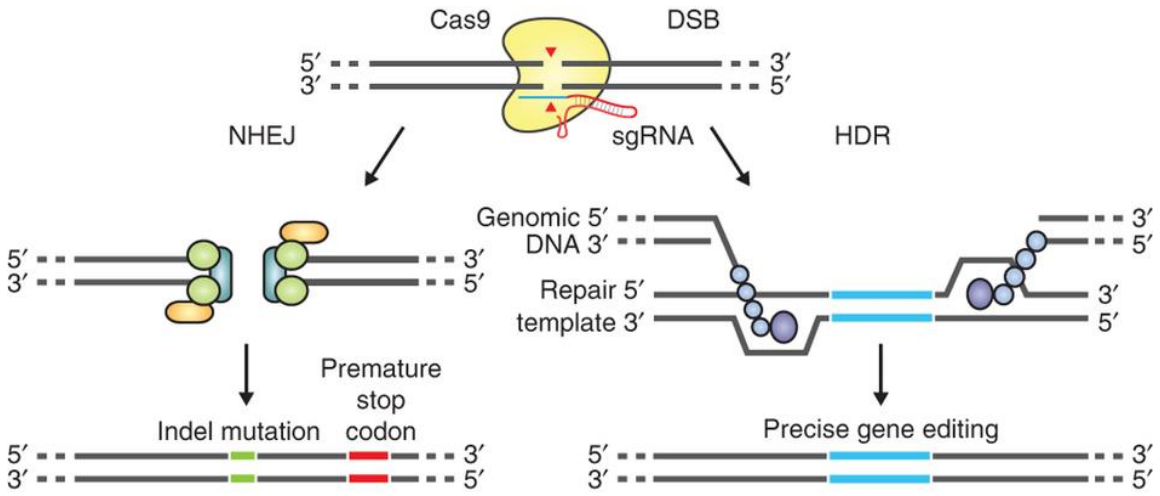

Figure 1.4 Schematic representation of CRISPR/Cas9 mechanism of action. Cas9 is targeted to a specific genomic region by the sgRNA and cleaves the DNA, generating double-strand breaks. These breaks can be repaired in one of two ways: via error-prone NHEJ, in which the DNA repair machinery ligates the DNA ends back together, so randomly generating indel mutations, or via HDR, when a repair template is provided for homologous recombination. While the NHEJ pathway can lead to gene knockout by the introduction of a premature stop codon, HDR allows precise gene editing (Ran et al, 2013).

One of the most important characteristics of this new approach is its versatility as proven by its successful application to a number of different model systems, e.g. to perform gene knockout or modification in human and mouse cells (Cho et al. 2013; Xue et al. 2016; Wang et al. 2013), zebrafish (Hwang et al. 2013) and *Drosophila* (Yu et al. 2013). Moreover, Gilbert and colleagues demonstrated the modulation of gene expression using the CRISPR/Cas9 system by fusing an enzymatically dead Cas9 to transcription effector domains with distinct regulatory functions, either activators or inhibitors (Gilbert et al. 2013). In this way, the authors were able to stably modulate gene expression in both human and yeast cells.

Given its simplicity and speed, the CRISPR/Cas9 approach soon became the tool of choice for genome-wide knockout screens, representing a valid alternative to RNA interference (Sanjana et al. 2014), and different genome-scale gRNA libraries were generated to target genes in mammalian cells (Koike-Yusa et al. 2014; Chen et al. 2015) and *Drosophila* (Bassett et al. 2015). Lastly, many groups have also developed multiplex CRISPR strategies to achieve the knockout of multiple genes at the same time in a variety of model systems:

human cell lines (Sakuma et al. 2014; Kabadi et al. 2014), intestinal organoids (Andersson-Rolf et al. 2016), zebrafish (Yin et al. 2015) and *Drosophila* (Port et al. 2014).
In summary, this section has highlighted some of the most crucial aspects of the CRISPR revolution and how it has changed our approach to genetic studies; the next paragraph will instead focus on how this technology has been employed for disrupting gene expression in a conditional manner.

1.4 WNT signalling pathways

All of the technologies described in detail so far for modelling the small intestine *in vitro* and for gene editing have formed a major part of my PhD studies investigating the regulatory mechanisms of the WNT signalling pathway, a fundamental player in the maintenance of homeostasis of intestinal stem cells (Clevers et al. 2014).

WNTs are a class of 19 evolutionarily conserved, secreted lipoglycoproteins in mammals that are involved in a variety of biological processes, such as proliferation, differentiation, migration and control of embryonic development, as well as adult homeostasis (Niehrs 2012). WNTs can bind to a multitude of Frizzled receptors and co-receptors and their combinatorial binding determines the downstream signalling events that subsequently occur (Dijksterhuis et al. 2014). These have been classified into two main branches: a β-catenin-dependent, or "canonical", WNT pathway and a β-catenin independent, or "non-canonical", pathway (Semenov et al. 2007; Macdonald et al. 2007). Although some WNTs preferentially activate the "canonical" pathway over the "non-canonical", and vice versa, the signalling outcome is predominantly dependent upon the cellular context.

This section will describe the essential traits of both β-catenin dependent "canonical" and β-catenin independent "non-canonical" WNT signalling pathways (**Figure 1.5**).

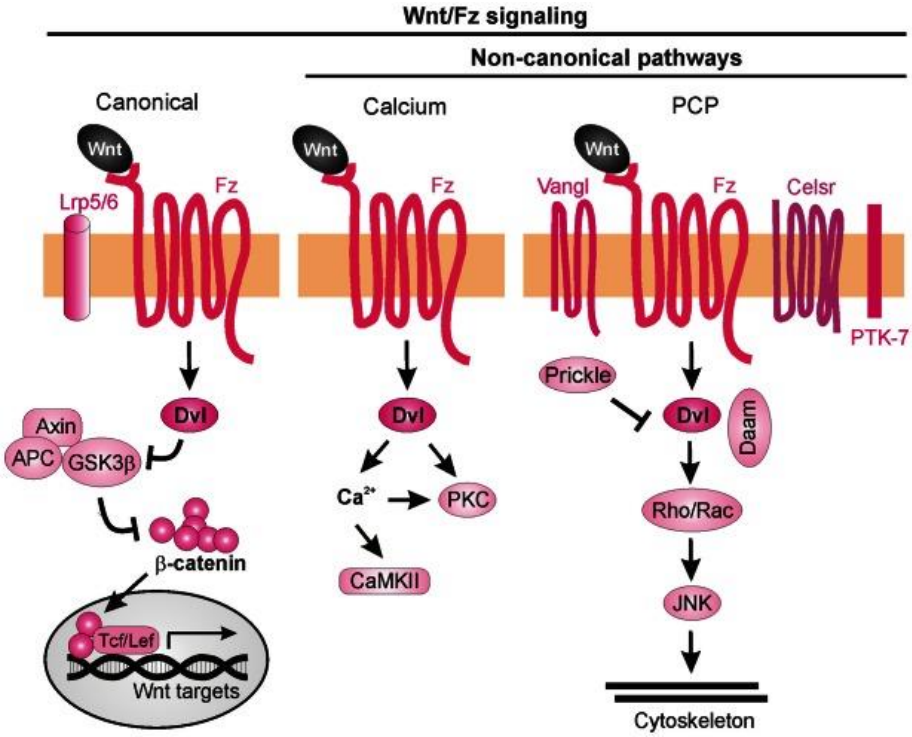

Figure 1.5 Overview of the different WNT signalling pathways. WNT ligands can transduce their signal through two types of pathway: the WNT/β-catenin canonical pathway and the non-canonical pathways. The former is characterised by the binding of WNT to Frizzled (Fz) and its co-receptors Lrp5/6. This leads to the recruitment of DVL to the plasma membrane and inhibition of the destruction complex, allowing the translocation of β-catenin to the nucleus and its binding to the transcription factors TCF/LEF, inducing the expression of target genes (left). The non-canonical pathways mainly consist of two branches (right); in the Calcium pathway, WNT binding to Fz leads to DVL recruitment and thence to an increase in cytosolic Ca^{2+} that in turn activates a series of calcium-dependent kinases (CaMKII). In the PCP pathway, transmembrane proteins like Vangl, Celsr and PTK7 assist Wnt docking to Fz that determines the recruitment and activation of the intracellular proteins DVL, Prickle and DAAM. This leads to the activation of the small GTPases Rho and Rac that in turn stimulate JNK to promote actin cytoskeleton remodelling. Figure adapted from Aviles et al. 2013.

1.4.1 The "canonical" WNT/β-catenin pathway

The "canonical" WNT/β-catenin pathway is the most well-studied of the two pathways and is characterised by WNT interaction with Frizzled and its co-receptor LRP5/6.

In the absence of WNT stimulation, β-catenin is sequestered in the cytoplasm by the so-called "destruction complex", whose function is to target it for degradation. This complex is formed from a number of different proteins, such as adenomatosis polyposis coli (APC), AXIN, glycogen synthase kinase 3 (GSK3) and casein kinase 1 (CK1). When β-catenin is recruited by the complex it is phosphorylated by GSK3 and CK1, leading to its subsequent ubiquitination by β-TrCP, which signals it for proteasomal degradation (Yanagawa et al. 2002; Behrens et al. 1998).

Conversely, when WNT ligands are present, they bind to the cysteine-rich domain (CRD) of Frizzled and to its co-receptor LRP5/6 (MacDonald & He, 2012; Janda et al. 2012). The formation of this ligand-receptor complex is followed by conformational changes that lead to the recruitment of the scaffolding protein Dishevelled (DVL) to take part in the "signalosome". As a consequence, LRP6 is phosphorylated and this induces a dramatic relocalisation of AXIN from the cytoplasm to the plasma membrane, followed by the dismantling of the β-catenin destruction complex (Bilic et al. 2007). In this way, β-catenin is stabilised and can translocate into the nucleus, where it associates with the transcription factors TCF/LEF (T cell factor/lymphoid enhancer-binding factor) to drive the expression of WNT target genes, amongst which *Cyclin D1*, *c-myc*, *Axin2* and *Lgr5* are some of the most well-known (Tetsu & McCormick 1999; He et al. 1998; Jho et al. 2002; Barker et al. 2007). A widely used method to measure WNT/β-Catenin activity levels is the TOP-flash assay, which is based on a TCF/LEF luciferase reporter and provides a direct readout for the activity of the canonical pathway (Molenaar et al. 1996).

Given its high degree of conservation throughout evolution, it comes as no surprise that the canonical WNT pathway acts as a key mediator in many cellular processes; above all, its centrality in regulating stem cell differentiation and proliferation emerges in the context of both embryonic and adult stem cells (Reya & Clevers 2005). Interestingly, whilst some groups have shown that WNT signalling prevents the differentiation of mouse ESCs into

epiblast stem cells (ten Berge et al. 2011), others have reported that an increase in WNT/β-catenin activity has been observed before these cells exit from pluripotency and commence lineage specification (Turner et al. 2014). As previously discussed, WNT signalling is also fundamental for adult stem cell self-renewal and the maintenance of homeostasis in the intestine (Barker et al. 2007). In addition, it also plays a crucial role in the homeostasis of other adult tissues, such as the hair follicle (Lim et al. 2016) and the mammary gland (van Amerongen et al. 2012). In fact, linage tracing approaches using the *Axin2*–CreERT2 mouse line have highlighted the importance of an autocrine WNT/β-catenin signalling loop in the maintenance of a quiescent stem cell population in the hair follicle bulge, and similarly in the mammary epithelium it was shown that $Axin2^+$ progenitor cells could contribute to both luminal and basal epithelial lineages.

Therefore, it is of primary importance that WNT/β-Catenin activity is tightly regulated in order to avoid an uncontrolled expansion of the stem cell pool that could lead to tumorigenesis; in this regard, the role of the E3 ubiquitin ligase RNF43 acquires a particular relevance in terms of tuning the membrane levels of Frizzled and will be discussed in detail later on.

1.4.2 β-catenin independent WNT signalling pathways

The term “non-canonical”, or β-catenin independent, WNT signalling refers to a diverse range of pathways that are triggered by the interaction of WNT ligands with Frizzled and alternative co-receptors to the LRPs (van Amerongen et al. 2008). Importantly, these pathways employ different downstream signalling modalities which do not rely on the transcriptional role of β-catenin.

One example of a β-catenin-independent signalling cascade is the WNT-Ca^{2+} pathway. It was first observed in the zebrafish embryo, where WNT stimulation caused an increase in cytosolic calcium levels (Slusarski et al. 1997). Following WNT docking to Frizzled, heterotrimeric G proteins associated with the receptor are activated and, consequently, this stimulates phospholipase C (PLC) to activate the cascade responsible for Ca^{2+} release

in the cytoplasm. Lastly, this calcium increase activates calmodulin-dependent kinase II (CAMKII) that mediates the final transcriptional events (De 2011). Dysregulation in this pathway has been associated with cancer, inflammation and neurodegenerative diseases.

The other well-known β-catenin-independent pathway is the WNT/planar cell polarity (PCP) pathway that has been better characterised when compared to WNT/ Ca^{2+} signalling. In this case, WNT signals are transduced through the interaction of the ligand with Frizzled and its co-receptors ROR1/2 or PTK7, and this induces the recruitment of intracellular proteins like DVL, DAAM and Prickle to activate the small GTPases RAC1 and RHOA. These molecules stimulate, respectively, the JUN N-terminal kinase (JNK) and RHO kinase, and as a consequence the actin cytoskeleton is remodelled and cell shape and polarity are redefined (Oishi et al. 2003). In fact, the PCP pathway plays a major role in those morphogenetic processes occurring during vertebrate embryonic development by governing cell migration during gastrulation and neural tube closure (Simons & Mlodzik 2008; Ho et al. 2012).

This pathway was shown to have an antagonistic relationship to canonical WNT/ β-catenin signalling; for instance, it was observed *in vitro* that the PCP-associated WNT-5A signal antagonises the β-catenin-dependent signalling cascade by competing with WNT-3A for Frizzled binding and by inhibiting Wnt-3A-dependent LRP6 phosphorylation (Sato et al. 2010). Nevertheless, it is not appropriate to draw a neat separation between “canonical” and “non-canonical” WNT pathways, given that the same ligands and receptors can engage various signalling cascades depending on the cellular context and also considering that some components are shared between the different pathways, such as Dishevelled (Gao & Chen 2010). In this regard, since both WNT/β-catenin and PCP pathways are mediated by Frizzled receptors, it is reasonable to assume that both signalling cascades are subject to the same mechanisms of regulation at the level of the receptor (Hao et al. 2012).

In the next paragraph, I will discuss the role of *Rnf43* and its homologue *ZnrF3* in regulating the turnover of Frizzled, which is a critical node in the global modulation of the activity of WNT-driven signalling pathways.

1.5 RNF43 & ZNRF3, novel key players in WNT pathway regulation

1.5.1 *Rnf43* & *Znrf3* are important tumour suppressors in the small intestine

Aberrant WNT signalling activity has been widely associated with many diseases, including cancer. For this reason, it is of the utmost importance that the final signalling output of WNT cascades is tightly controlled by feedback mechanisms.

In 2012, two groups independently identified a novel class of important regulators of WNT-driven signalling pathways: two E3 ubiquitin ligases, RNF43 (RING finger protein 43) and its paralogue ZNRF3 (Zinc/RING finger protein 3), which target the Frizzled family receptors for degradation, hence inhibiting WNT signalling responses (Koo et al. 2012; Hao et al. 2012).

Rnf43 and *Znrf3* are both WNT target genes encoding transmembrane proteins containing a Really Interesting New Gene (RING) domain that, via negative feedback, promote endocytosis-mediated degradation of WNT receptors and co-receptors in an ubiquitination-dependent manner (**Figure 1.6 A-C**). The internalised molecules are then degraded in the lysosome, thus ensuring optimal surface levels of Frizzled and attenuating WNT signalling activity.

In addition to the intracellular RING domain, which has E3 ligase activity, RNF43 and ZNRF3 also contain a protease-associated domain or PA, an extracellular domain for protein-protein interactions. A recent study reported that this region might be involved in target recognition prior to ubiquitination by interacting with the extracellular, cysteine-rich domain (CRD) of Frizzled (Tsukiyama et al. 2015). Interestingly, these proteins belong to an evolutionarily conserved family of transmembrane E3 ubiquitin ligases, the PA-RING family, that are all characterised by the same domain organisation and which will be described in detail later on.

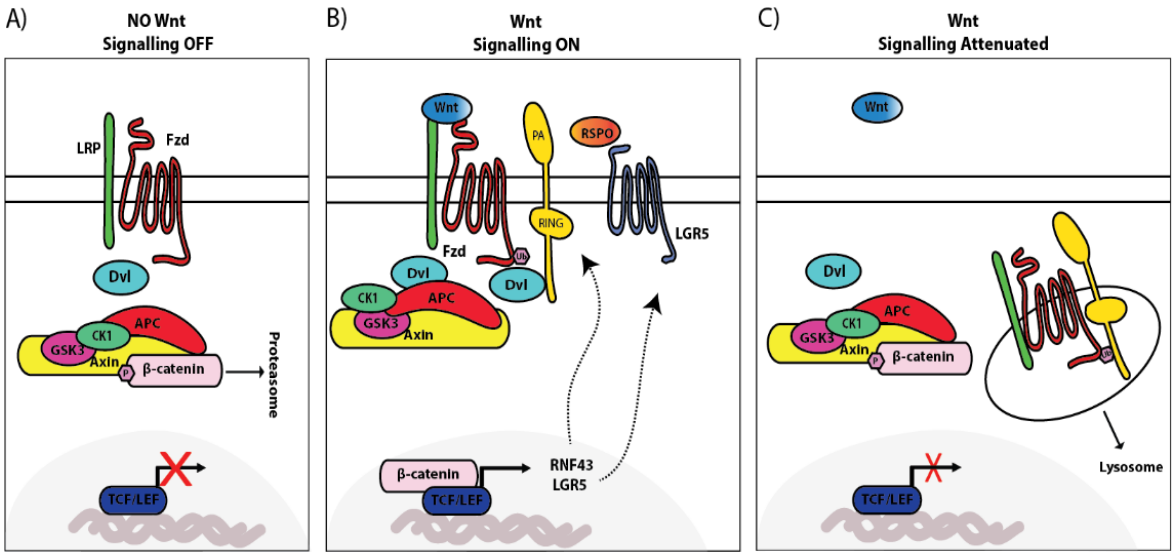

Figure 1.6 Model of negative feedback regulation of the WNT/β-catenin pathway by RNF43 and ZNRF3. **A)** Resting stage (no WNT stimulation), in which the destruction complex degrades cytoplasmic β-catenin and WNT signalling is shut off. **B)** Upon WNT stimulation, Frizzled and LRP5/6 receptors recruit destruction complex components to the plasma membrane, so causing its inactivation; this leads to the accumulation of β-catenin and its subsequent translocation to the nucleus, where it induces gene expression of WNT target genes, such as Rnf43/Znrf3 and Lgr5 **C)** RNF43 and ZNRF3 reach the plasma membrane where they ubiquitinate Frizzled, and consequently promote its endocytosis and lysosomal degradation. Frizzled clearance from the cell surface renders the cell less sensitive to WNT stimulation and, in this way, WNT signalling is attenuated.

In situ hybridization experiments showed that both *Rnf43* and *Znrf3* are uniquely expressed at the bottom of intestinal crypts in $Lgr5^{+}$ stem cells, and gene expression profiling revealed that their expression correlates with that of intestinal stem cell genes, such as *Lgr5*, *Olfm4* and *Ascl2* (**Figure 1.7**). In fact, in this context, mouse genetic studies have demonstrated that these two genes have a fundamental role as tumour suppressors: ablation of both *Rnf43* and *Znrf3* (*R&Z*) in the intestinal epithelium resulted in the rapid formation of adenomas (**Figure 1.8b**) that ultimately develop into tumours, due to hyper-activation of WNT signalling (**Figure 1.8d**). These tumours were found to be strictly dependent upon WNT for their growth, as the inhibition of WNT secretion resulted in growth arrest (Koo et al. 2015). It is noteworthy that when compared to other known negative modulators of WNT signalling, R&Z mutants were the first to show rapid tumorigenesis at a rate which phenocopied *Apc* mutants, so demonstrating their physiological importance. In fact, it is important to recall that *Apc* mutations are

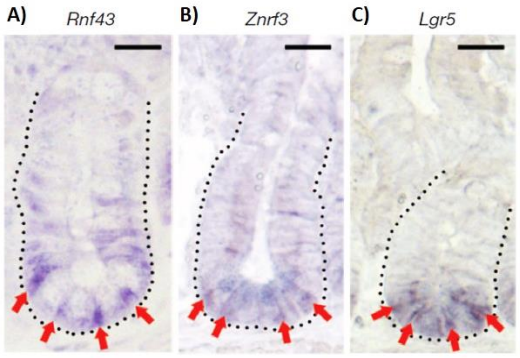

Figure 1.7 Lgr5^{+} stem cell genes: Rnf43 and Znrf3. *In situ* hybridization showing expression of *Rnf43* **(A)**, *Znrf3* **(B)** and *Lgr5* **(C)** in the mouse small intestinal crypt (dotted line indicates the intestinal epithelial lining of the crypt). Crypt Base Columnar cells (CBC cells) in between Paneth cells are indicated with red arrows. Scale bars, 20 mm. (Koo et al., 2012).

responsible for familiar adenomatous polyposis (FAP) as wells as an increased risk of sporadic colorectal cancers (Rowan et al. 2000).

The mechanistic importance of RNF43 and ZRNF3 as E3 ligases is not an isolated case when considering the role of this class of enzymes in the regulation of stem cell-niche interactions; a further example is the E3 ubiquitin ligase Mib1 (Mind-bomb-1), which is known to have an analogous role in Notch signalling by promoting the endocytosis of the Notch ligands Delta and Jagged in niche cells, resulting in the activation of Notch signalling in stem cells (van Es et al. 2005; Koo et al. 2005; Koo et al. 2007).

Given their fundamental role in modulating WNT activity in intestinal stem cells, RNF43 and ZNRF3 are considered essential for tissue homeostasis by preventing uncontrolled expansion of the stem cell compartment. However, it is also necessary that, in turn, R&Z activity is precisely controlled in order to avoid the loss of the stem cell compartment over time. The R-spondins (RSPO), WNT pathway agonist ligands, play a key role in the regulation of RNF43/ZNRF3 turnover, together with their concomitant receptors LGR4/5/6. R-spondins are soluble niche factors that can bind to the LGR5 receptor and induce the formation of a ternary complex with R&Z (Zebisch et al. 2013; Hao et al. 2012). Recently, it has been shown that these events are instrumental for the membrane clearance of RNF43 and ZNFR3, resulting in enhanced WNT responsiveness (de Lau et al. 2014); accordingly, the double KO of *Lgr4* and *Lgr5* results in intestinal crypt loss (de Lau et al. 2011).

In conclusion, RNF43 and ZNRF3 can be classified as essential negative modulators of the WNT signalling pathway that act at the receptor level, preventing uncontrolled expansion of the stem cell compartment and providing a major contribution to tissue homeostasis. Therefore, it comes as no surprise that mutations affecting components of

the RNF43/LGR5/RSPO axis can frequently be found in different types of cancer (Hao et al. 2016).

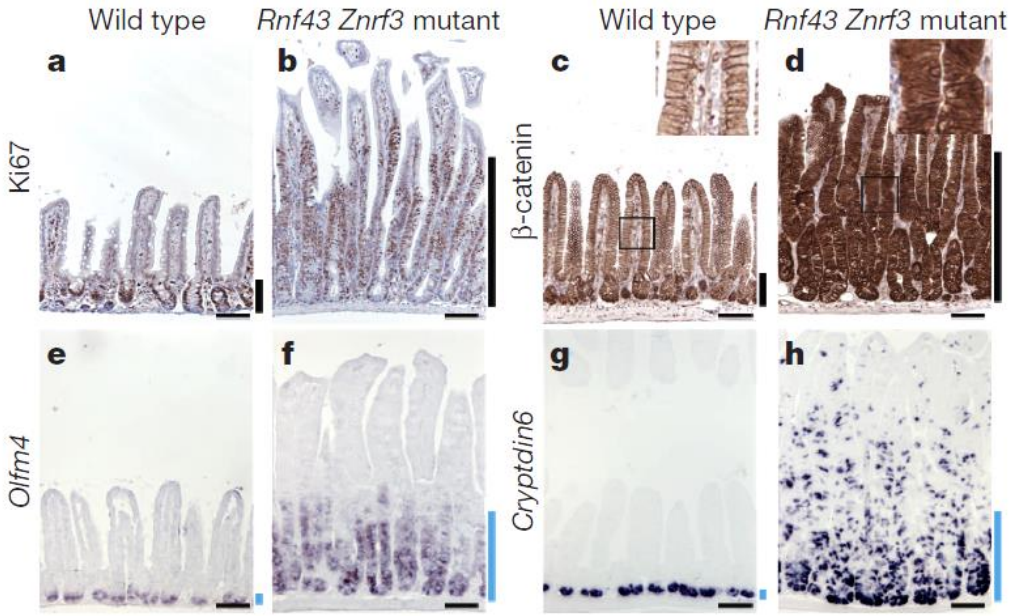

Figure 1.8 Rnf43 and Znrf3 compound mutant mouse phenotypes in the small intestine. Removal of both *R&Z* in the small intestine leads to strongly increased cell proliferation, as demonstrated by Ki67 staining (**a, b**), WNT/β-catenin activation (**c, d**) and stem cell (**e, f**) and Paneth cell (**g, h**) metaplasia, marked respectively by *Olfm4* and *Cryptidin6* expression (Koo et al, 2012).

1.5.2 RNF43 and R-spondin are often mutated in cancer

Alterations shifting the balance between the RNF43-mediated negative feedback loop and R-spondin-mediated positive modulatory activity towards augmented WNT signalling can often be encountered in a variety of human tumours. In particular, those cancer types that have been previously characterised as being driven by uncontrolled WNT/ β-catenin activity are also likely to harbour abnormalities in RNF43 or RSPO; it is also worth mentioning that *Rnf43* mutations were found to be mutually exclusive with *Apc* and β-catenin mutations (Giannakis et al. 2014), confirming their redundant roles in the outcome of WNT pathway activation.

Inactivating somatic mutations in *Rnf43* were observed in over 18% of colorectal adenocarcinomas and endometrial carcinomas (Giannakis et al. 2014) and in 21% of mucinous ovarian carcinoma samples (Ryland et al. 2013), as well as in gastric (K. Wang et al. 2014) and pancreatic cancers (Jiao et al. 2014). In addition, mutations in RNF43 were also reported to be present in benign pancreatic tumours, intraductal papillary mucinous neoplasm and mucinous cystic neoplasm (Wu et al. 2011) and in 9.3% of intrahepatic cholangiocarcinomas (Ong et al. 2012).

According to the Catalogue Of Somatic Mutations In Cancer (COSMIC), the most common mutational events in *Rnf43* consist of nonsense and frameshift mutations that lead to a truncated protein, which supports the classification of *Rnf43* as a tumour suppressor. Notably, two main hotspot mutations causing frameshifts were identified, G659fs and R117fs, representing, respectively, 41.7% - 48.0% and 8.3% - 12.0% of RNF43 mutations in colon and endometrial cancer (Giannakis et al. 2014).

Another interesting observation is that *Rnf43* mutations are more frequent in microsatellite-instable tumours compared to microsatellite-stable ones; this is the case for gastric cancer, colorectal cancer and endometrial carcinoma (Hao et al. 2016).

Although it is functionally redundant with RNF43, ZNRF3 is less frequently mutated in cancer. Mutations in *Znrf3* could only be found in 21% of adrenocortical carcinomas, which is the type of cancer showing the highest frequency of *Znrf3* mutations (Assie et al. 2014).

This difference in relative mutation frequencies might be due to different expression levels of the two proteins.

Additionally, abnormalities in R-spondin proteins are also found in cancer. In particular, it has been observed that translocations of *Rspo-2* (3%) and *Rspo-3* (8%) such that their expression is under the control of stronger promoters are recurrent in microsatellite stable (MSS) colon cancer (Seshagiri et al. 2012; Shinmura et al. 2014). Usually RSPO-2 and RSPO-3 are found to be fused to EIF3E and PTPRK, respectively, and their expression levels are increased in tumour samples. Interestingly, the same type of fusion products were recently observed in traditional serrated colorectal adenomas at an even higher frequency (Sekine et al. 2016) and these translocations were found to be mutually exclusive with APC or β-catenin mutations. Furthermore, *Rspo-2*/*3* translocations have been identified in other types of tumours, such as prostate cancer and non-small cell lung cancer (Karkera et al. 2014).

In conclusion, these data taken together show that alterations in the R-spondin/RNF43 module are often implicated in various types of cancer, again supporting the physiological relevance of RNF43 as a tumour suppressor. In light of this, it is especially important to elucidate the mechanisms through which RNF43 promotes the ubiquitination, internalisation and degradation of Frizzled, not only because this could lead to new insights into the WNT pathway but also because it might reveal some novel interactors of RNF43 with an equally important function.

1.5.3 Role of Dishevelled in the mechanism of action of RNF43

Despite its crucial role in fine-tuning the WNT pathway and its prominent activity as a tumour suppressor, the precise mechanism of action and regulation of RNF43 remain poorly understood. Nevertheless, two recent pieces of work have helped to broaden our understanding of RNF43-mediated downregulation of Frizzled by revealing a novel and unexpected role for Dishevelled as an adaptor for the recruitment of RNF43 to Frizzled (Jiang et al. 2015; Tsukiyama et al. 2015).

The first observation made by Cong and colleagues was that surface levels of both Frizzled and LRP were significantly increased in *Dishevelled* triple KO cells, even though WNT/β-catenin activity was reduced (Jiang et al. 2015). Hence, they investigated the ubiquitination and endocytosis of Frizzled in more detail and found that ubiquitination of the WNT receptor and its internalisation were greatly impaired in *Dvl* KO cells.

To investigate further at a molecular level, the group performed a series of co-immunoprecipitation experiments that highlighted a region in the intracellular domain of RNF43 that is responsible for Dishevelled-2 binding, subsequently termed the Dishevelled-interaction region or DIR. This region was mapped by Cong and colleagues to be between aa 326-454, whereas Tsukiyama's group instead identified a more C-terminal region as being implicated in DVL binding (aa 477-596) and observed that this interaction is only required for the suppression of non-canonical WNT signalling. In contrast to the former report, they showed by a combination of flow cytometry and luciferase reporter assays that the binding of RNF43 to DVL2 is not required for the surface clearance of Fzd4 or for the suppression of WNT/β-catenin signalling.

Interestingly, Cong's group found the DEP (Dishevelled, EGL-10 and Pleckstrin) domain of Dishevelled to be essential for the downregulation of Frizzled, even though the DVL2-ΔDEP protein retains the ability to interact with RNF43. In fact, the biggest limitation of this work is that it failed to identify a region of Dishevelled that is necessary and sufficient to interact with RNF43. Possible explanations could be the existence of multiple points of contact between the two proteins or the possibility that the interaction is not direct and might be mediated by a third party.

These considerations, together with some of the discrepancies between the two studies, underlie the need of further investigation into the dynamics of Frizzled-RNF43-DVL complex formation, as additional players might be required for FZD internalisation. A detailed characterisation of these molecular events could pinpoint novel interactors of RNF43 that may also be important regulators of its activity.

1.6 The PA-RING family of E3 ubiquitin Ligases

Numerous signalling pathways govern the most basic and essential cellular functions and their tight regulation is fundamental to prevent dysregulation and alterations of these important processes (Giancotti 2014). Among various modulatory strategies, a commonly used system is the establishment of negative feedback loops using ubiquitination to target proteins for degradation. The fine tuning of the immune response by the suppressors of cytokine signalling (SOCS) is an exemplary case of an inhibitory feedback mechanism based on ubiquitination (Tamiya et al. 2011). SOCS proteins are induced by cytokine stimulation, functioning as E3 ubiquitin ligases that then degrade cytokine receptors and consequently inhibit the JAK/STAT pathway (Tamiya et al. 2011; Babon J, Leila N. Varghese 2014).

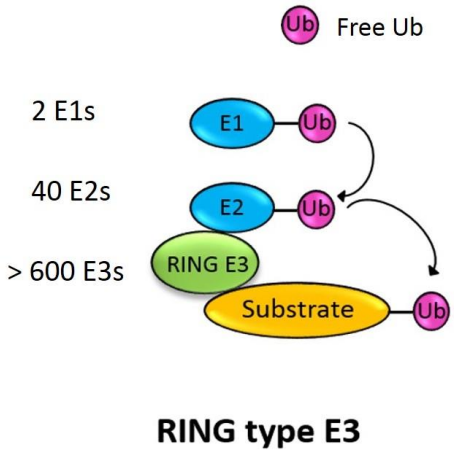

Figure 1.9 Ubiquitination process. The first step in the ubiquitination chain reaction is the formation of a thioester bond between free Ubiquitin (Ub) and the ubiquitin-activating E1 enzymes. Ubiquitin can then be transferred to an ubiquitin-conjugating E2 enzyme and finally to the E3 ubiquitin ligase that modifies a lysine residue on the target protein with an ubiquitin molecule and which confers substrate specificity to the process. The scheme refers to RING-type E3s in particular, but the E3 class is vast and comprises other types such as U-box, HECT and RBR E3 ligases. In total, over 600 E3 ligases are present in mammalian cells versus 40 E2 and only two E1 enzymes. (Clague et al. 2015).

In recent years, interest has been growing in ubiquitination as a regulatory modification in multiple biological processes (Strikoudis et al. 2014; Jia & Sun 2011; Metzger et al. 2012), with particular relevance to the control of membrane signalling and cell surface remodelling (MacGurn et al. 2012). In particular, E3 ubiquitin ligases have turned out to be extremely important players in the regulation of membrane signalling as they represent the most abundant class of enzyme in the ubiquitination cascade (Clague et al. 2015) and are responsible for substrate specificity (**Figure 1.9**).

Several examples of E3 ubiquitin ligases acting on signalling receptors have been reported, such as the HECT-domain containing ligase Nedd4 that promotes the ubiquitination and internalisation of the RTK receptors, EGFR (Lin et al. 2010) and FGFR (Persaud et al. 2011), or the RING finger E3 Cbl,

which is responsible for the attenuation of EGF signalling by EGF receptor ubiquitination and endocytosis (Umebayashi 2008). The mechanism of action of these proteins greatly resembles that of RNF43 and ZNRF3, the RING E3 ligases that promote the endocytosis-mediated degradation of the WNT receptor via negative feedback (Koo et al. 2012; Hao et al. 2012). As previously described, RNF43 and ZNRF3 share a common structural architecture consisting of an extracellular protease-associated domain (PA), a transmembrane domain and an intracellular RING domain. Bioinformatics analysis based on the screening of human sequences in GenBank revealed a 45-63% sequence similarity and the same structural organisation with 10 other human E3 ubiquitin ligases (**Figure 1.10 A-C**). This led to the identification of a novel conserved gene family, termed the PA-RING family (Koo et al. 2012). The members of this family show a high degree of homology between different species and, although most of them have not been well characterised yet, it is reasonable to hypothesise that they might share a certain degree of functional redundancy as well.

The next sections will focus on this newly identified family of E3 ubiquitin ligases, whose members have recently emerged as important regulators of membrane proteins in various cellular processes. I will discuss the roles of the most well characterised members and speculate on the putative role of the others by linking them to their orthologous genes in other species.

1.6.1 The Goliath-related protein family

As previously outlined, the PA-RING family has been reported to be highly conserved throughout evolution from yeast to human and evolutionary history as reconstructed in the Ensembl Compara database (Vilella et al. 2009) showed ancient proteins with the same domain architecture in plants and fungi (Bocock et al. 2009).

In early Metazoan evolution two clusters derived from these proteins (Lau et al. 2014): from the first cluster, PLR-1 is one of the earliest remaining representatives in C. *elegans* (Moffat et al. 2014; Bhat et al. 2015), whereas from the second cluster, the Goliath gene

family of E3 ubiquitin ligases evolved in *Drosophila* (Bouchard & Côté 1993). These genes have orthologues in many other vertebrates (Guais et al. 2006), such as *GREUL1* or *RNF128* in X. *laevis* (Borchers et al. 2002), c-*rzf* or *RNF13* in the chicken embryo (Tranque et al. 1996) and *G1RP* or *Rnf130* in mouse (Baker & Reddy 2000).

The *Drosophila* family is composed of only two members, *Goliath* and *Godzilla*, that exhibit strong homology to the human PA-RING members *Rnf130* and *Rnf167*, respectively (Yamazaki et al. 2013). *Goliath* was the first PA-RING member to be identified and was originally described as a developmentally important gene encoding a zinc-finger-motif protein involved in the regulation of gene expression during mesoderm formation (Bouchard & Côté 1993). Later, another E3 ligase was identified, Godzilla, displaying the same structural organisation as Goliath. Both proteins contain a PA domain that is located extracellularly and considered to be implicated in protein recognition (Mahon & Bateman 2000), in addition to a RING domain that is intracellular and contains six conserved cysteine and two histidine residues which coordinate Zn^{2+} ions and are essential for the ubiquitin ligase activity (Yamazaki et al. 2013). These ligases have been reported to act as key regulators of recycling endosome trafficking; they are expressed in endosomes, where they direct the ubiquitination of the v-SNARE protein VAMP3 and consequently inhibit transferrin receptor recycling (Yamazaki et al. 2013). Interestingly, this function is analogous to that of its human orthologue, *Rnf167*, which is similarly responsible for VAMP3 ubiquitination and degradation.

This does not represent the only case of evolutionary preservation of gene function among the PA-RING members in different species. For instance, the C. *elegans* orthologue of RNF43 and ZNRF3, PLR-1, also negatively regulates WNT receptor turnover and therefore inhibits the WNT signalling pathway (Moffat et al. 2014). This function has been associated with the regulation of the cellular response to WNTs during neuronal development in C. *elegans,* which is crucial for the establishment of the polarity of the nervous system (Bhat et al. 2015). In addition, PLR-1 lowers surface levels of the Frizzled co-receptors CAM-1/ROR and Lin28/RYK and targets them to endosomes, comparable to the function of its mammalian orthologues that are known to induce the internalisation of Frizzled together with its co-receptor, LRP.

In conclusion, these examples suggest that Goliath-related PA and RING domain-containing proteins have not only conserved their structural architecture but also their functional roles throughout evolution.

1.6.2 The mammalian PA-RING family

In mammals, the PA-RING family of E3 ubiquitin ligases consists of 12 transmembrane proteins divided into four distinct branches (Koo et al. 2012, **Figure 1.10 A**). As might be expected, most of its members are still poorly characterised and many aspects about them remain unexplored. However, there are a few exceptions, such as *RNF128*, *RNF13* and its homologue *RNF167* that, together with *RNF43* and *ZNRF3*, represent the most extensively characterised PA-RING members.

Rnf128, also known as *GRAIL* (gene related to anergy in lymphocytes) was firstly identified as a gene encoding an endosomal E3 ubiquitin ligase upregulated in anergized $CD4^+$ T cells (Anandasabapathy et al. 2003) and implicated in immune self-tolerance through the inhibition of cytokine production (Mueller 2004). The importance of RNF128 in the induction of T cell anergy was also demonstrated *in vivo* by showing that its constitutive expression leads to the development of an anergic phenotype in naïve $CD4^+$ T cells (Seroogy et al. 2004). An enzymatically inactive form of RNF128 was consistent in its ability to abrogate this induction process. These data suggest that the ubiquitination activity of RNF128 is required for the induction of tolerance in naïve T cells. In support of this, it was shown that RNF128 acts as a gatekeeper of unresponsiveness in T cells by promoting TCR-CD3 ubiquitination and degradation (Nurieva et al. 2010); $RNF128^{-/-}$ T cells are hyper-responsive to TCR stimulation and RNF128-deficient mice display an enhanced susceptibility to autoimmune diseases.

The juxtaposition of the PA and RING finger domains across the lipid bilayer was shown to be crucial for the molecular mechanism of action of RNF128. This spatial organisation is considered to be instrumental for the binding of transmembrane substrates of RNF128, which include the TCR complex and its costimulatory molecules, CD40 (Lineberry et al.

2008) and CD83 (Su et al. 2009). It is proposed that the PA domain serves as an extracellular recruitment platform to capture the target, which is then subsequently ubiquitinated by the intracellular RING domain.

In terms of other members of the family, *Rnf13* and *Rnf167* are homologous genes that encode endosomal membrane proteins involved in intracellular vesicular trafficking (Lussier et al. 2012; Zhang et al. 2013). In particular, *Rnf13* regulates SNARE complex assembly by ubiquitinating the SNARE-associated protein, Snapin (Zhang et al. 2013), while *Rnf167* acts as a negative regulator of cellular endosome trafficking by targeting the SNARE protein VAMP3, analogous to its orthologue in *Drosophila* (Yamazaki et al. 2013). Both ligases are targeted to endosomal membranes by their PA domain and point mutations that affect their cellular localisation can be detected in a number of human tumours (van Dijk et al. 2014); nevertheless, the most frequent mutations in *RNF13* and *RNF167* result in loss of function of their ligase activity. Recently, it has been observed that *Rnf13* mutant mice are prone to develop a high number of metastatic foci in the lungs (Cheng et al. 2015), hence, it can be hypothesised that this protein and its homologue may function as tumour suppressors similar to their paralogues *Rnf43* and *Znrf3*.

Besides the members described so far, the PA-RING family comprises several other proteins; however, the information available on them is still rather limited. Some members have been linked to certain pathologies, such as pulmonary diseases and urinary bladder cancer in the case of *Rnf150* (Press 2015; Zaravinos et al. 2011) or Barrett's Oesophagus in the case of *Rnf130* (Wang et al. 2014). Two other ligases, *Rnf148* and *Rnf133*, have been associated with the process of sperm maturation (Anon 2014; Liu et al. 2013; Nian et al. 2008), whereas the *Rnf43* homologue *Rnf215* has not been characterised yet. A general summary of the mammalian PA-RING proteins can be found in **Table 1.1**.

In light of this, it becomes clear that many questions are still open and many aspects of members of this family are worth investigating. For example, the majority of PA-RING proteins have not been linked to the regulation of any particular signalling pathway yet, most of their targets remain unknown, and in many cases their *in vivo* function has never been addressed. It has to be acknowledged, though, that potential genetic redundancy could represent a limiting factor in the study of members belonging to the same gene

family, as exemplified by the case of *Rnf43* and *Znrf3*: adenoma formation could be observed only when ablating both genes in parallel in the murine intestine (Koo et al. 2012). It is therefore not unreasonable to speculate that PA-RING family members may differ in their target specificity and physiological role, but it is likely that their mechanism of action in regulating the abundance of membrane proteins has been preserved throughout evolution.

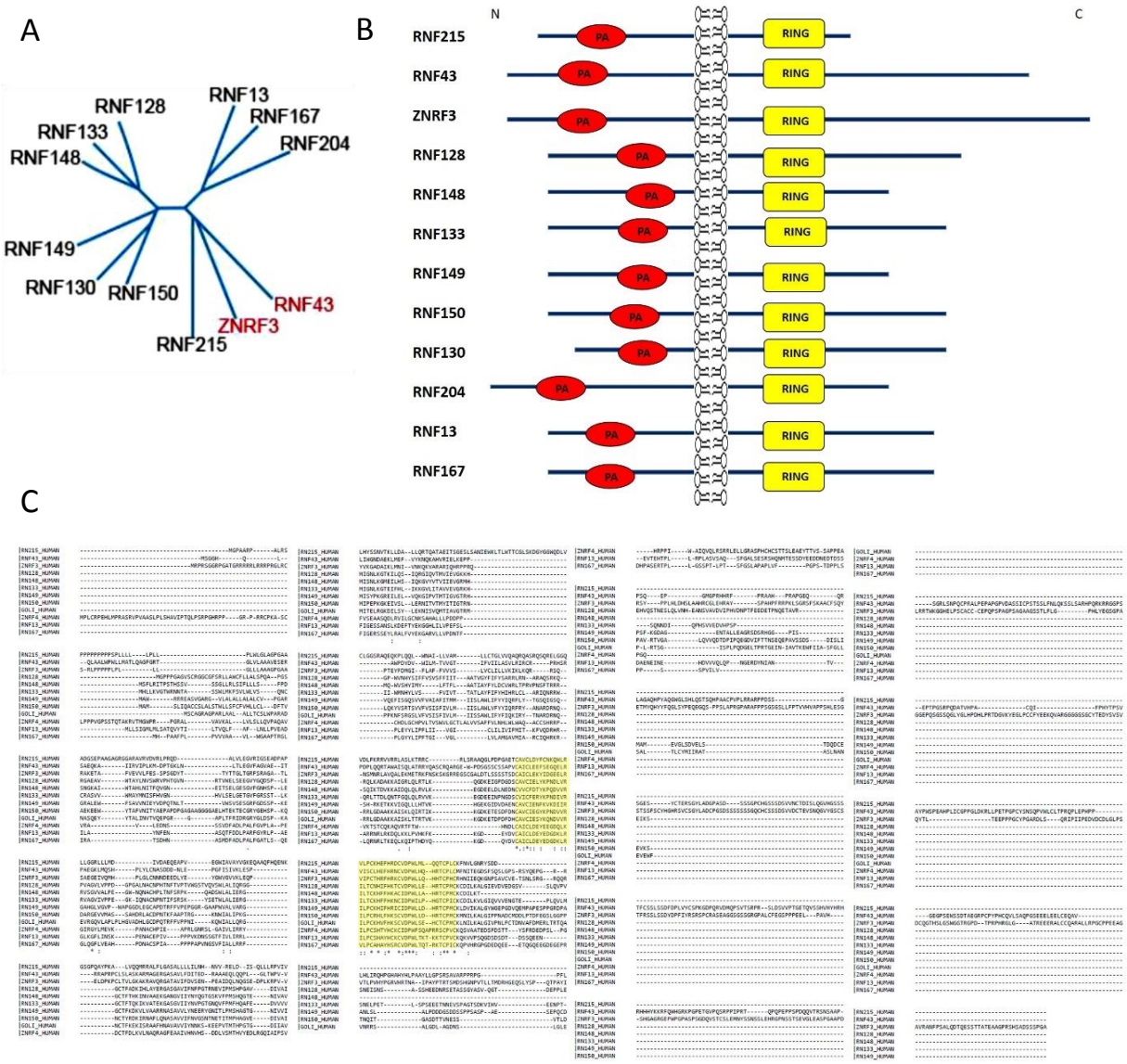

Figure 1.10 The PA-RING family of E3 ubiquitin ligases. **A)** Phylogenetic tree of the newly identified members of the PA-RING family in humans (Koo et al. 2012). **B)** Schematic representation of protein domain organisation of PA-RING family members, where PA is the protease-associated domain. **C)** Sequence alignment of all PA-RING members, where the RING domain is highlighted in yellow (ClustalW2).

Table 1.1 Summary of reported traits of PA-RING family members.

	Tissue Expression*	**Cellular Localisation ****	**Targets**	**Putative Role**	***In vivo* model**
RNF215	n/a	n/a	n/a	n/a	n/a
RNF150	n/a	n/a	n/a	Common differentially expressed gene in urinary bladder cancer.	n/a
RNF130	Broadly expressed. Upregulated in complete H-mole tissues and in Barrett's Oesophagus samples.	n/a	n/a	Originally identified in *Drosophila* as a transcription factor involved in the formation of the mesoderm in the embryo. Transcription factor involved in apoptosis in the mouse.	n/a
RNF149	Broadly expressed.	n/a	BRAF	Attenuation of the increase in cell growth induced by wild-type BRAF. Associated with FDG uptake in PET and survival in patients with resected non-small cell lung cancer.	n/a
RNF148	Testis and low expression in pancreas.	n/a	n/a	Testicular interstitial gene. Its expression is regulated by histone deacetylases.	n/a
RNF133	Expressed during spermatogen-esis.	ER localisation	n/a	May play a role in sperm maturation.	n/a
RNF128	High in the SI, liver, kidney, muscle and bone marrow.	Endo-membrane system	TCR-CD3, CD40, CD83, CD151, TBK1	Negative regulator of the T-cell receptor, role in haematopoiesis. Mutations associated with chronic kidney disease.	KO mice develop auto-immune disease

RNF13	Broadly expressed, overexpressed in pancreatic cancer.	Late endosomes	Snapin	Assembly of the SNARE complex, mediation of ER stress-induced apoptosis through the IRE1α-TRAF2-JNK signalling pathway.	KO mice show accelerated muscle regenerati-on and enhanced metastasis.
RNF167	Broadly expressed.	Endo-membrane system	AMPAR, VAMP3, Arl8B	Selective regulator of AMPAR-mediated neurotransmission. Abrogates recycling endosome trafficking, regulates lysosome positioning.	n/a
RNF204	n/a	ER localisation	Calnexin	Regulator of Calnexin turnover and ER homeostasis.	n/a

* Information from the EMBL-EBI Expression Atlas.

** According to *COMPARTMENTS,* Subcellular localization database.

1.7 Aims of my PhD

In recent years, RNF43 emerged as an important negative regulator of the WNT signalling pathway. It is a transmembrane E3 ubiquitin ligase localised at the plasma membrane, where it promotes ubiquitination and subsequent degradation of the WNT receptor Frizzled and its co-receptor LRP. RNF43 activity acquires a prominent role in the murine small intestine where it prevents uncontrolled expansion of the stem cell compartment and significantly contributes to tissue homeostasis. However, despite this crucial role in the fine regulation of the WNT pathway, the precise regulatory mechanisms of RNF43 remain poorly understood.

For this reason, during my PhD I aim to elucidate details of the precise mechanism of action of RNF43, beginning with the identification of genes with a functional connection to RNF43 itself by using a new screening strategy that combines CRISPR/Cas9 technology and

intestinal organoid culture. The use of this screening strategy with RNF43 provides a paradigm for other PA-RING proteins; for instance, different members could exhibit similar functions as regulators of transmembrane proteins such as, e.g., signalling receptors.

The identification of this novel gene family has opened up various questions and possible lines of investigation, some of which my thesis proposes to address by studying the potential involvement of other PA-RING members in the regulation of the WNT pathway, as well as other signalling pathways, and the identification of PA-RING members' targets.

Tackling these points, in combination with the identification of genes functionally related to RNF43, will help us potentially gain new insights into the WNT signalling pathway and broaden our understanding of the specificity and mechanism of action of each of these novel E3 ligases.

To summarise, my thesis has the following specific aims:

1) The identification of novel genes that are involved in the mechanism of action of RNF43, and the subsequent characterisation of their role both *in vitro* and *in vivo*, in order to understand in detail the molecular mechanisms through which RNF43 promotes Frizzled endocytosis and degradation;

2) The characterisation of additional PA-RING family members, in order to:
   - assess whether there are any other members of this family that are involved in the WNT signalling pathway in addition to RNF43 and ZNRF3
   - identify novel targets for selected PA-RING family members.

Chapter 2

Materials and Methods

2.1 Materials

2.1.1 Devices, consumables and chemicals

Devices, consumables and chemicals are listed in **Tables S1** and **S2** of Appendix A.

2.1.2 Kits and enzymes

All Kits and enzymes used are listed in **Tables S3** and **S4** of Appendix A.

2.1.3 Plasmids

All DNA constructs used are listed in **Table S5** of Appendix A.

2.1.4 Cloning and genotyping primers

Primers for cloning and PCR genotyping are listed in **Tables S6 – S10** of Appendix A.

2.1.5 RT-qPCR primers

Primers for RT-qPCR are listed in **Tables S11** of Appendix A.

2.1.6 Primary/Secondary Antibodies

Primary and secondary antibodies with relative dilution factors are listed in **Tables S12** of Appendix A.

2.2 Methods

2.2.1 Vector generation

PiggyBac constructs for dox-inducible RNF43 overexpression

In order to generate pBhCMV-hRNF43-mCherry, pPB-CAG-rtTA2ACas9_Neo and pPB-CAG-rtTA_Hyg, cDNAs of human RNF43, S. pyogenes WT Cas9 and Hygromycin resistance were PCR-amplified using Phusion® High-Fidelity Polymerase (NEB) and cloned into PiggyBac-based vectors containing inducible tet-responsive transgenes using the In-Fusion® HD Cloning Kit (Clontech) according to manufacturer's instructions. RNF43 and rtTA expression constructs were always transfected in combination with the Super PiggyBac Transposase expression vector in a 2:2:1 ratio. All the PiggyBac plasmids were a kind gift from Prof. Austin Smith's laboratory.

Vectors for inducible overexpression of PA-RING family members

To obtain vectors for inducible overexpression of the other PA-RING family members, their cDNAs were cloned into pcDNA™4TO (Thermo Fisher) by In-Fusion cloning; the peculiarity of this vector is the presence of Tetracycline operator sequences that are recognised by the Tet repressor in T-REx™-293 cells.

Similarly, these cDNAs were cloned downstream of the floxed dsRed cassette in the retroviral vector pMSCV-loxp-dsRed-loxp-3xHA-Puro-WPRE (Addgene).

Generation of CRISPR concatemer vectors for multiple gene KO

Single guide RNAs for CRISPR knockout were designed using the Zhang lab webtool (http://crispr.mit.edu/) and their sequences modified by the addition of specific overhangs for cloning into MSCV-puro concatemer vectors (Andersson-Rolf et al. 2016).

As a first step, oligos were pooled together in one reaction for their annealing and phosphorylation by T4 PNK and T4 DNA ligases (NEB) with the following thermocycler settings: 37°C for 30 minutes, 95 °C for 5 minutes, ramp down to 25 °C at 0. 3 °C/minute and 4 °C. Generation of 2 gRNA-containg MSCV vector was achieved by Golden Gate cloning as described in Ran et al., 2013. For incorporation of 3 and 4 gRNAs, annealed oligo mix was diluted 1:100 and Golden Gate cloning was performed with the following settings: 37°C for 5 minutes and 21°C for 5 minutes for 50 cycles, then 37°C for 5 minutes and 4°C.

All cloning reactions were treated with Plasmid-safe exonuclease (Cambio) for 30 minutes at 37°C and other 30 minutes at 70°C.

Concatemer vectors were used in a 1:1 ratio with a WT Cas9 expression plasmid (Addgene).

Generation of Daam1 expression vectors

Human *DAAM1* cDNA was purchased from TransOMIC, PCR-amplified using Phusion® High-Fidelity Polymerase and cloned into pcDNA4TO backbone with different tags via In-fusion cloning.

Generation of gRNA expression vectors

A vector from the Church lab containing a gRNA to target GFP (Addgene) was used as a template in an inverse PCR reaction using Phusion® High-Fidelity Polymerase. The aim was to exchange the pre-existhing gRNA with a new one. The PCR mix was then digested with DpnI (NEB) for 2 hours 37°C. Ligation was performed with T4 DNA Ligase (NEB) for 1-2 hours at room temperature.

All reaction mixtures were directly used for transformation into either 10G (Cambridge Bioscience) or Stellar (Takara) competent bacteria, DNA was purified using a Miniprep kit (Qiagen) and plasmids were checked by restriction digest and Sanger sequencing. Once the success of the cloning was confirmed, DNA was purified with a Plasmid Midiprep kit (Qiagen). See **Tables S6-8**, **S13** and **S4** of Appendix A for information about cloning primers, PCR programs and enzymes respectively.

2.2.2 Cell culture

Cell lines

Mouse embryonic stem cells (E14Tg2a) were cultured feeder-free on 0.1% gelatin-coated dishes in in Serum-LIF medium supplemented with 2i (CHIRON + PD03) without antibiotics or alternatively, in basal N2B27 medium supplemented with 2i.

Platinum-E cells (Cell Biolabs) were grown in DMEM + 10% FBS and Penicillin-Streptomycin in the presence of Puromycin (1 µg/ml) and Blasticidin (10 µg/ml).

T-REx™-293 cells (Life Technologies) and **HEK293 cells** (SCI TC facility) were cultured in DMEM + 10% FBS and Penicillin-Streptomycin, supplemented with 10 µg/ml Blasticidin only in case of T-REx™-293 cells.

HS27 human skin fibroblasts (SCI TC facility) were grown in GMEM (Sigma) supplemented with 1x non-essential amino acids (Life Technologies), 1 mM sodium pyruvate, 2 nM L-Glutamine (Life Technologies), 50 µM β-mercaptoethanol (Sigma) and 10% FBS.

Cells were mitotically inactivated for 3 hours at 37°C with 10 µg/ml Mitomycin C (Sigma).

All cells were kept in a tissue culture incubator at 37°C and 5% CO_2 and split in a variable ratio depending on confluency every 2-4 days. All cultures were mycoplasma free.

See **Table S14** of Appendix A for medium composition.

Cell transfection by lipofection

Transfections were performed using the Lipofectamine2000 Transfection Reagent (Invitrogen) following the manufacturer's instructions, when cells reached 60-70% of confluency. Medium was replaced the day after.

Cell transfection by electroporation

Mouse ESC were resuspended in phosphate buffered saline without calcium and magnesium (Sigma) and mixed with a total of 50 µg of DNA per 10^6 cells. The mixture was transferred to a 4 mm cuvette (Biorad) and electroporation was performed using the Gene Pulser XCell electroporation system (Biorad) with the following settings: 240 V, 500 uF, unlimited resistance.

Following drug selection, single colonies were picked into 96-well plates and cells were subsequently lysed with freshly-made lysis buffer for 2 hours at 56°C (see **Table S16** of Appendix A for lysis buffer composition). Clones were genotyped by long-range PCR using LongAmp polymerase (NEB) following manufacturer's protocol.

Isolation of single clones by cell sorting

To obtain clonal populations of HEK293, cells were washed twice in PBS and filtered through a 70 µm cell strainer and sorted into 96-well plates as single cells on a Beckman Coulter high-speed MoFlo cell sorter. Clones were lysed and genotyped as described above.

ESC rederivation

Embryos at E2.5 stage were flushed out of the oviduct using a syringe with a blunt needle with M2 medium (Sigma) containing Penicillin-Streptomycin. Embryos were transferred by mouth pipetting to a 35 mm culture dish containing pre-equilibrated BlastAssist medium (Origio) supplemented with 2i and incubated at 37°C for 3 days.

After blastocysts had hatched (E5.5), embryos were moved to 4-well dishes, previously coated with a layer of inactivated human fibroblasts, and culture medium was changed to 2i-Lif with Penicillin-Streptomycin. Embryos were kept in the incubator at 37°C for 10 to 14

days until trophectoderm cells attached to feeders, allowing inner cell mass (ICM) outgrowth. When the ICM outgrew into a primary colony, this was mechanically split into fragments using a pulled glass pipette. The subsequent dissociation of ICM-derived colonies into single cells was performed by Accutase treatment for 5 minutes at 37°C and cells were transferred to 6-well plates for expansion. Cultures were then adapted to feeder-free conditions within two passages and cells were genotyped as previously described.

ESC retroviral transduction

Platinum-E cells were transfected with 9 μg of the retroviral expression vector pMSCV-puro (Clontech) containing single gRNAs against *Daam1* and *Daam2*. After two days, viruses were harvested by passing the media through a 0.45 μm filter and viral supernatant was mixed with 4 μg/ml Polybrene and added to newly-derived ESC plated on Laminin (Sigma) for overnight incubation. After 24 hours the viral mixture was discarded, cells were washed in PBS and their media changed to 2i-Lif. Culture media was supplemented 2 days later with Puromycin (1 μg/ml) for selection of transduced cells.

2.2.3 Organoid culture and genetic manipulation

Intestinal crypt isolation

Mice were dissected to collect the small intestine from the cecum to the stomach. Crypts derived from duodenum, jejunum and ileum were used to establish organoid culture.

Firstly, the intestine was flushed by a 10 ml syringe with pre-chilled PBSO (without Calcium and Magnesium), cut longitudinally and spread open by using forceps.

Villi were removed by gently scraping the intestine with a coverslip, 5 mm pieces were obtained and transferred to a 50 ml tube with pre-chilled PBS0. The remaining villi were washed away by vigorous shaking. Then the tissue was incubated 15 minutes on a rocking platform with 25ml of Gentle Cell Dissociation Reagent (Stem Cell Technologies) and enrichment for crypts in solution was confirmed by checking a drop under the microscope. The solution was spun at 1200 rpm for 3 minutes and pellet resuspended in 1 ml of PBS0.

After spinning at 500 xg for 5 minutes, Matrigel was added to the pellet considering 20 µl of matrix per well and approximately 50-100 crypts were seeded in each well of a pre-warmed 48-well plate. The plate was incubated at 37°C for 10 minutes to let the Matrigel solidify and 250 µl of WENR+Nic medium added on top.

Organoid culture and maintenance

Murine intestinal organoids were derived from small intestinal crypts of WT, VillinCreERT2 and RZ-DKO VillinCreERT2 mice and embedded in Matrigel. Culture media was refreshed every 2-3 days and organoids were split with a 1:3 ratio every 6-7 days. For passaging, Matrigel domes were disrupted and organoids were mechanically fragmented into single-crypt domains which were spun at 600 xg for 5 minutes. The pellet was resuspended in fresh Matrigel and seeded in pre-warmed 48-well tissue culture plates (for culture medium composition see **Table S15** of Appendix A).

Organoid transfection by lipofection

Organoids were cultured at high density in WENR+Nic media in preparation to this procedure so that they displayed a cystic morphology and contained a higher number of stem cells. Organoids were mechanically disrupted and spun at 900 xg for 5 minutes; the pellet was resuspended in TrypLE Express and incubated at 37°C for 5 minutes. The dissociation process was terminated by adding 500 µl of EN media supplemented with Y-27632 (Rho-Kinase inhibitor) and CHIRON without antibiotics and fragments were spun at 900 xg for 5 minutes (for EN medium composition see **Table S15** of Appendix A). In parallel, two separate mixes containing 50 µl Opti-MEM Reduced Serum Medium (Gibco) plus 4 µl of Lipofectamine 2000 or 1.6 µg of DNA were prepared and incubated for 5 minutes at room temperature; they were then pooled together and incubated for 30 minutes. This Lipofectamine-DNA mixture was combined with 100 µl of cell suspension in a 48-well tissue culture plate and then spinouculated at 32°C, 600 xg for 1 hour. This was followed by another 6 hour incubation at 37°C, after which the mix was spun at 500 xg for 5 minutes. The pellet was resuspended in 20µl of Matrigel and seeded in one well of a pre-warmed

48-well tissue culture plate. WENR+Nic media supplemented with Y-27632 was overlaid. Selection of transfected organoids with 100 µg/ml Hygromycin B started 2-3 days later.

Organoid transfection by electroporation

Two days prior to electroporation, culture media was changed from WENR+Nic to EN without antibiotics, supplemented with Y-27632 and CHIRON. Organoids were treated with 1.25% v/v DMSO 24 hours before electroporation and were subsequently dissociated into small clusters of 10-20 cells by TrypLE Express treatment for 3-5 minutes at 37°C. After spinning for 5 minutes at 500 xg, cells were counted and a minimum of 10^5 cells was used per condition. Organoid pellet was resuspended in 1 ml of BTXpress buffer (Harvard Apparatus) and mixed with a total amount of 10-20 µg of DNA. The cell-DNA mixture was then transferred to the cuvette and electroporation performed according to the following settings using the NEPA21 Super Electroporator (NEPA Gene):

	Poring pulse	**Transfer pulse**
Voltage	175 V	20 V
Pulse length	5 msec	50 msec
Pulse interval	50 msec	50 msec
Number of pulses	2	5
Decay rate	10%	40%
Polarity	+	+/-

This was followed a 30 minute incubation with 400µl BTXpress buffer + Y-27632 to allow cells to recover, after which they were spun at 400 xg for 3 minutes. Then the pellet was resuspended in Matrigel and EN medium supplemented with Y-27632, CHIRON and DMSO was overlaid. After 24 hours medium was changed to EN + Y-27632 + CHIRON and 4-5 days later normal organoid medium was applied.

Isolation of single organoids by manual picking

After drug selection, single organoids were manually isolated in safety cabinet under a light microscope. Matrigel was gently disrupted without damaging the organoids that were pooled together in a Petri dish containing DMEM/F-12 supplemented with HEPES (10mM), L-glutamine (20mM) and Penicillin-Streptomycin (1x). Single organoids were aspirated in the tip of a p20 pipette and placed into a 1.5 ml tube containing 10 µl of WENR+Nic + Y-27632 medium. Organoids were then seeded directly in a 48 well plate by adding 10 µl of Matrigel and pipetting up and down to fragment single organoids into pieces. WENR+Nic + Y-27632 medium was overlaid when Matrigel had solidified and refreshed every 2 days.

Organoid retroviral transduction

Virus production. Platinum-E cells were transfected with 24 µg of the retroviral vector pMSCV-loxp-dsRed-loxp-3xHA-Puro-WPRE (Addgene) containing the cDNA of PA-RING family members. After two days, viruses were harvested by passing the media through a 0.45µm filter and spinning it at 8000 xg at 4°C for 12 hours. The next day, the supernatant was discarded and the pellet was resuspended in transduction medium: WENR+Nic supplemented with Y-27632 and polybrene (8µg/ml).

Organoid fragmentation. Organoids were mechanically disrupted and spun at 900 xg for 5 minutes. Pellet was then resuspended in TrypLE Express and incubated at 37°C for 5 minutes. The dissociation process was terminated by adding 500 µl of WENR+Nic medium and fragments were spun at 900 xg for 5 minutes and the pellet was resuspended in transduction medium.

Viral transduction. The organoid fragments were combined with the retroviral suspension in a 48-well tissue culture plate and then spinouculated at 32°C, 600 xg for 1 hour. This was followed by another 6 hour incubation at 37°C, after which the mix was spun at 900 xg for 5 minutes. The pellet was resuspended in 50µl of Matrigel and seeded in one well of a pre-warmed 48-well tissue culture plate. Transduction media without polybrene was overlaid. Two/three days after transduction, selection of infected organoids with 1 µg/ml Puromycin began. After they reached full size, culture media was changed to ENR + Puromycin so that they could regain their budding structures within two weeks. Expression of the gene of

interest was induced with 1µM 4-hydroxytamoxifen (4-OHT) for 12 hours and then culture conditions were changed to EN (RSPO withdrawal).

2.2.4 Other techniques and assays

Quantitative RT-PCR

Total RNA was extracted from HEK293 and mESC using RNeasy Mini kit (Qiagen) and from intestinal organoids using RNeasy Micro kit (Qiagen). On-column DNase digestion was performed to avoid contamination from genomic DNA and 1 µg of RNA was retro-transcribed using M-MLV Reverse Transcriptase (Promega). Quantitative RT-PCR reactions were run in triplicates or quadruplicates using iQSYBR Green Supermix (Biorad) according to the manufacturer's instructions. Average gene expression was normalized the reference gene GAPDH.

Immunofluorescence

Cells were washed twice with PBSO and fixed in 4% PFA for 20 minutes at room temperature. Then they were permeabilised in 0.2% Triton X-100 (Sigma) for 15 minutes and blocked in 5% donkey serum (Sigma) and 0.1% Triton X-100 or in 10% BSA (Sigma) for 1 hour at room temperature. Primary antibody was incubated overnight at 4°C and the excess was washed away on the following day, prior to incubation with secondary antibody for 1 hour at room temperature. DAPI (Sigma) was added while performing the final washes in PBS and cells were mounted in RapiClear (Sunjin lab).

Image acquisition

Images of intestinal organoids and HEK293 cells were acquired with the Evos *fl* inverted digital fluorescence microscope, equipped with the following lenses and filters: 10x (AMG, 10x Plan AMEP-4632) dry objective, 20x (AMG, 20x Plan FL AMEP-4624) dry objective; filters for DAPI, GFP, RFP and Texas Red. Confocal microscopy was instead conducted on mESC using the software LAS AF and Leica SP5 TCS confocal microscope.

Flow cytometry

Cells were pelleted 2 days after transfection, resuspended in 200 µl of ice-cold FACS buffer (0.1% BSA PBS) and incubated with primary antibody on ice for 45 minutes. Cells were then washes twice with 200 µl of ice-cold FACS buffer and incubated on ice with secondary antibody for 30 minutes. After two washes, pelleted cells were resuspended in 500 µl of ice-cold FACS buffer, filtered and analysed using the BD LSRFortessa™ cell analyser. Subsequently, data were analysed with the FlowJo software.

Western blotting

Cells were lysed on ice for 30 minutes in a buffer containing complete protease-inhibitor cocktail tablets (Roche) and centrifuged at maximum speed for 30 minutes at 4°C. Protein concentration was measured using Pierce™ BCA Protein Assay Kit (Thermo Fisher) and equal amounts were loaded on polyacrylamide gel and run at 140 V for 1.5 hours. Proteins were subsequently transferred to an Immobilon-FL PVDF 0.45 µm membrane (Millipore) using the Trans-Blot® Turbo™ Transfer apparatus (Biorad) and the membrane was blocked for 1 hour with a 5% milk blocking buffer at room temperature. This was followed by an overnight incubation in primary antibody solution at 4°C. The membrane was then washed, secondary antibody was applied for 1 hour at room temperature and detection was performed using ECL prime Western blotting Detection system (GE Healthcare). See Tables **S17-18** of Appendix A for Western blot buffer composition.

Immunoprecipitation

Two days after transfection, cells were treated with 10 mM MG132 (PeptaNova) for 4-6 hours to inhibit proteasome activity. On the next day, cells were harvested and lysed on ice as previously described. Then 15 µl of Protein G Resin (Invitrogen) were incubated with 1 µl of 4 µg/µl mouse monoclonal antibody for 1 hour at 4°C. After washing, the bead/antibody conjugate was incubated with the cell lysates at 4°C overnight. The resin was then washed 5 times with lysis buffer before elution in 15 µl of 5X Laemli buffer. Samples were kept 95°C for 5 minutes and analysed by Western Blot.

Ubiquitination assay

HEK293T cells were transfected 2 days prior to analysis with HA-Ubiquitin and V5-Frizzled5 constructs. Frizzled5 was then pulled down using V5-bound Protein-G-sepharose beads (Invitrogen) and its ubiquitination levels assessed by Western Blot against HA.

Endocytosis assay

Subcellular localization of SNAP-tagged Frizzled5 (SNAP-FZD5) was analysed in DAAM KO HEK293 cells compared to WT cells, with or without RNF43 co-expression. Surface SNAP-FZD5 was labelled with SNAP-Alexa549 (NEB) for 15 minutes at room temperature in the dark, cells were washed and the labelled receptor was chased for 30 and 120 minutes.

Surface Proteome Analysis

Dox-inducible E3-overexpressing T-REx™-293 cells were treated overnight with 1 µg/ml doxycycline (Sigma) to induce overexpression of the E3 ubiquitin ligase of interest. Samples were prepared in triplicate and surface proteins from were enriched by using Pierce Cell Surface Protein Isolation Kit (Thermo Fisher) according to manufacturer's instructions; surface proteins were first labelled with Sulfo-NHS-SS-Biotin, cells were then lysed and Biotin-labelled surface proteins were affinity-purified by a using NeutrAvidin agarose resin. The resin was extensively washed with PBS to remove traces of detergents, before biotinylated proteins were eluted by incubating the resin for 1 hour at room temperature with 5 mM dithiothreitol (DTT) and 0.5% RapiGest SF surfactant (Waters) in 50 mM ammonium bicarbonate. A second and third elution were obtained by incubating the resin with 8 M urea/ 2M thiourea and 5 mM DTT in ammonium bicarbonate.

Each elution was handed over to the Proteomics Core facility of Masaryk University (Czech Republic) for alkylation with iodoacetamide, digestion with Lys-C (Promega) and overnight trypsin treatment. Each sample variant was analysed separately three times by nano-ultra performance liquid chromatography (LC)–tandem mass spectrometry (MS/MS) on an RSLCnano/Orbitrap-Elite system (Thermo Fisher) with a 90 minute LC gradient. MS was recorded by Orbitrap analyzer with a resolution of 60000 at 400 m/z; MS/MS, after Higher-energy collisional dissociation, was recorded by Orbitrap analyzer with a resolution of

15000 at 400 m/z. MS/MS data processing was performed using Proteome Discoverer™ software (version 1.4) and applying the following search algorithms: Mascot (version 2.4.1) and SEQUEST. UniProtKB-Human (version from 16.9.2015) was searched as a protein database and contaminant proteins were filtered out by referring to cRAP contaminant database (http://www.thegpm.org/crap). A minimum of one unique peptide and peptide identifications with q value <0.01 were considered for protein identification. Dox-treated samples were compared to non-treated samples and a ratio was calculated by dividing the normalized area for each protein in the Dox^+ samples by the Dox^- samples.

2.2.5 Mouse procedures

Mouse handling

Rosa26-floxed STOP-Cas9 mouse was imported from Jackson Laboratories. In this mouse line, Cre recombinase-dependent expression of Cas9 endonuclease is directed by a CAG promoter and, in combination with single guide RNAs and Cre, it can lead to gene disruption, as described in Platt et al., 2014.

This line was crossed with a VillinCre-ERT2 that expressed the Cre recombinase fused to the estrogen receptor under the Villin promoter. ESC were then rederived from Rosa26-floxed STOP-Cas9::VillinCre-ERT2 mice, infected with gRNAs against *Daam1* and *Daam2* and used to generate chimeras. In the chimeras, Cas9 expression was induced in mouse intestine by one intraperitoneal administration of 3 mg/20g mouse weight of Tamoxifen in corn oil (Sigma). Tamoxifen administration led to translocation of Cre-ERT2 into the nucleus and subsequent excision of the stop codon that prevents Cas9 expression.

All mouse breeding and experimental procedures were subjected to ethical approval and performed under the terms of the Animals (Scientific Procedures) Act, 1986. All mice were kept in pathogen-free conditions and all the work was performed according to the United Kingdom Home Office regulations.

Chimeric mouse generation

Chimeras were generated by blastocyst microinjection of newly-derived ESC by the Stem Cell Institute Transgenic Facility.

Intestine collection and preparation

Intestinal samples were obtained 7 and 14 days after tamoxifen injection. Mice were euthanized by cervical dislocation, dissected and the intestine removed for fixation in Formalin overnight at room temperature on a rocking platform. After fixation, samples were rinsed twice in PBS and kept in 70% Ethanol.

2.2.6 Immunohistochemistry

Samples were paraffin-embedded, sectioned and stained by the Stem Cell Institute Histology Core Facility.

Antigen retrieval was performed by boiling the slides for 15 minutes at 95°C in 0.01 M Citric Buffer (pH 6.0), and then slides were washed several times in PBS. Peroxidase Block was added on top for 5 minutes at room temperature, slides were again washed and incubated for 1 hour at room temperature with the blocking/permeabilisation solution (0.1% Tween/ 2% NDS). Primary antibody solution was applied overnight at 4°C, slides were then washed and incubated for 30 minutes with the polymer-HRP labelled secondary antibody (DAKO Envision Kit). This was followed by DAB colour development and finally sections were counterstained with Mayer's Haematoxylin, dehydrated and mounted.

Chapter 3

Development of an inducible system for the identification of RNF43-related genes

3.1 Aims of the chapter

RNF43 is an E3 ubiquitin ligase crucial for fine regulation of the WNT signalling pathway at the plasma membrane through ubiquitination of Frizzled. Because the precise molecular events of this process, including the regulation of RNF43, still need to be clarified, my aim is to identify novel genes that have a functional connection to RNF43; I believe that this represents the fundamental starting point in order to understand in detail how RNF43 is capable of controlling membrane clearance of the WNT receptor.

For this purpose, an alternative gene-screening approach was created which would in parallel provide functional information on the candidate genes; such a strategy required a system of inducible RNF43 overexpression, referred to here as iRNF43 for simplicity, in combination with CRISPR/Cas9 knockout of genes encoding putative interactors of the RNF43 intracellular domain.

In particular, the specific aim of this chapter is the establishment of a solid and reliable screening platform for the identification of functional partners of RNF43 which meets the following requirements:

1) The induction of RNF43 overexpression results in a clear phenotypic effect supposedly due to WNT pathway downregulation (e.g. changes in cell morphology, cell death); as this represents the readout of the system, it must not leave any room for misinterpretation.

2) Knockout of genes that are required for RNF43 function should counter the effect of its overexpression and be able to revert the phenotypic change associated with overexpression.

The next section will describe two different iRNF43 systems that have been generated and tested to establish the most appropriate screening platform.

3.2 Results

3.2.1 iRNF43 mESC-based screening platform

In order to capitalise on a previously described WNT-dependent system, mouse embryonic stem cells (mESC) were cultured in N2B27 medium supplemented with 10% WNT-conditioned medium and LIF (Leukaemia Inhibitory Factor), as it was previously reported that mESC can be maintained in an undifferentiated state under these conditions in a feeder-free culture by virtue of a synergistic action of WNT and LIF (Ogawa et al. 2006). Therefore, mESC cultured in this condition were initially considered as an ideal screening platform, since they represent a particularly convenient system for genetic screens,

including large scale screens, and also because the WNT/β-catenin pathway has been shown to play a major role in the maintenance of mESC pluripotency (ten Berge et al. 2011; Nusse et al. 2008). For instance, addition of WNT3a to mESC was reported to strongly promote their self-renewal and chemical inhibition of the WNT negative regulator GSK3 was seen to facilitate ESC pluripotency (Sato et al. 2004).
Based on these reports, I hypothesised that WNT pathway inhibition caused by RNF43 overexpression would make ESC lose their pluripotency.

In light of the above considerations, the first system established for the CRISPR/Cas9 knockout screen was a stable line of mESCs with constitutive expression of rtTA-Cas9 and doxycycline-inducible expression of *RNF43* together with a mCherry red fluorescent protein as a reporter. To generate this cell line the Tet-On method for inducible gene expression and the PiggyBac Transposon system were employed, as summarised in the schematic of **Figure 3.1**. The exploitation of this Transposon-based strategy for stable integration of transgenes into the genome offered several advantages over the more traditional lentivirus-based approaches, such as its time effectiveness, no limits in cargo capacity as wells as no need of producing viral particles beforehand.
In my system, *RNF43*-mCherry overexpression was triggered by the addition of doxycycline and within 4 days of doxycycline addition, it was possible to observe a dramatic cell morphology change in the WNT+LIF + dox condition (**Figure 3.2**): RNF43 overexpressing-ES colonies lost their round and domed shape to become flat and much less compact.
As a substantial body of literature shows that the role of the WNT/β-catenin pathway in both ESC pluripotency and differentiation is rather controversial (Kelly et al. 2011; Wray et al. 2011; ten Berge et al. 2011), I sought to probe more deeply what this morphological change meant. For instance, I speculated that the morphological changes observed in RNF43-overexpresisng cells could have been due to ESC differentiation caused by WNT pathway shutdown, as LIF alone was shown to be unable to sustain ESC pluripotency (Ogawa et al. 2004).

To thus determine if *RNF43* overexpression led to ESC differentiation, eGFP was targeted into the *Rex1* locus to generate eGFP knock-in iRNF43 ESC. *Rex1* is a commonly used marker

for naïve undifferentiated ES cells (Toyooka et al. 2008) that is rapidly downregulated at the onset of differentiation (Guo et al. 2011).

If overexpression of *RNF43* caused the morphological changes observed due to downregulation of WNT signalling and concomitant differentiation of the mESC colonies, as depicted in **Figure 3.3**, then I would expect doxycycline to induce a progressive reduction in Rex1-eGFP expression as the mESCs differentiate, concomitant with an increase in *RNF43*-mCherry expression. In this context, knockout of genes that are essential for the mechanism of action of RNF43 should prevent the loss of Rex1 expression in RNF43-overexpressing cells.

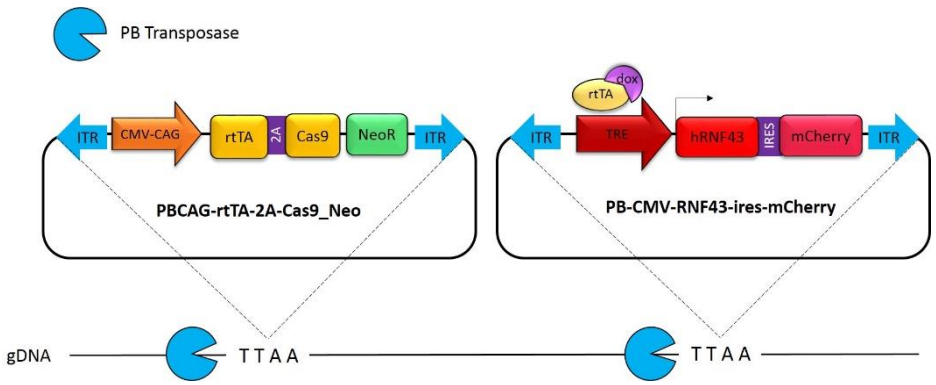

Figure 3.1 PiggyBac constructs for iRNF43-mCherry mESC generation. Schematic representation of the PiggyBac vectors used to generate a stable mESC line that constitutively expresses Cas9 and inducibly expresses RNF43-mCherry upon doxycycline treatment by exploiting the Tet-On system. In one vector, the Cas9 sequence is linked to the reverse tetracycline trans-activator (rtTA) by a 2A peptide sequence (left), while the other vector carries the human cDNA sequence of *RNF43* fused to the IRES-mCherry reporter downstream of the Tet-responsive element (TRE; right). When doxycycline is provided, it binds to the rtTA activator that can then translocate into the nucleus, bind to the TRE region and activate RN43-mCherry transcription. Use of the PiggyBac SuperTransposase allows random, stable integration of the constructs into the genomic DNA (gDNA).

However, when the system was investigated by both flow cytometry and confocal imaging this hypothesis was rejected as the majority of iRNF43-expressing ESC still retained Rex1-eGFP expression after 5 days under WNT+LIF + dox conditions in spite of morphology

changes (**Figure 3.4**). Furthermore, both treated and non-treated samples in WNT+LIF showed higher levels of background differentiation compared to the control (Serum+LIF + 2i: CHIRON + PD03, inhibitors of glycogen synthase kinase 3 and mitogen-activated protein kinase).

I speculated then that the observed morphological change might have been an effect of RNF43 overexpression on the non-canonical WNT PCP (Planar Cell Polarity) pathway; for instance, RNF43 was reported to also inhibit this β-catenin independent signalling branch that regulates cytoskeleton organisation (Hao et al. 2012).

These data, taken together, indicated that the iRNF43 ESC line was not a suitable platform for the CRISPR knockout screening because of the lack of a clear readout. Hence, it was needed to establish a different system, one in which the role of the WNT pathway was unequivocally crucial and well characterised.

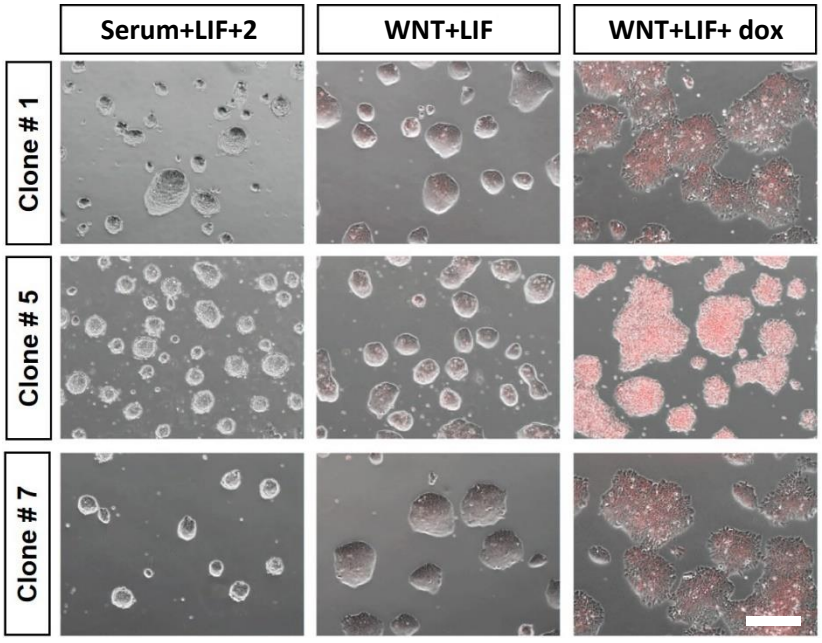

Figure 3.2 Doxycycline treatment test to iRNF43 mES clones. Three different iRNF43-mCherry ESC clones were subjected to doxycycline treatment. After 4 days, RNF43-mCherry expression is clearly detectable in all the cells under WNT+LIF + dox conditions. In particular, clone #5 shows a dramatic morphological change upon *RNF43* overexpression, whereas colonies retain an undifferentiated morphology in both control Serum+LIF+2i (SL2i) and WNT+LIF conditions. Scale bar =400 µm.

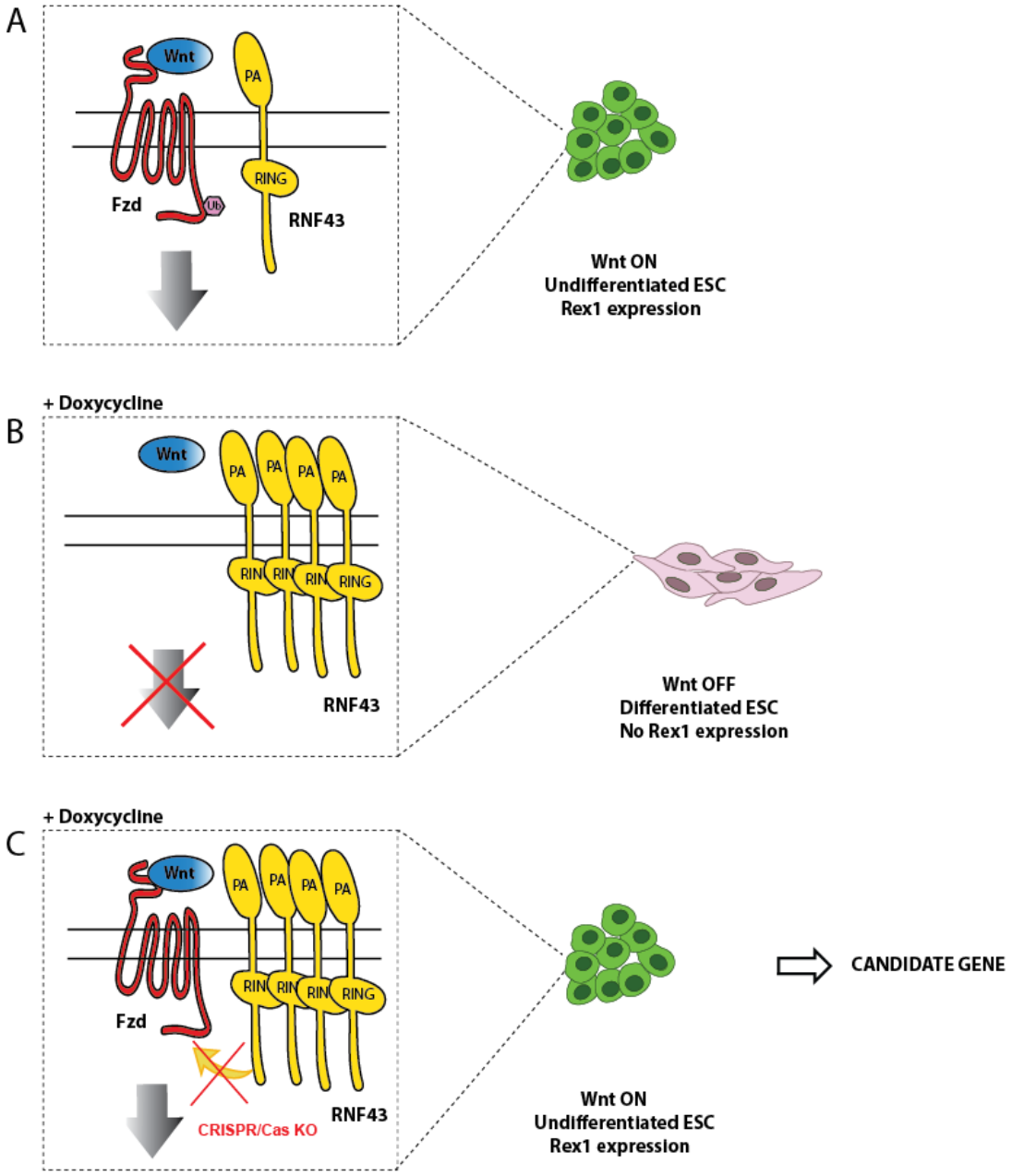

Figure 3.3 Working hypothesis for CRISPR/Cas9 screening in Rex1-GFP iRNF43 mESC. **A)** When Rex1-GFP iRNF43 ESC are cultured in WNT + LIF, the WNT ligand binds to its receptor Frizzled (Fzd), the signalling cascade is activated and cells present an undifferentiated morphology concomitant with Rex1-GFP expression. **B)** Upon doxycycline treatment, RNF43 is overexpressed and Fzd cleared from the cell surface, causing WNT signalling shut down. Since cells undergo profound morphology changes, we hypothesise they could be differentiating, which would result in loss of Rex1 expression. **C)** If doxycycline treatment leads to differentiation, performing knockout of genes that are functionally essential for RNF43 action could prevent the loss of undifferentiated morphology and Rex1 expression.

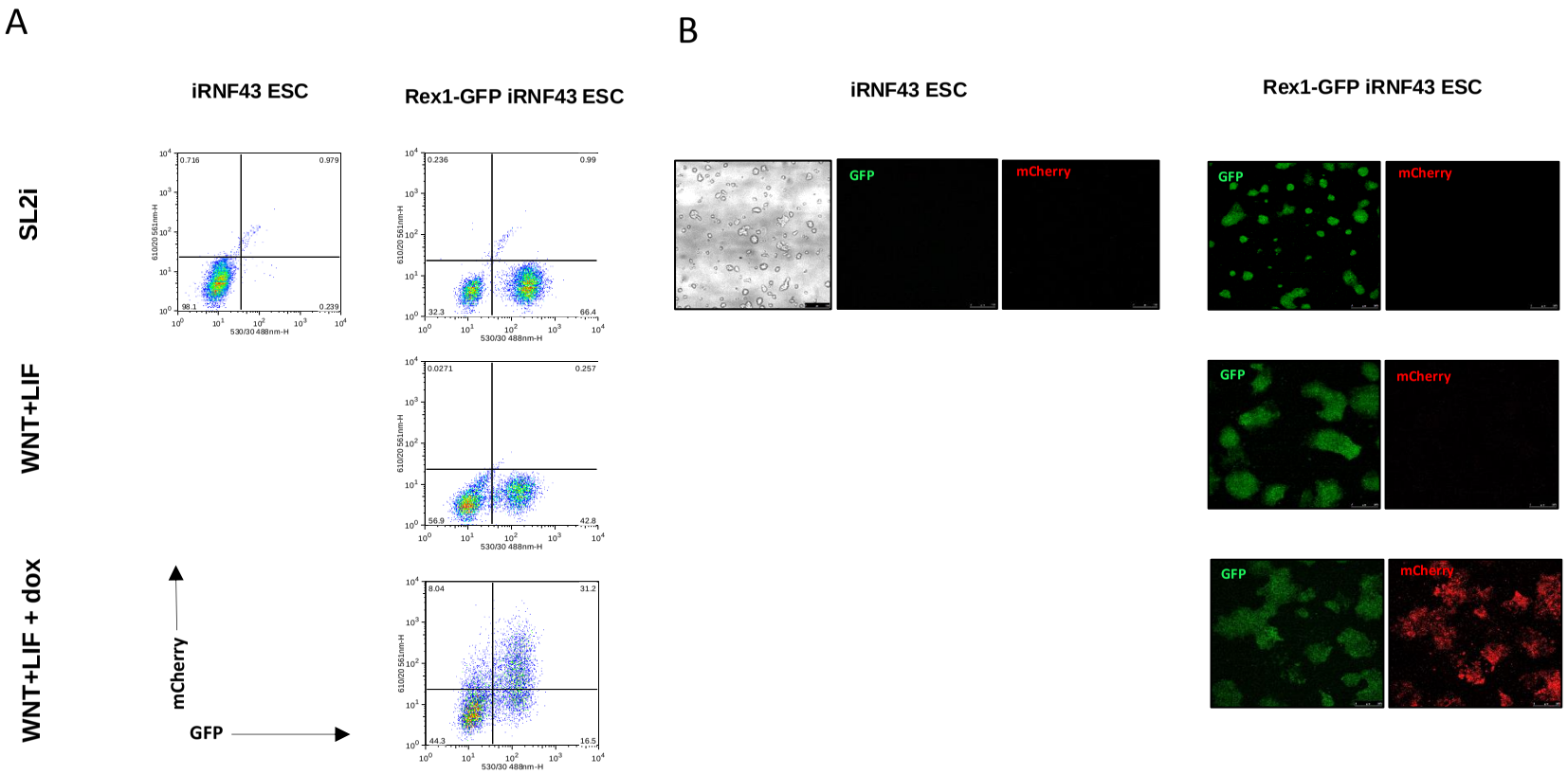

Figure 3.4 iRNF43 mES cells retain Rex1 expression after 5 days of doxycycline treatment. **A)** Flow cytometric analysis of Rex1-GFP iRNF43 ESC compared in three different culture conditions: Serum+LIF+2i (SL2i), WNT+LIF and WNT+LIF + dox. The non-targeted iRNF43 parental line cultured in SL2i serves as a negative control. Upon doxycycline induction only 8% of Rex1-GFP iRNF43 ES cells overexpresses RNF43-mCherry while downregulating the Rex1-GFP reporter ($mCherry^{+}GFP^{-}$). In addition, considerable levels of background differentiation (GFP^{-} cells) are present in both control conditions, SL2i and WNT-Lif. **B)** Confocal imaging confirms the same results: Rex1-GFP iRNF43 ES cells retain GFP expression in WNT+LIF + dox, despite their differentiating morphology. Scale bar=100 µm.

3.2.2 iRNF43 organoid-based screening platform

Based on the results obtained with iRNF43 ESC, I decided to focus on mouse intestinal organoids for my screening platform. Although less straightforward for screening purposes than ES cells, intestinal organoids are heavily dependent on WNT/β-catenin signalling for their maintenance and survival, and clear phenotypes in this system are associated with alterations in WNT pathway activity.

Therefore, a stable organoid line with doxycycline-inducible overexpression of RNF43-mCherry was generated in a manner similar to that of the iRNF43 ESC lines by exploiting the PiggyBac Transposon systems (**Figure 3.5**), and subjected to doxycycline treatment. After 36 hours, all induced organoids showed a strong and homogeneous expression of mCherry and no leaky mCherry expression could be detected in non-treated samples (**Figure 3.6**).

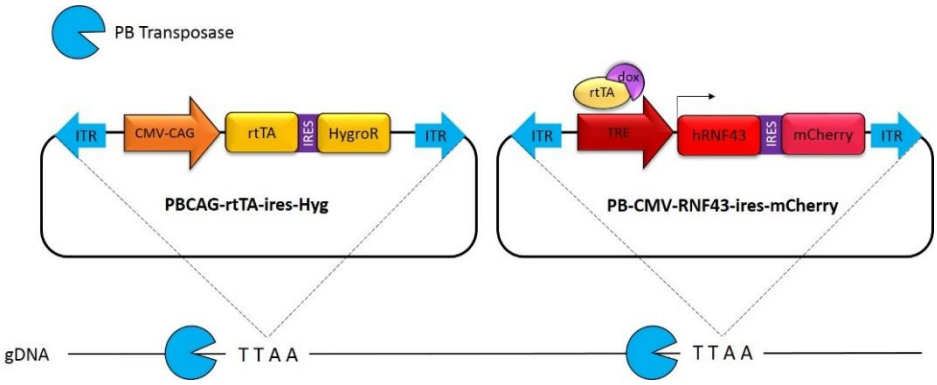

Figure 3.5 PiggyBac constructs for iRNF43-mCherry intestinal organoid generation. Schematic representation of the PiggyBac vectors used to generate a stable mouse intestinal organoid line that constitutively expresses the reverse tetracycline trans-activator (rtTA) and inducibly expresses RNF43-mCherry upon doxycycline treatment by exploiting the Tet-On system. The human cDNA sequence of RNF43 fused with the IRES-mCherry reporter is located downstream of the Tet-responsive element (TRE); when doxycycline is provided, it binds to the rtTA activator that can then translocate into the nucleus, bind to the TRE region and activate RNF43-mCherry transcription. Use of the PiggyBac SuperTransposase allows random, stable integration of the constructs into the genomic DNA (gDNA).

In line with the importance of WNT signalling in the maintenance of intestinal stem cells, it was anticipated that overexpression of the WNT pathway negative regulator RNF43 would reduce the viability of intestinal organoids. To test whether *RNF43* overexpression affected the viability of my system as predicted, organoids were cultured in doxycycline-containing medium for 3 to 5 days, passaged and maintained under these conditions until the culture was lost over time (**Figure 3.7**).

Since organoid death/ survival seemed to be a clear phenotypic readout for my genetic screening, I hypothesised that organoids depleted of RNF43 functional interactor genes would remain viable in doxycycline-containing medium, as outlined in the updated model in **Figure 3.8**. More specifically, depleting an essential component for the action of RNF43 should abolish Frizzled internalisation and so restore WNT activity levels back to normal. This will therefore allow organoids to survive even in the context of *RNF43* overexpression.

In summary, intestinal organoids with doxycycline-inducible overexpression of RNF43 proved to be a much more appropriate system for my screening platform development, as RNF43 overexpression could effectively cause organoid death, a clear phenotypic effect resulting from WNT pathway inhibition.

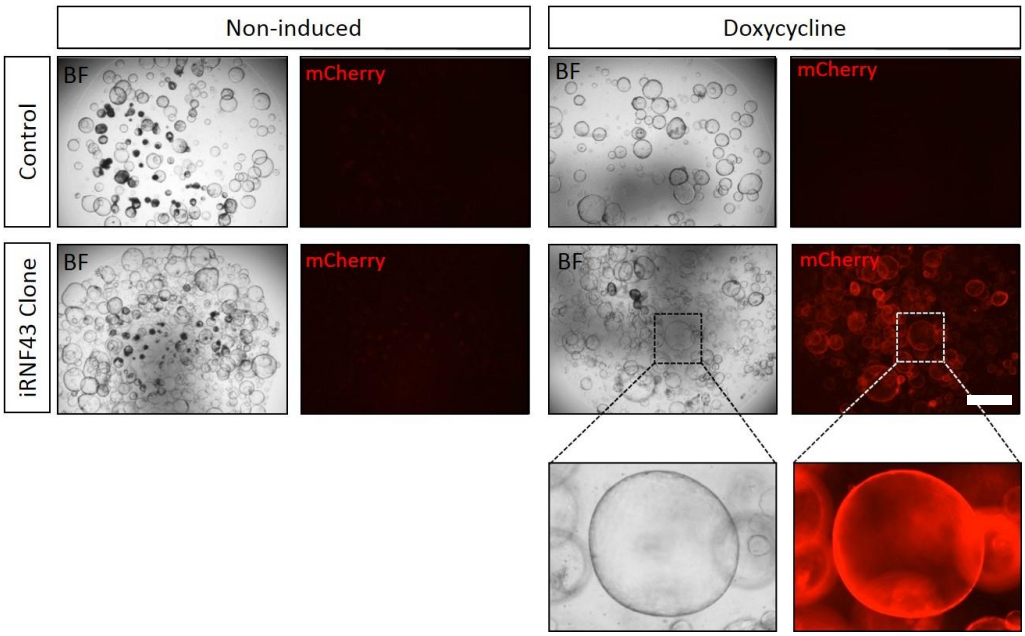

Figure 3.6 Doxycycline treatment test to iRNF43 mouse intestinal organoids. iRNF43-organoid clonal population showing strong and homogenous overexpression of *RNF43*-mCherry 36 hours after doxycycline treatment. No *RNF43* leaky expression can be observed in the non-induced organoids. Scale bar= 1000 µm.

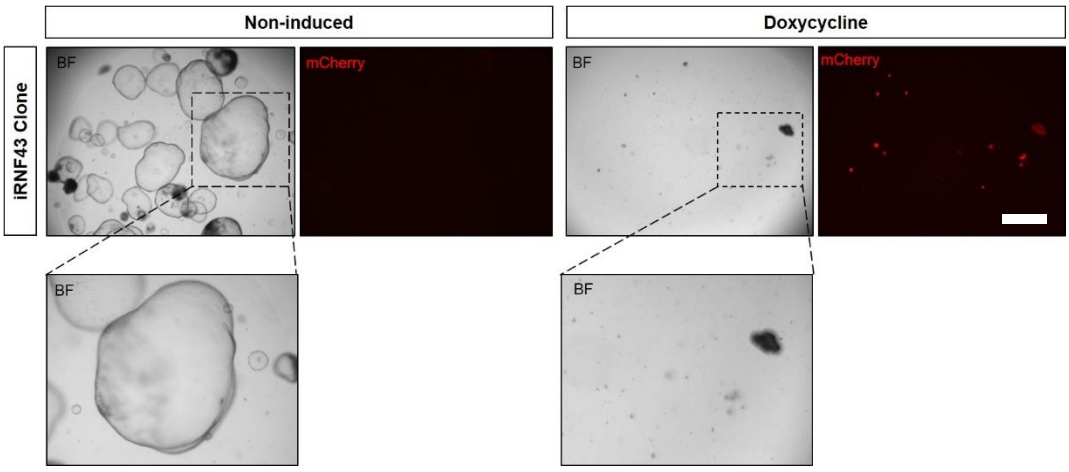

***Figure 3.7 iRNF43* intestinal organoids die after prolonged RNF43 expression.** After 3-5 days of doxycycline treatment, followed by passaging under the same culture conditions, iRNF43 organoids start showing a drastic reduction in their viability. As expected, *RNF43* overexpression leads to intestinal organoid death. Scale bar= 1000 µm.

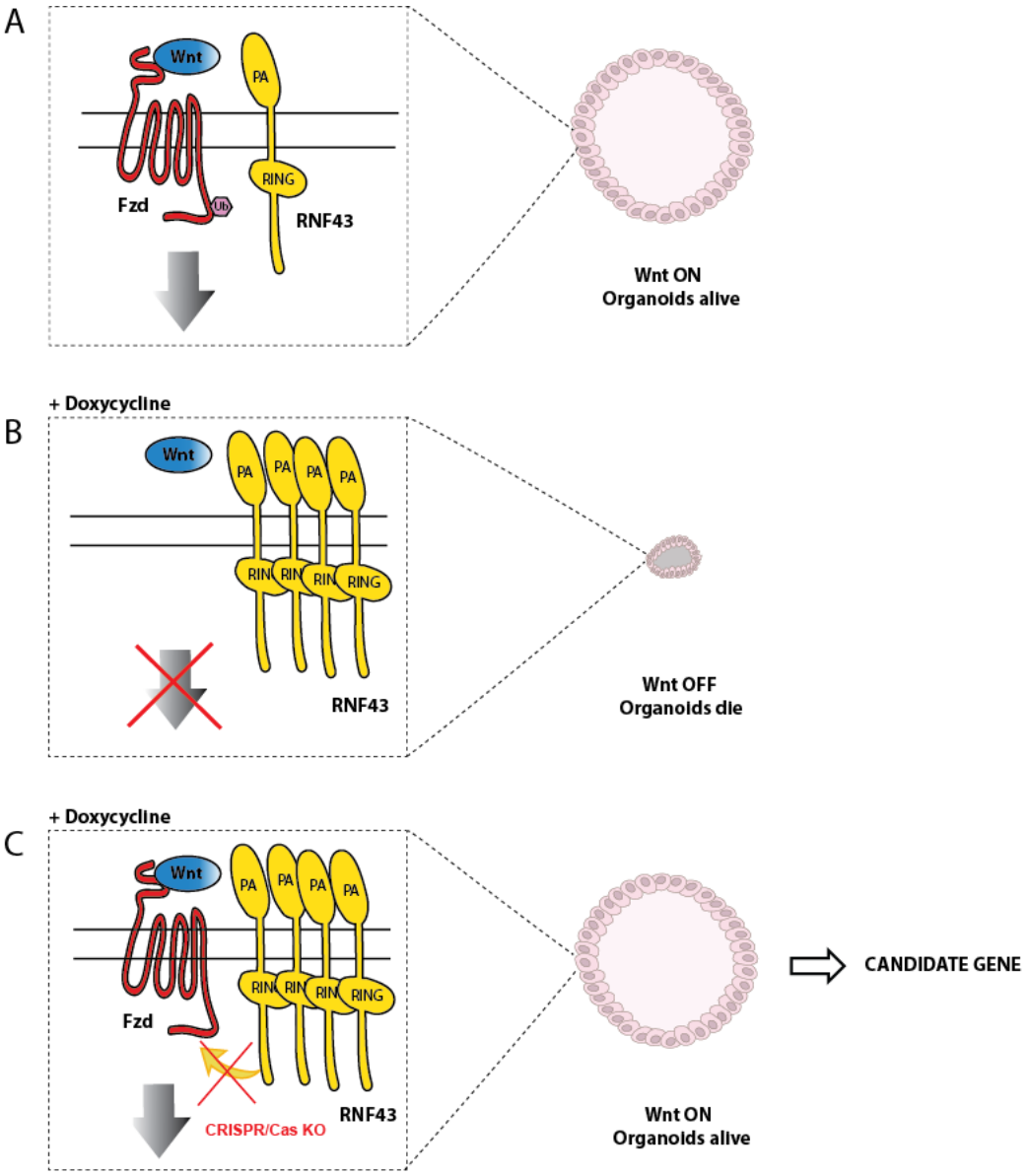

Figure 3.8 Working hypothesis for CRISPR/Cas9 screening in iRNF43 mouse intestinal organoids. **A)** In non-induced iRNF43 organoids, WNT binds to its receptor Frizzled (Fzd) to activate the pathway and this sustains organoid growth and viability. **B)** Upon doxycycline treatment, *RNF43* is overexpressed and FZD cleared from the cell surface, causing WNT signalling inhibition. As a result, organoids die over time. **C)** Under conditions of RNF43-overexpression, knockout of genes that are functionally essential for the mechanism of action of RNF43 could prevent organoid death, even though RNF43 is overexpressed.

3.2.3 iRNF43 organoid line validation

The previous section has described the establishment and preliminary testing of the iRNF43 organoid line and pointed out those characteristics that theoretically make it a suitable knockout-screening platform for the identification of genes encoding RNF43 functional interactors. Nevertheless, further validation of the system was required before carrying out the actual screening experiments that will be the focus of the next chapter.

As already stated, the underlying idea behind my screening strategy is that knockout of genes with a functional connection to RNF43 can interfere with Frizzled internalisation and prevent organoid death, which is the phenotype associated with *RNF43* overexpression (**Figure 3.8**). However, the ablation of other genes can also lead to organoid survival when RNF43 is overexpressed; for instance, the loss of any downstream negative effectors of the WNT pathway can also prevent organoid death. This is due to downstream activation of the WNT pathway that can bypass the inhibitory effect of RNF43 at the plasma membrane and the ablation of such downstream genes can be exploited to check that my system works according to predictions.

Thus, iRNF43 organoids were transfected with a Cas9-expressing plasmid and gRNA-expressing vectors against *Axin1* and *Axin2* as well as Rnf43 and *Znrf3* (*RZ*), then induced with doxycycline and passaged under these culture conditions (**Figure 3.9**). Furthermore, transfected organoids were also subjected to withdrawal of the essential medium components WNT and RSPO, as a control to verify that CRISPR-mediated gene knockout had occurred; a schematic summary on the expected outcomes in terms of organoid survival under the different culture conditions can be found in **Figure 3.10**.

As AXIN is a key component of the β-catenin destruction complex, its knockout is known to strongly boost WNT activity, as β-catenin cannot be degraded. In terms of organoid culture conditions, this translates into complete WNT ligand-independent β-catenin activity. Therefore, not only could *Axin*-knockout organoids be cultured in doxycycline-containing medium, but they could also survive without any of the essential organoid medium components, RSPO and WNT, represented by growth under WEN (WNT-EGF-Noggin) + Nic (Nicotinamide) and ENR (EGF-Noggin-RSPO) + IWP2 conditions, where IWP2

is a chemical inhibitor of the Porcupine palmitoyltransferase which is essential for WNT protein secretion. In this regard, it is important to recall that wildtype intestinal organoids can autonomously produce WNT ligands as they contain Paneth cells that are responsible for WNT3 production (Farin et al. 2012). For this reason, they do not require WNT-conditioned medium to survive but, when treated with IWP2 that blocks WNT secretion from Paneth cells, they die unless they have some loss-of-function mutations in downstream negative effectors of the WNT pathway.

Furthermore, my organoid platform and its compatibility with CRISPR gene editing tools were further validated by performing *RZ* knockout. As expected, loss of *RZ* was not sufficient to counteract the deleterious effect of *RNF43* overexpression and *RZ* KO organoids died when treated with doxycycline, whilst being independent of RSPO addition when uninduced (growth under the WEN + Nic condition). As shown by Koo *et al.* in 2012, intestinal organoids lacking *Rnf43* and *Znrf3* are known to survive in medium lacking addition of RSPO, whereas control organoids die in the absence of RSPO.

In conclusion, functional testing of the iRNF43 organoid line using CRISPR/Cas9 confirmed the reliability and robustness of my screening strategy and underlines the decision to perform the knockout screen for genes encoding RNF43-interacting proteins in this system.

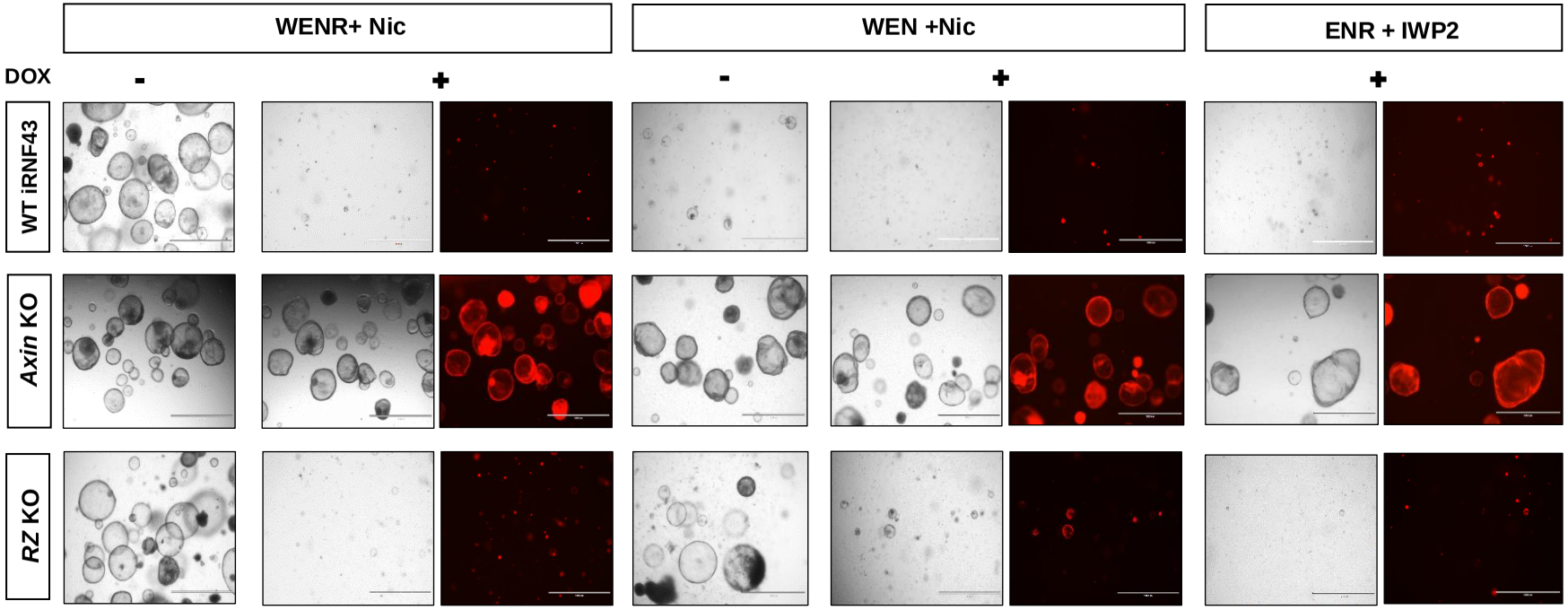

Figure 3.9 CRISPR knockout of specified genes validates the iRNF43 intestinal organoid model. Whilst WT iRNF43 organoids are not able to survive when RNF43 is overexpressed or when RSPO (WEN + Nic) or WNT (ENR + IWP2) are absent from their culture medium, *Axin* KO iRNF43 organoids are viable under all conditions due to downstream constitutive activation of the WNT pathway. In addition, knockout of *Rnf43* and *ZnrfF3* (RZ) is not sufficient to rescue the effect of *RNF43* overexpression and RZ KO iRNF43 organoids phenocopy the WT parental line, with the only difference being that they can survive in the absence of RSPO (WEN + Nic -dox). Scale bar=1000 µm.

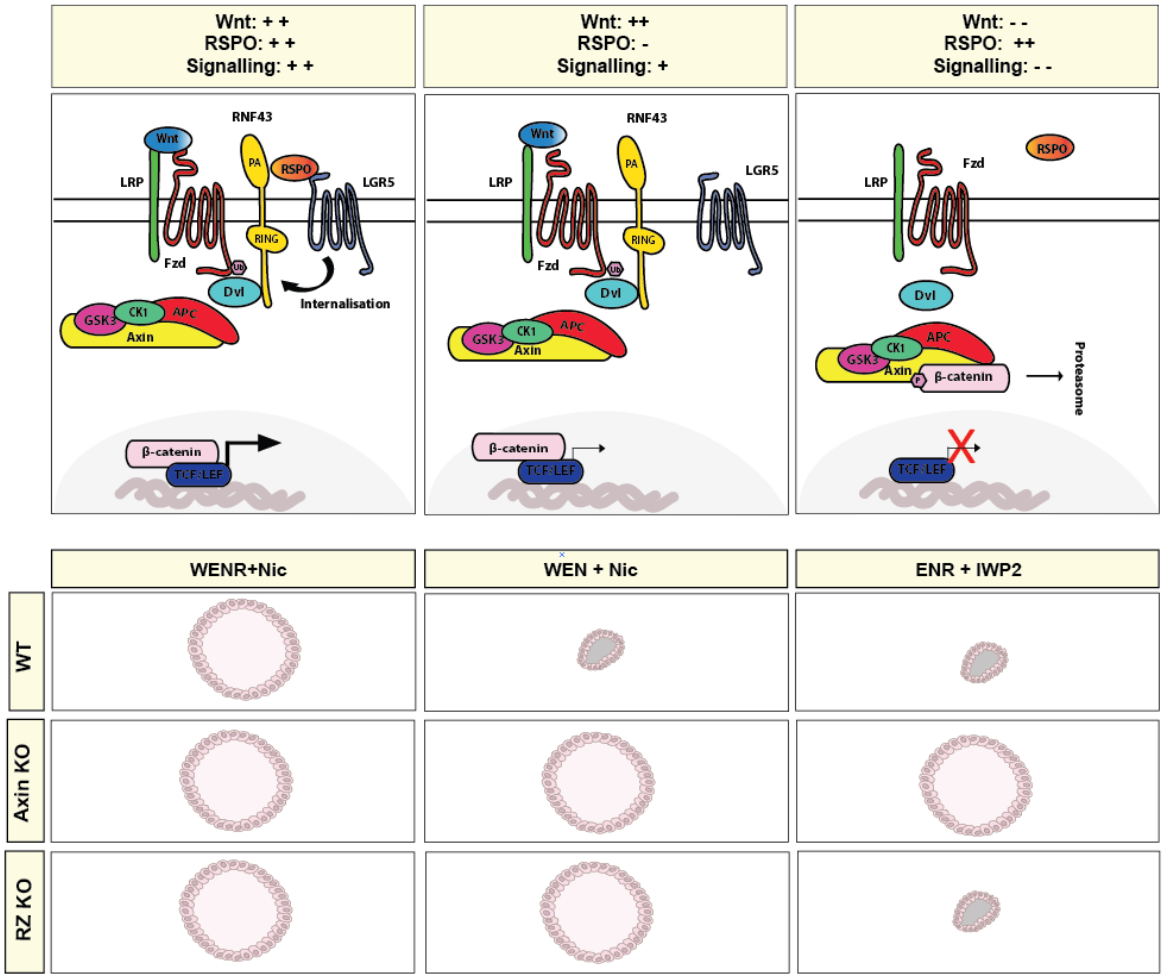

Figure 3.10 Schematic diagrams outlining WNT pathway activity and organoid survival under different medium conditions.

The top panel summarises the WNT/β-catenin pathway in intestinal organoids cultured under three different medium conditions. In the standard WENR+ Nic condition (left), signalling is activated by the concomitant presence of WNT and RSPO ligands, the latter leading to RNF43 internalisation. During RSPO withdrawal (WEN+ Nic, middle), RNF43 is no longer removed from the cell surface and its inhibitory activity does not allow sufficient levels of WNT signalling for organoid survival. Finally, during WNT withdrawal (ENR + IWP2, right), the total absence of signalling-initiating ligands results in complete pathway shut down.

The bottom panel summarises the outcomes in terms of organoid survival under different culture conditions depending on organoid genotype: WT organoids can only survive when the culture medium is supplemented with both RSPO and WNT, while *Axin* mutant organoids can survive regardless of the presence or absence of those components. *RZ* KO organoids do not need RSPO to promote RNF43 internalisation but are still sensitive to WNT depletion.

3.4 Summary and conclusions

In order to build a novel knockout-screening platform to test candidate genes for their functional connection to RNF43, two different inducible RNF43-overexpression systems were generated and tested.

The first system to be established was an iRNF43 mouse embryonic stem cell line, for mainly two reasons: firstly, mESC are particularly suitable for screening purposes and secondly, their pluripotency maintenance has been previously shown to be dependent on WNT pathway activity (ten Berge et al. 2011; Nusse et al. 2008).

Given these premises, I speculated that RNF43 overexpression and consequent WNT signalling downregulation would lead to ESC differentiation; however, prolonged doxycycline treatment did not result in the downregulation of the pluripotency marker *Rex1*, even though cells acquired a more differentiated morphology. Such phenotypical effect could simply be the result of actin cytoskeleton rearrangements following RNF43 overexpression; for instance, this E3 ligase was also reported to affect the WNT PCP pathway (Hao et al. 2012), which is responsible for cell shape regulation (Oishi et al. 2003).

The fact that the WNT pathway has also been associated with ES cell lineage diversification (Aubert et al. 2002) could be a possible explanation for the observed phenotype, together with the consideration that the precise role of WNT/β-catenin signalling in the maintenance of pluripotency, as well as the induction of differentiation, has always been regarded as controversial.

For example, it was observed that the expression of a form of β-catenin which could not promote transcription did not impede the formation of undifferentiated colonies and that ablation of β-catenin itself could result in normal mES colonies within a few passages (Kelly et al. 2011; Wray et al. 2011). In addition to this, an increase in WNT transcriptional activity was reported to mark the early phases of the exit from pluripotency in ESC (Trott & Martinez Arias 2013).

In light of these conflicting reports, it would appear that the WNT/β-catenin pathway can regulate both ES cell pluripotency and differentiation in a context-dependent manner and this makes it difficult to anticipate the effect of its downregulation on the ESC state. For

this reason, I was not able to establish a clear link between RNF43 overexpression and ESC differentiation and I decided to switch from ES cells to intestinal organoids for the development of my screening system.

In comparison to mESCs, the role of WNT/β-catenin signalling in intestinal stem cells is more defined and this makes intestinal organoids a much simpler model system for identifying RNF43-related genes. WNT ligands are known to be essential stem cell niche factors in the murine intestine, responsible for promoting intestinal stem cell proliferation and maintenance of their self-renewal (Sato&Clevers, 2013); consistent with their role in the intestine, the same ligands are indispensable for the growth and maintenance of intestinal organoids, a system that therefore fully relies on the WNT/ β-catenin pathway for its survival (Sato et al. 2011).

Given the clear role of WNT signalling in maintaining organoid viability, an organoid line with inducible *RNF43* overexpression was successfully generated and tested for viability effects upon doxycycline treatment. Further testing by the application of CRISPR/Cas9 validated iRNF43 organoids as a reliable and robust knockout screening platform. Specifically, knockout of the WNT negative regulator *Axin* could support organoid survival under a number of different culture conditions, regardless of *RNF43* overexpression, and the absence of RSPO and/or WNT. Lastly, I also confirmed that depletion of *RZ* was not able to rescue the RNF43 overexpression phenotype, although non-induced organoids could survive in the absence of RSPO; an additional indicator that CRISPR technology can be successfully applied to my screening system.

Taken together, these data validate my initial hypothesis on the working principles of a CRISPR/Cas9 knockout screen performed in RNF43-overexpressing organoids, as depicted in **Figure 3.8**.

Chapter 4

CRISPR/Cas9-mediated knockout screening of RNF43-interacting proteins

4.1 Aims of the chapter

The focus of my work is the study of the mechanism(s) of action of RNF43, aimed at unravelling new players in Frizzled membrane clearance and RNF43 regulation. The previous chapter has described in detail the screening platform I designed as well as the organoid line established to identify potential novel genes with a functional connection to RNF43.

Here, I show how I selected the candidate genes encoding putative RNF43-interacting proteins to perform their knockout in iRNF43 organoids and how this system provided us with preliminary functional insights into the role of these genes in the context of RNF43.

Therefore, the main aspects this chapter intends to address can be summarised as follows:

1) Creation of a set of candidate genes for knockout screening following identification of mass spectrometry hits obtained from RNF43 Immunoprecipitation-Mass Spectrometry (RNF43 IP-MS) and subsequent generation of CRISPR constructs to target candidate genes and their paralogs;
2) Description of the CRISPR knockout screen of the candidate genes in iRNF43 intestinal organoids to shortlist those candidates whose depletion promoted organoid survival in the context of RNF43 overexpression;
3) Elucidation of where exactly in the context of WNT pathway regulation the identified candidates act, either in membrane-proximal events of Frizzled internalisation or in more downstream events of the signalling cascade.

4.2 Results

4.2.1 Selection of genes for CRISPR/Cas9 KO screening

After establishing the organoid-based screening platform, the next step was to select the genes to screen by knockout in the iRNF43 line. Following a goal-oriented approach, I focused on the investigation of genes encoding proteins that emerged as potential RNF43 interactors in RNF43 IP-MS (Immunoprecipitation-Mass Spectrometry).

These preliminary data had been previously generated by Dr. Koo by performing RNF43 pull-down followed by Mass Spectrometry (MS) analysis and the relative MS hit list was selected as a starting point in order to narrow down the number of candidate genes to be tested in organoids.

The available MS dataset referred to a total of 5 independent experiments of RNF43 pull-down followed by mass spectrometry analysis; for technical reasons, pull-down experiments had to be performed with three different RNF43 constructs: the full length (two technical replicates), the PA/TM RNF43 and ΔCRNF43 (two technical replicates).

The reason for this is that an unexpected cleavage of the full length protein was found to occur during sample processing prior to mass spectrometry analysis, resulting in truncation of the protein to only the intracellular domain of RNF43 ("full length RNF43", as indicated in **Figure 4.1**). To overcome this and avoid possible artifacts due to protein mislocalisation, a complementary deletion form containing the extracellular and transmembrane domains was generated (PA/TM RNF43) and employed to repeat the analysis. Interestingly, it was noticable that removal of the C-terminus (aa 524-784) from the full length protein greatly increased its stability (ΔCRNF43) and therefore the experiment was repeated once more including this form. The different forms of RNF43 that were employed in IP-MS experiments are outlined in **Figure 4.1**, with each of them providing information on interactions occuring in different domains of RNF43.

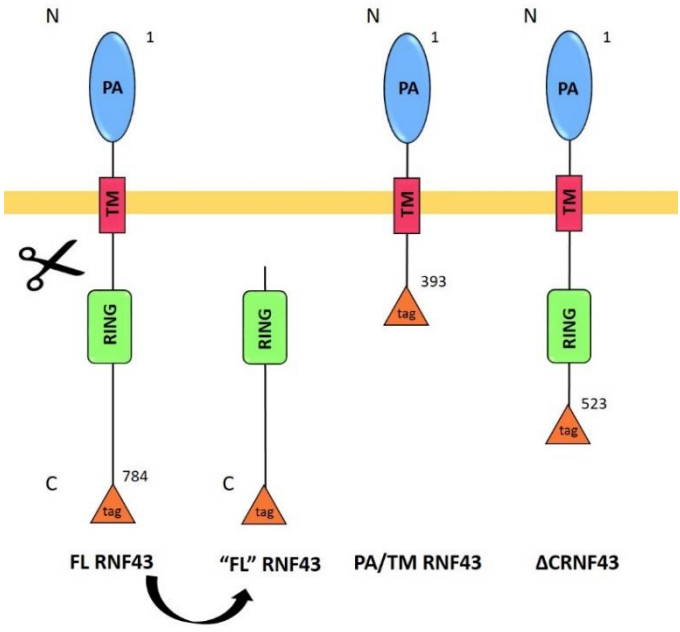

Figure 4.1 Different RNF43 constructs used in mass spectrometry experiments. Three different types of *RNF43* constructs were employed for RNF43 pull-down followed by mass spectrometry: the "full length" ("FL" RNF43), a fragment containing PA and TM domains only (PA/TM) and a form with all the functional domains but lacking the C terminus for stability purposes (ΔC RNF43). The PA/TM form was employed to compensate for a cleavage event during processing which left only the intracellular domain of FL RNF43 intact and the ΔC RNF43 form employed following recognition that removal of the C terminal portion resulted in increased stability.

For this study, particular attention was paid to those MS hits showing the greatest number of peptides in the experiments conducted on the "full length" and ΔCRNF43 forms; these hits were usually absent or had a low number of peptides in the PA/TM deletion form, suggesting that selected proteins were likely to interact with the cytoplasmic tail of RNF43. In this way, I thought possible to effectively identify molecules helping RNF43 to trigger Frizzled internalisation on the cytoplasmic side.

Other criteria taken into account to narrow down the list of genes for screening included their expression in the mouse intestine and their

known or putative function. For example, genes already known to be implicated in processes like ubiquitination, membrane trafficking, the WNT pathway and endocytosis were of particular interest. In light of the above considerations, it is therefore worth mentioning that not only were the top-ranked hits chosen for the genetic screening, but also those that seemed promising based on their function, irrespective of a low MS score. Lastly, one additional parameter considered in the selection process was the number of paralogs each gene had; for instance, genes with more than 2 paralogs expressed in the intestine were excluded, given the difficulty of obtaining simultaneous knockout of that many genes.

Thus, by combining all the MS data and considering the above-mentioned criteria, a list of 27 genes was drawn up. The complete list can be found in **Table 4.1**, together with information about paralogs, MS score and gene function.

In conclusion, this section has detailed the rationale for selecting the genes to be screened in iRNF43 organoids.

Table 4.1 Summary information about MS hits selected for CRISPR screen

#	GENES	PARALOGS*	MS SCORE**	Function
1	*UBR2*	*UBR3*	high	E3 ubiquitin-protein ligase
2	*SLC12A2*	*SLC12A8; SLC12A9*	high	Mediates sodium and chloride ion reabsorption
3	*WDR26*	-	high	Interacts with DDB1-CUL4A/B E3 ligase complexes
4	*ARMC8*	-	high	Armadillo repeat-containing protein 8
5	*EMERIN*	-	medium	Influences nuclear accumulation of beta-catenin
6	*ADAM17*	-	medium	Proteolytic release of several cell surface proteins
7	*AP2M1*	-	medium	Vesicle transport in different membrane traffic pathways
8	*VANGL1*	*VANGL2*	medium	Interacts with Dvl. Regulates wound healing in the intestine
9	*PLD1*	*PLD2*	medium	Implicated in numerous cellular pathways, including membrane trafficking
10	*ZMYND19*	-	medium	Deubiquitinating enzyme
11	*TMED10*	-	medium	Involved in vesicular protein trafficking, mainly early secretory pathway
12	*BAG6*	-	medium	Misfolded protein binding and ubiquitin protein ligase binding
13	*ZYG-11B*	*ZER1*	medium	Component of the E3 ubiquitin ligase complex ZYG11B-CUL2-Elongin BC.

14	*IGSF8*	*PTGFRN*	medium	Prostaglandin regulatory-like protein
15	*SPTLC1*	-	medium	Serine palmitoyltransferase
16	*BRI3BP*	*TMEM109*	low	Involved in tumorigenesis
17	*SYNTENIN -1*	*SYNTENIN-2*	low	May play a role in vesicular trafficking
18	*DAAM1*	*DAAM2*	low	Interacts with Dishevelled and Rho
19	*DVL2*	*DVL1, DVL3*	low	Transducer of WNT signals to downstream effectors
20	*SORT1*	*SORL1; SORCS1*	low	Required for protein transport from the Golgi apparatus to the lysosomes
21	*UBL4A*	-	low	Component of the Bag6 complex
22	*SEC16A*	*SEC16B*	low	Secretory cargo traffic from the endoplasmic reticulum to the Golgi
23	*RAB8A*	*RAB15; RAB10*	low	Regulators of intracellular membrane trafficking
24	*LMAN2*	-	low	Involved in the transport and sorting of glycoproteins
25	*AP2A2*	*AP2A1*	low	Vesicle transport in different membrane trafficking pathways
26	*TMEM59*	-	low	Regulator of autophagy and protein processing
27	*SH3BP4*	*MACC1*	low	Transferrin receptor endocytosis

* According to *TreeFam* database of animal gene trees. Only genes expressed in the murine intestine

** Low score: <3 peptides; high score: > 9 peptides

4.2.2 Single guide RNA vector generation for multiple gene knockout

The final readout of my CRISPR knockout screening is a phenotypic effect caused by gene deletion in RNF43-overexpressing organoids; however, if a gene has multiple paralogs with similar functions, a phenomenon known as “genetic compensation” may occur when a single gene is knocked out and its role is replaced by a similar gene (Diss et al. 2014). Since this can mask any potential phenotypic effect, in my screening I aimed to perform knockout of the selected MS hits as well as their paralogous genes in order to overcome the limitations of single-gene knockout approaches.

To achieve multiple gene knockout using CRISPR/Cas9 technology, our group has recently developed a one-step method to clone up to four different gRNAs into a single vector (Andersson-Rolf et al. 2016). As the backbone is composed of several consecutive gRNA expression cassettes, the construct has been termed a CRISPR-concatemer. Each cassette is approximately 400 bp and contains two inverted *Bbs*I restriction sites, a U6 promoter driving gRNA expression and a gRNA scaffold. During a cloning process involving Golden Gate assembly each *Bbs*I site is replaced by a pre-annealed gRNA oligo with matching overhangs and permanently lost (**Figure 4.2**). Thus, our strategy exploits the unique nature of Type IIS restriction enzymes, like *Bbs*I, in cleaving target DNA outside of their recognition sequences; in this way, each cassette can have a different sequence with customised overhangs flanking *Bbs*I core sites and this can mediate the incorporation of different gRNA fragments at specific positions within the vector.

The great advantage of this method is the ease of cloning multiple annealed gRNAs into the same vector in a straightforward one-step reaction, which is highly efficient because it is based on consecutive cycles of digestion and ligation until all *Bbs*I sites are lost, as outlined in **Figure 4.3**. In addition, this tool is also extremely flexible since several versions of the vector exist differing in the number of gRNA cassettes (for cloning two, three or four gRNAs).

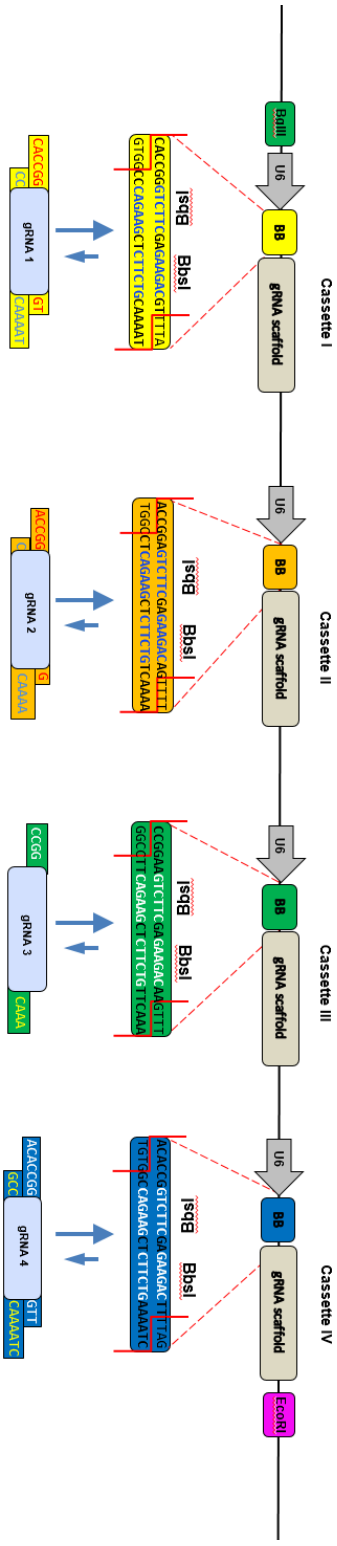

***Figure 4.2* Schematic representation of the CRISPR-concatemer vector with four cassettes.** The schematic represents a 4 gRNA-concatemer vector with each 400bp-cassette containing a U6 promoter, two inverted repeated *Bbs*I sites (indicated as BB) and the gRNA scaffold, in that order. The strategy exploits the Type IIS restriction enzyme *Bbs*I that recognises asymmetric DNA sequences and cleaves outside of its recognition sequence so that each cassette can have different overhangs and each gRNA can be cloned into a specific position in a one-step reaction. During the *shuffling* reaction, *Bbs*I sites are replaced by gRNA oligos with matching overhangs (as indicated by the blue arrows) and consequently lost (Merenda et al, 2017. *In press*).

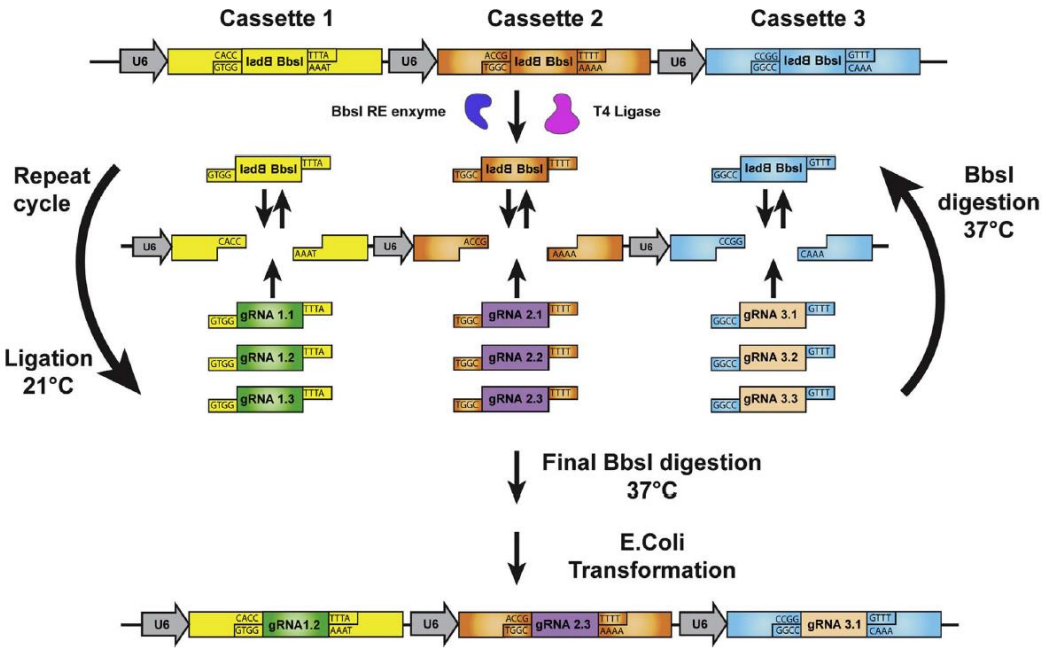

Figure 4.3 Schematic outlining the cloning strategy to integrate multiple gRNAs into the CRISPR-concatemer vector. The scheme illustrates the Golden Gate, or *shuffling*, reaction by which multiple annealed oligos are incorporated into a single concatemer vector by repeated cycles of *Bbs*I digestion (37°C) and ligation (21°C). Each gRNA expression cassette has custom-designed overhangs that originally constitute *Bbs*I recognition sites. When *Bbs*I digests the vector, its restriction sites are replaced by annealed gRNA oligos that are integrated thanks to their vector-matching overhangs. In this way, the *Bbs*I sites are lost and the gRNAs cannot be removed during the following rounds of digestion (Andersson-Rolf et al, 2016).

Another advantage to our CRISPR-concatemer approach is its versatility, as it can be used to perform simultaneous knockout of several genes as well as to increase CRISPR knockout efficiency by targeting the same gene with multiple gRNAs.

For the planned screening, I generated constructs containing three or four different gRNAs, depending on the number of paralogs for each candidate: for genes with only one paralog, I designed two gRNAs to target each gene and cloned these into the 4 gRNA-concatemer vector (*e.g PLD1/2*), whereas for genes with no paralogs three gRNAs were designed to target the same gene and thus increase the efficiency of knockout (*e.g.* Bag6).

In this way, gRNAs against all the selected MS hits and their paralogs were generated, specific overhangs were added to each end (**Supplementary Table S7**) and the resulting oligonucleotides were cloned into the required CRISPR-concatemer vectors.

To perform the CRISPR knockout screening, the gRNA concatemer vectors were introduced together with a Cas9 expression plasmid into iRNF43 organoids by electroporation (Merenda et al., 2017). Thanks to careful optimisation of the electroporation protocol for this organoid line using the NEPA21 Super Electroporator, it was possible to achieve very high levels of transfection efficiency (up to 70% with generic GFP-expression plasmids) so that I could confidently assume that the majority of the cells received both the gRNA expression vector and the Cas9 plasmid (**Figure 4.4 B**).

In summary, gRNA vectors were generated for the selected genes as part of a CRISPR-concatemer strategy for multiple gene knockout in RNF43-overexpressing organoids.

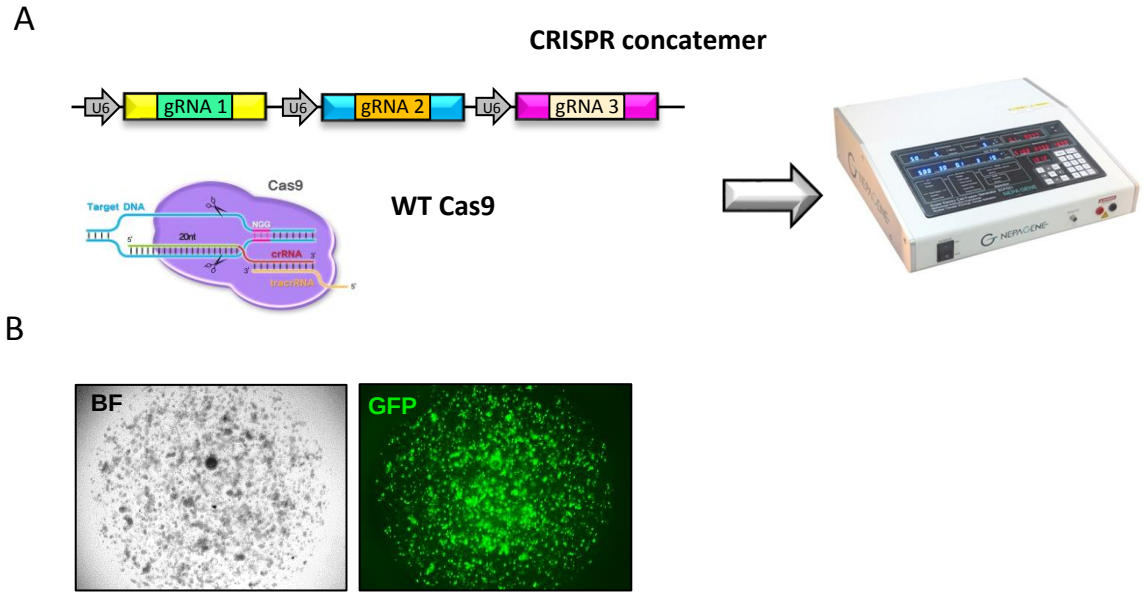

Figure 4.4 Intestinal organoid transfection by electroporation. **A)** CRISPR-concatemer vectors containing gRNAs targeting the selected MS hits and their paralogs are co-transfected with an equal amount of a WT Cas9 expression plasmid into intestinal organoids by using the NEPA21 Super Electroporator. **B)** Images of intestinal organoids electroporated with an eGFP-expressing plasmid showing a high transfection efficiency thanks to protocol optimisation.

4.2.3 Candidates of interest revealed by the CRISPR screen

Following recovery from electroporation, iRNF43 organoids were subjected to prolonged doxycycline treatment and their survival was monitored after several rounds of splitting in order to functionally screen the selected MS hits (**Figure 4.5 B**). The same number of cells was seeded into each well and all wells were spilt in parallel at the same ratio for each round of splitting.

Once again, knockout of the destruction complex component Axin was employed as a positive control, a proxy for the correct functioning of my screening system, as described in the previous chapter. In brief, *Axin1/2* KO organoids can survive indefinitely despite prolonged *RNF43* overexpression due to downstream activation of the pathway, in contrast to WT iRNF43 organoids which die around passage #2 when cultured in dox-supplemented medium.

While knock out of most of the candidates resulted in organoid death after 2-3 passages, the depletion of *Daam1/2* could render organoids insensitive to RNF43 overexpression (**Figure 4.5 C**). *Daam* mutant organoids were comparable to *Axin1/2* KO organoids in terms of their size, levels of RNF43 overexpression (indicated by the mCherry reporter) and growth rate; for example, they could be passaged at the same time and in the same ratio as Axin1/2 KO organoids for over 6-7 passages.

Interestingly, knockout of *Dvl* also produced organoids capable of surviving prolonged doxycycline treatment, confirming previously reported observations according to which DVL is assisting RNF43 in promoting Frizzled internalisation (Jiang et al. 2015). Furthermore, as DAAM (DVL Associated Activator of Morphogenesis) is known to interact with DVL, albeit in the context of the WNT planar cell polarity (PCP) pathway, it was striking to see it emerging during the screening and I thus decided to further examine its role in the mechanism of action of RNF43.

Nevertheless, DAAM is not the only potential interactor in RNF43-mediated downregulation of Frizzled my CRISPR screen in iRNF43 organoids revealed. A few other candidates from the MS hit list emerged as interesting molecules to study in the context of RNF43 activity and, even more broadly, WNT pathway regulation. For example, knockout

of *Ubl4a*, *Sec16a* and *Slc12a2*, together with their paralogs, resulted in organoids viable for over 6-7 passages in doxycycline-supplemented medium, similar to Axin KO organoids (**Figure 4.6**).

In contrast to *Daam*, none of these genes has ever been associated with the WNT pathway before. *Ubl4a* is a known interactor of Bag6 that promotes tail-anchored protein biogenesis (Kuwabara et al. 2015), *Slc12a2* encodes a solute carrier that mediates sodium and chloride reabsorption and SEC16A acts as a scaffold to recruit COPII components and facilitate protein export from the endoplasmic reticulum to the secretory pathway (Sprangers & Rabouille 2015).

Considering that these biological roles refer to broad cellular processes, it might not be easy to pinpoint a direct contribution of the candidates to WNT pathway regulation, as they could directly or indirectly affect multiple signalling components in parallel. On the other hand, it is intriguing to consider the specific function these genes may have in the mechanism of action of RNF43 and/or WNT pathway regulation.

Nonetheless, I decided to focus on DAAM for further characterisation as it already had a specific role in WNT regulation described in the literature.

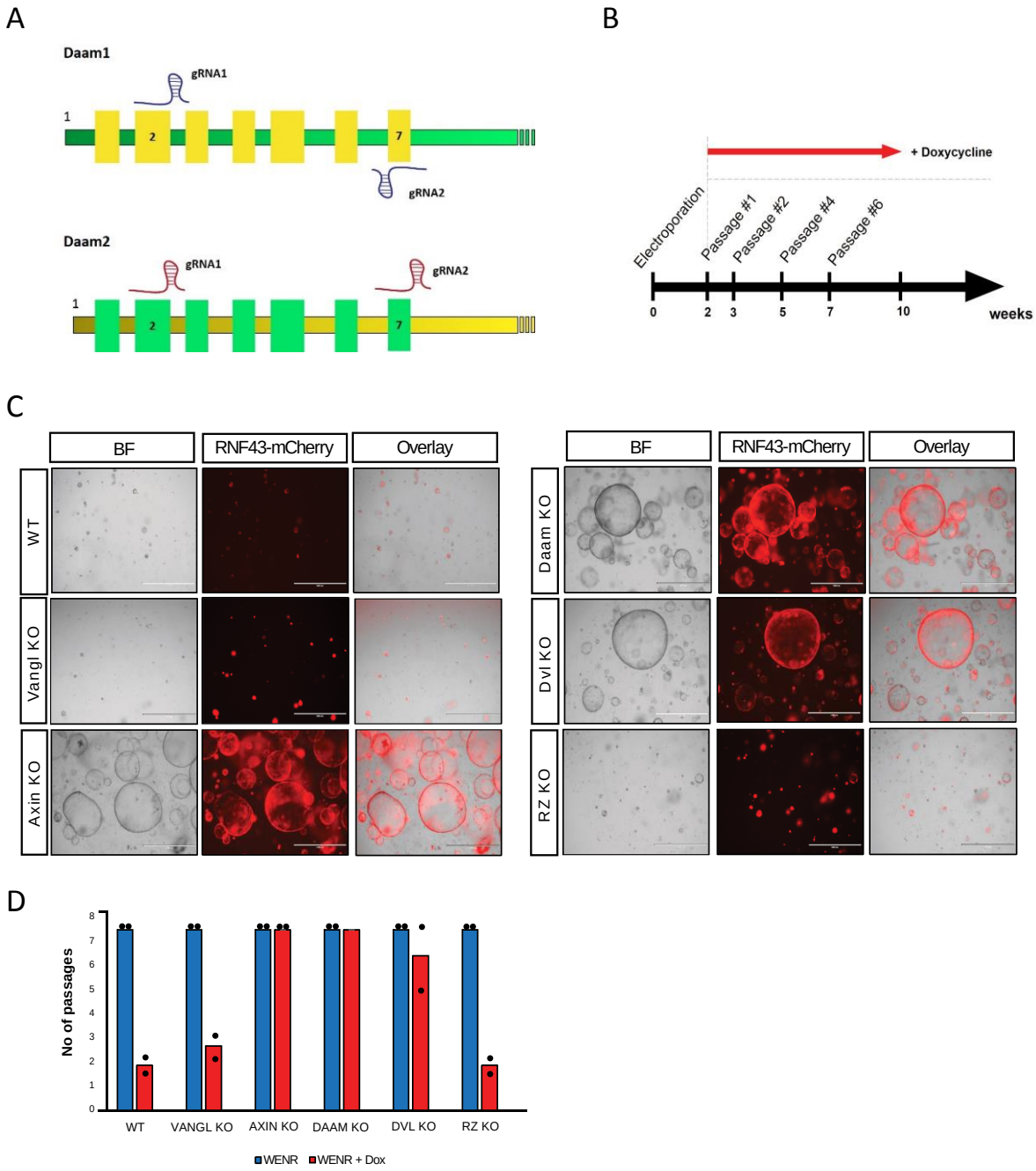

Figure 4.5 Daam1/2 knockout renders intestinal organoids insensitive to RNF43 overexpression. **A)** Schematic representation of *Daam1* and *Daam2* genes with the relative targeted exons. Two gRNAs were used to target each gene. **B)** The scheme illustrates the experimental timeline followed when performing CRISPR knockout and doxycycline induction. Approximately 2 weeks after electroporation, RNF43 overexpression was induced by addition of doxycycline and surviving organoids were cultured under these conditions for over 6 passages. **C)** Representative images of iRNF43 organoids in WENR +Nic + dox medium. After passage # 3, all WT iRNF43 organoids were dead but *Daam1/2* KO organoids were still alive, similar to *Axin1/2* KO organoids. Dvl knockout could also sustain organoid survival during RNF43 overexpression, whereas knocking out *R&Z* could not. Scale bar= 1000 µm. **D)** Bar chart displaying iRNF43 organoid survival in terms of number of passages according to genotype in WENR medium with or without doxycycline (red and blue bars, respectively). Data from two independent biological replicates.

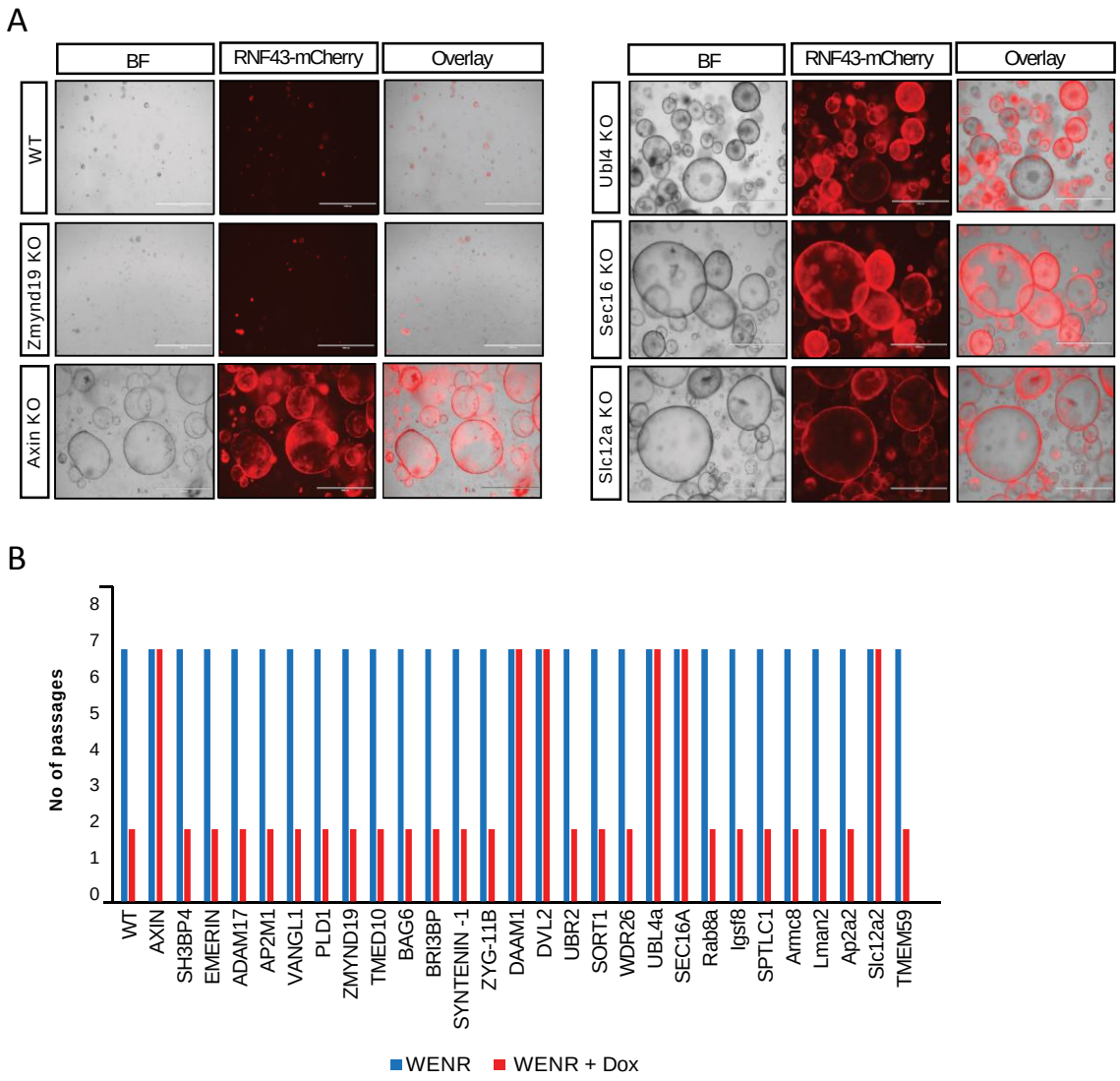

***Figure 4.6 Additional positive hits identified during CRISPR screening*. A)** Images of iRNF43 organoids in WENR +Nic + dox medium. After passage # 3, all iRNF43 WT organoids were dead, whereas knockout of the following genes enabled organoids to survive in dox-supplemented medium for over 6 passages, thus phenocopying *Axin1/2* KO organoids: *Ubl4a, Sec16a/b* and *Slc12a2/8/9*. Scale bar= 1000 µm. **B)** Bar chart displaying iRNF43 organoid survival in terms of number of passages according to genotype in WENR medium with or without doxycycline (red and blue bars, respectively). The chart includes all MS hits screened (see also Table 4.1).

4.2.4 DAAM is identified as a potential component of RNF43-mediated Frizzled internalisation

Since the previously described CRISPR screen does not provide any information on where in the pathway DAAM might act, growth factor withdrawal experiments in WT background organoids were necessary to understand whether the candidate was taking part in RNF43-related events at the plasma membrane or was instead implicated in more downstream events (described in **Figure 4.7**).

Therefore, *Daam* KO organoids were subjected to withdrawal of both RSPO and WNT (EN and EN+IPW2 conditions, respectively) and their behaviour compared in parallel to the same set of controls, including WT, *Axin* KO and *RZ* KO organoids.

As expected, WT organoids died after 1-2 passages in both culture conditions, while *Axin* mutants remained viable in both media conditions for several passages. What was interesting to observe was that knockout of *Daam* could perfectly mimic the *RZ* KO organoid phenotype, with *Daam* KO organoids insensitive to the absence of RSPO but sensitive to the complete absence of WNT (**Figure 4.8**). This allowed us to conclude that DAAM was likely to be involved in membrane-proximal events, potentially promoting Frizzled ubiquitination and internalisation together with RNF43.

These data are preliminary and obviously need to be integrated with additional *in vitro* evidence in order to prove a direct link between DAAM and RNF43. The biochemical assays employed to assess Frizzled endocytosis and ubiquitination in a *Daam*-mutant background will be outlined in the next chapter.

I next asked whether knockout of both paralogs, *Daam1* and *Daam2*, was required to mediate such an effect in intestinal organoids, or whether loss of only one of them was responsible for it. To address this, the same withdrawal experiments were carried out but compared the behaviour of only single mutant organoids to controls, as summarised in **Figure 4.9 B, C**. Notably, knockout of *Daam1* was sufficient for organoids to display insensitivity to RPSO withdrawal; this was actually not surprising considering that murine intestinal organoids predominantly express *Daam1* (**Figure 4.9 D**). Importantly, these experiments were repeated from the beginning with independent sets of gRNAs, allowing

us to exclude the possibility that the observed phenotypes were a consequence of possible off-target effects (**Figure 4.9 A**).

In conclusion, the knockout of *Daam* in intestinal organoids rendered them insensitive to RNF43 overexpression or to the absence of RSPO. These data indicate that DAAM is likely to participate in RNF43-mediated downregulation of Frizzled, possibly through direct interaction and the formation of a ternary complex with Dishevelled.

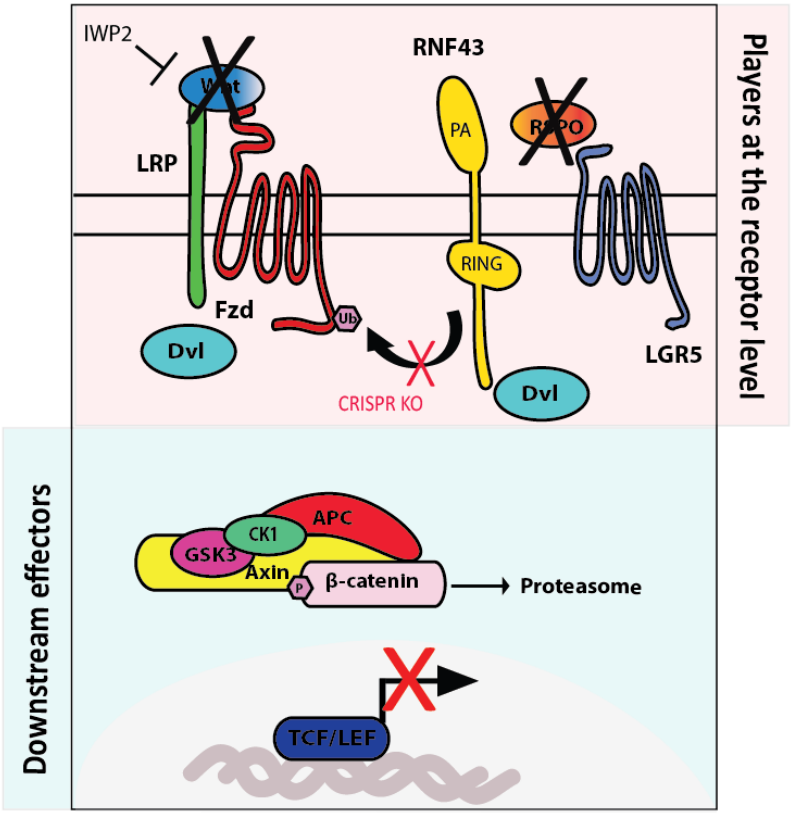

Figure 4.7 Schematic diagram of the different levels of regulation of the WNT pathway. The scheme illustrates how RSPO and WNT withdrawal experiments can pinpoint if a candidate gene functions at the receptor level (pink rectangle) or in more downstream events of the WNT pathway (blue rectangle). For the former, since CRISPR knockout of genes involved in the mechanism of action of RNF43 can interfere with its inhibitory activity, intestinal organoids should become insensitive to the absence of RSPO. However, WNT ligands will still be essential in order to trigger pathway activation. For the latter, organoids depleted of downstream effectors of the WNT pathway would be completely unaffected by absence of either growth factor (*e.g. Axin* KO).

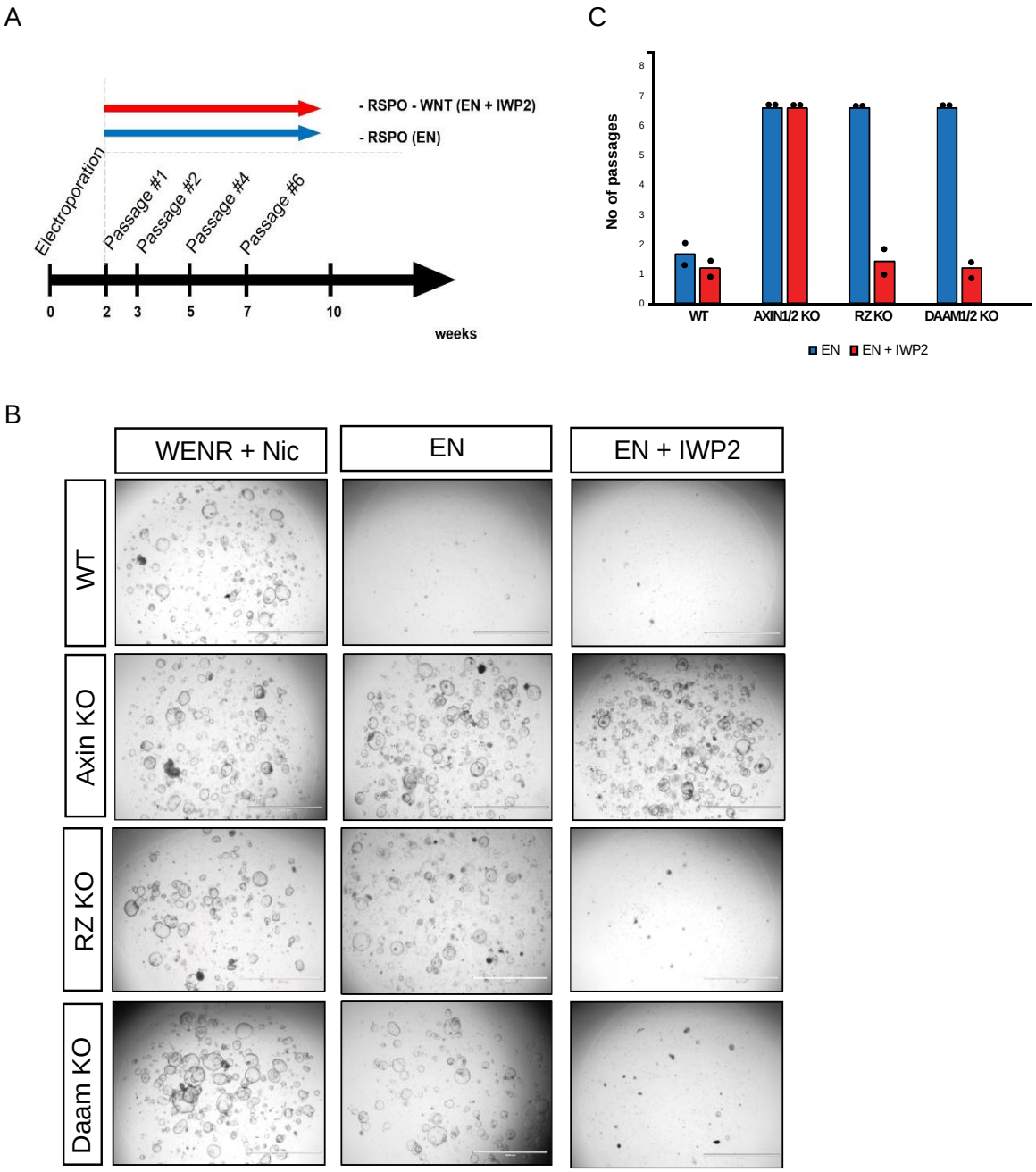

Figure 4.8 Daam1/2 knockout intestinal organoids are insensitive to RSPO withdrawal but are still dependent on WNT. **A)** The scheme illustrates the experimental timeline followed when performing CRISPR knockout and growth factor withdrawal experiments in intestinal organoids with a WT background. Approximately 2 weeks after electroporation, organoids were cultured both in the absence of RPSO (blue arrow) and WNT (red arrow) to determine viability. **B)** Images of intestinal organoids under three different culture conditions: WENR +Nic, EN (-RSPO) and EN +IWP2 (-WNT;-RSPO). After two passages, WT organoids could not survive under any of the withdrawal conditions, while *Axin1/2* KO organoids could be cultured in both. *Daam1/2* KO organoids instead displayed similar behaviour to *RZ* KO organoids, by being able to survive in the absence of RSPO but being sensitive to the absence of WNT. Scale bar= 2000 µm. **C)** Bar chart displaying organoid survival in terms of number of passages according to genotype in EN and EN +IWP2 culture conditions (blue and red bars, respectively). Data from two independent biological replicates.

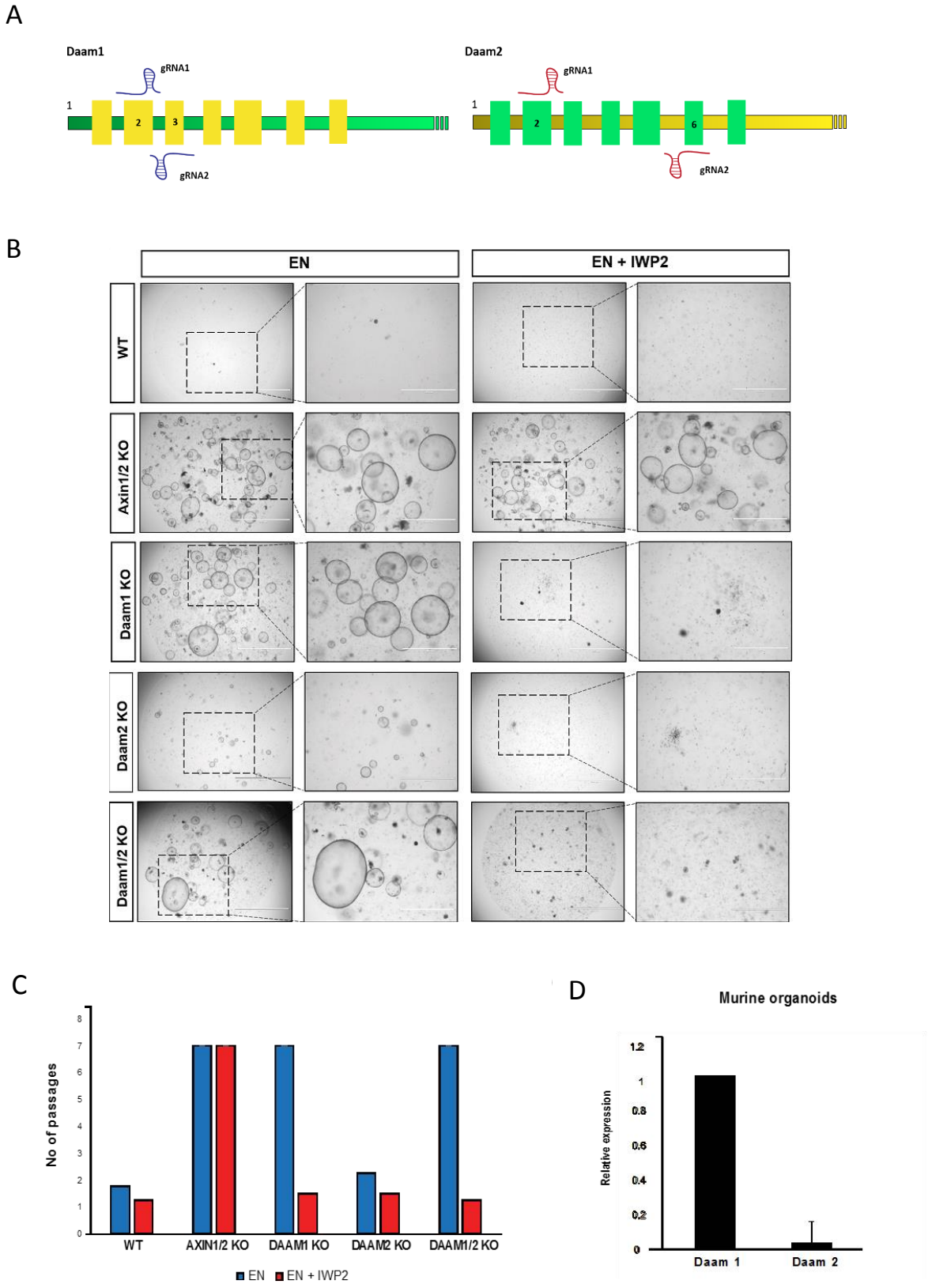

Figure 4.9 Daam1 knockout is sufficient for intestinal organoid survival in the absence of RSPO. *Continues on next page.*

***Figure 4.9 Daam1 knockout is sufficient for intestinal organoid survival in the absence of RSPO*.**
A) Schematic representation of *Daam1* and *Daam2* genes with the relative targeted exons. Different sets of gRNAs were employed, compared to previous experiments. **B)** Images of intestinal organoids in EN (RSPO withdrawal) and EN +IWP2 (WNT and RSPO withdrawal) media, with magnified areas (dotted outline) to the right. After two passages, no WT organoids could survive under any of the withdrawal conditions, while *Axin1/2* KO organoids could be cultured in both. Daam1 single knockout could mimic the effects of *Daam1/2* double KO, with organoids surviving under EN but dying under EN +IWP2 conditions. By contrast, knocking out *Daam2* only did not support organoid growth in EN. Scale bar= 1000 µm. **C)** Bar chart displaying organoid survival in terms of number of passages according to genotype under EN and EN +IWP2 culture conditions (blue and red bars, respectively). **D)** Relative abundance of *Daam2* transcripts in mouse intestinal organoids compared to *Daam1*.

Although *Daam* remained my major focus, RSPO and WNT withdrawal experiments were conducted for the other candidates too, in order to gain more insight into their roles. While *Sec16* KO phenocopied *RZ* and *Daam* KO, with organoids surviving only under EN conditions, the knockout of *Slc12a* surprisingly resulted in viable organoids under both withdrawal conditions, thus phenocopying *Axin* mutants (**Figure 4.10**). By contrast, *Ubl4* KO organoids rapidly died under both EN and EN+IWP2 conditions, similar to the WT control, suggesting that *Ubl4* is not a strong candidate for further work.

In summary, complementing my doxycycline screening with growth factor withdrawal experiments in organoids turned out to be an effective strategy to determine at what level in the WNT cascade my candidates were likely to be involved.

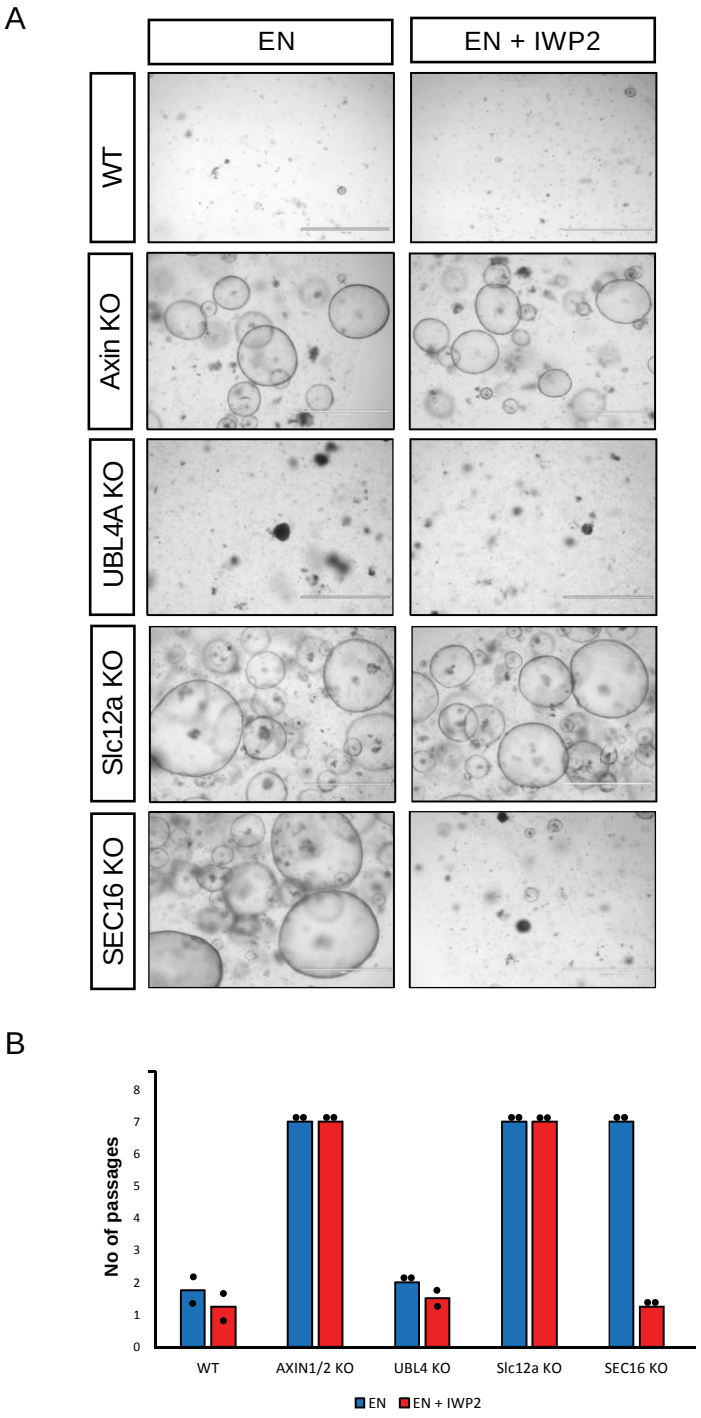

Figure 4.10 Further candidates tested using growth factor withdrawal. **A)** Images of intestinal organoids under growth factor withdrawal conditions: EN (-RSPO) and EN +IWP2 (-WNT;-RSPO). After two passages, WT organoids could not survive under any of the withdrawal conditions, while *Axin1/2* KO organoids could be cultured in both. Surprisingly, KO of *Slc12a* could phenocopy *Axin* knockout, with organoids surviving in both growth factor-deprived media, and KO of *Sec16* could phenocopy *RZ* KO, with organoids able to survive without RSPO but not without WNT. By contrast, Ubl4 KO organoids behaved like the WT control and died within a few passages. Scale bar= 1000 µm. **B)** Bar chart displaying organoid survival in terms of number of passages according to genotype under EN and EN +IWP2 culture conditions (blue and red bars, respectively).

4.3 Summary and conclusions

An important first step in understanding the details of the mechanism of action of RNF43 is the identification of genes with a functional connection to RNF43 and the WNT pathway in general.

Here I have shown how I successfully built a reliable and robust intestinal organoid-based screening platform with the intent of identifying RNF43-related genes. The system turned out to be particularly useful in order to screen selected mass spectrometry hits potentially interacting with the intracellular portion of RNF43. In particular, the choice of selectively focusing on potential RNF43 cytoplasmic interactors finds its motivation in the intent of identifying molecules taking part in the membrane-proximal events of RNF43-mediated Frizzled downregulation.

As a result, the following genes emerged as promising candidates from the CRISPR knockout screening in iRNF43 organoids: *Daam*, *Sec16*, *Slc12a* and *Ubl4* (**Figure 4.11**). I observed that knocking out each of these genes allowed organoids to survive regardless of RNF43 overexpression, suggesting that these gene products might have a role either in promoting RNF43-mediated surface clearance of Frizzled or in inhibiting WNT activity by other means.

Hence, I conclude that my strategy validates at least some of the RNF43-MS hits, since it can immediately provide corroborative functional data on the screened candidates; this is a considerable advantage if compared to traditional validation approaches, such as co-immunoprecipitation or the yeast two-hybrid screen. For instance, these assays provide information on the physical interaction between two proteins but are often carried out under non-physiological conditions, whereas organoid-based assays are performed in a contextual mammalian culture system.

My system could be employed to screen even more candidates from the RNF43 IP-MS list in order to test more hits and, theoretically, it might also be possible to develop an analogous approach for other negative regulators of the WNT pathway in order to identify their functionally related molecules.

However, this screening strategy is not flawless and has some intrinsic limitations; for example, if a gene is essential for cell survival its knockout will result in organoid death soon after electroporation; in this case it would not be possible to subject organoids to doxycycline induction and screening could not be performed. Combining the current strategy with a Cas9-inducible system would be a potential method to overcome this limitation.

Furthermore, another aspect worth taking into account when conducting a knockout screening is the eventuality that a gene is involved in multiple cellular processes and/or has multiple functions; under these circumstances, the observed screening outcome might be the result of indirect modulation of RNF43 or WNT/β-catenin pathway activity via unknown mechanisms. Thus, not all of the hits emerging from the CRISPR screening in iRNF43 organoids are necessarily involved in membrane-proximal events. For this reason, growth factor withdrawal experiments are required and organoid data need to be supported by additional *in vitro* data too, which will be the focus of the next chapter.

Lastly, although the screening can be extended to other MS hits, it will still only be possible to screen a limited number of candidates, given the labour-intensive nature of organoid culture that renders it unsuitable for high-throughput experiments.

Despite the above-mentioned drawbacks, overall my screening approach was highly effective in identifying interesting candidate genes that are worthy of further investigation. These candidates might be involved either in Frizzled clearance or in RNF43 regulation and/or maturation and trafficking to the plasma membrane, an obvious candidate for this being the COPII coat assembly protein SEC16. Importantly, this study could bring some interesting new insights into WNT/β-catenin pathway regulation, since it is the first time these genes are being associated with it.

Daam immediately caught my attention as a putative player in Frizzled downregulation, as it is already known to interact with Dishevelled, and it is intriguing to view it as a potential missing link to the unanswered questions raised by previous work on the role of Dishevelled in RNF43 activity (Jiang et al. 2015; Tsukiyama et al. 2015). In fact, the precise mechanism by which these two proteins cooperate is still unclear and it has been even suggested that their interaction might not be direct.

Following its clear ability to phenocopy R&Z, and given its previously described specific association with the WNT pathway, *Daam* was the candidate that I decided to focus on and I have thus tried to address its role in RNF43-mediated Frizzled clearance from the cell surface using both *in vitro* and *in vivo* approaches, as described in the next chapter.

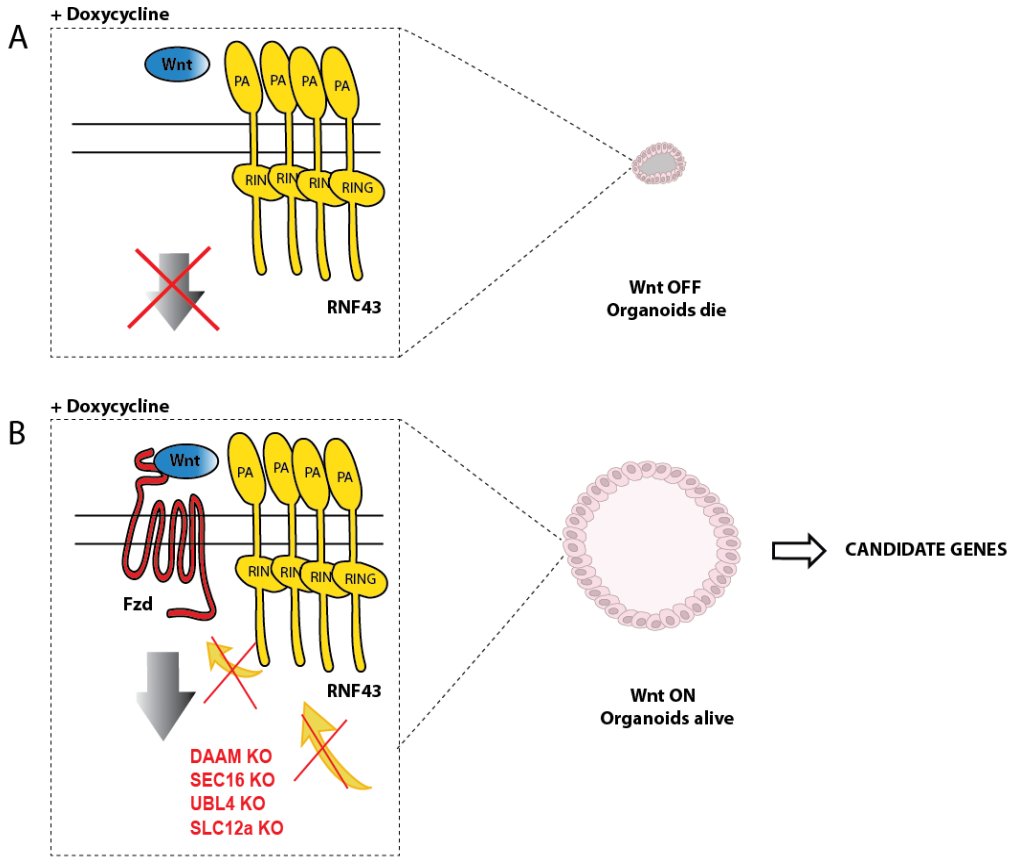

Figure 4.11 Schematic summary of candidate genes identified in the CRISPR knockout screen in iRNF43 intestinal organoids. When iRNF43 organoids are treated with doxycycline, Frizzled is depleted from the cell surface causing WNT pathway shut down and organoid death **(A)**; however, ablating the following genes selected from RNF43 IP-MS hit lists allowed iRNF43 organoids to overcome the harmful effects of RNF43 overexpression and survive in doxycycline-supplemented medium: *Daam, Sec16, Ubl4 and Slc12a* **(B)**.

Chapter 5

The role of DAAM in RNF43-mediated clearance of Frizzled from the plasma membrane

5.1 Aims of the chapter

The CRISPR/Cas9 screen in iRNF43 organoids combined with growth factor withdrawal experiments proved to be a fruitful approach resulting in the identification of novel candidates with functional links to RNF43 activity or WNT/β-catenin pathway regulation. In particular, DAAM1 could be pinpointed as a potential new regulator of RNF43-mediated Frizzled internalisation.

As a matter of course, DAAM has always been described in the context of the non-canonical WNT PCP pathway as a protein which interacts with Dishevelled to activate the small GTPases, RAC1 and RHOA, and promote cytoskeleton remodelling via JNK activation (Oishi et al. 2003). Nevertheless, what I aim for in this chapter is to characterise this protein in a

different context, which is the regulation of Frizzled surface levels within the canonical WNT/β-catenin signalling pathway.

In order to understand how DAAM might participate in Frizzled downregulation, I employed *in vitro*, cell-based assays to analyse receptor behaviour in the presence or absence of DAAM upon RNF43 overexpression, in terms of the following:

1) mature Frizzled levels;
2) dynamics of Frizzled endocytosis;
3) levels of Frizzled ubiquitination.

Furthermore, I also examined the physical interaction between epitope-tagged versions of RNF43 and DAAM.

Lastly, a separate goal of this study was the generation of a conditional DAAM1/2 double knockout mouse line to investigate the role of these genes *in vivo* in the murine intestine and to assess whether their depletion could still recapitulate the RNF43&ZNRF3 knockout phenotype.

5.2 Results

5.2.1 Characterisation of DAAM function *in vitro*

Organoid-based approaches highlighted DAAM as a potential interaction partner of RNF43, and the fact that this protein was already classified as interacting with Dishevelled (DVL) made it of particular interest in the context of regulation of Frizzled surface levels. Given its classification as a DVL interactor, I speculated that both DVL and DAAM together could be required for the efficient clearance of Frizzled from the cell surface and that perhaps DAAM was the missing piece within previously described DVL-mediated downregulation of Frizzled. Previous studies on this topic have failed to adequately describe the mechanism by which DVL promotes Frizzled clearance, although such studies did report cooperation of DVL with RNF43 (Jiang et al. 2015; Tsukiyama et al. 2015). Despite this advance, it is still unknown which region of DVL is responsible for RNF43 binding,

whether their binding is direct, and why RNF43 deletion mutants that have lost the ability to interact with DVL can still downregulate WNT/β-catenin pathway activity.

To investigate this topic further and to try to understand the role of DAAM within the context of DVL-mediated Frizzled clearance, *DAAM1* and *DAAM1/2* knockout cell lines were generated in order to perform cell-based assays in collaboration with Dr. Jihoon Kim. For this purpose, human embryonic kidney (HEK) 293T cells were chosen as they possess the complete and intact WNT pathway machinery and, for this reason, are often employed in the investigation of both canonical and non-canonical WNT signalling.

Thus, CRISPR/Cas9 technology was applied to HEK293T cells to obtain several clones with small frameshift mutations which were confirmed by TIDE analysis (Tracking of Indels by Decomposition, an online tool for quantitative assessment of CRISPR gene editing). While conducting TIDE analysis, it was possible to notice that some of the mutant clones displayed a small fraction of cells with a wildtype genotype; this could be due to contamination from WT cells during clone handling prior to genotyping or to reversion of frameshift mutations to in-frame modifications (**Figure 5.1 A**).

Thus, an alternative approach that allowed the generation of additional CRISPR knockout clones was pursued in order to achieve insertion/deletions of larger portions of DNA (~220 bp); in this way PCR-based genotyping could be utilised to identify mutant clones and the risk of reversion was eliminated (**Figure 5.1 B**). While depletion of DAAM1 protein could be confirmed by Western Blot for all the clones, loss of DAAM2 could not be verified due to the lack of a specific commercial antibody; in order to circumvent the problem, AbFrontier was requested to produce a rabbit polyclonal antibody against DAAM2.

Nevertheless, all the knockout clones described were employed in the analysis of the internalisation and ubiquitination behaviour of Frizzled5, a member of the WNT receptor family that was formerly reported as being prominently expressed in small intestinal epithelium (van Es et al., 2005).

First, Frizzled5 endocytosis upon RNF43 overexpression was compared to WT cells in all the *DAAM* mutant cell lines with small frameshift mutations; pulse chase experiments with a SNAP-tagged version of Frizzled5 were conducted at different time points and, interestingly, they revealed that Frizzled internalisation was impaired in *Daam1/2* KO cells

(**Figure 5.2**). For instance, while *RNF43* overexpression could induce rapid receptor internalisation in WT cells, very little internalisation was observed following *RNF43* overexpression in the two different *DAAM* double KO clones with small frameshift mutations. Although Frizzled endocytosis did still occur in mutant cells, it was greatly reduced and cells could retain surface receptor labelling even after 2 hours compared to wildtype.

A

Clones		Daam1	Daam2
C4	Daam1 KO	85% +1; wt 2%	wt
H11	Daam1/2 KO	12% -2; 9% -12; 12% -20	96% -17
B11	Daam1/2 KO	73% +1; wt 11%	91% +1

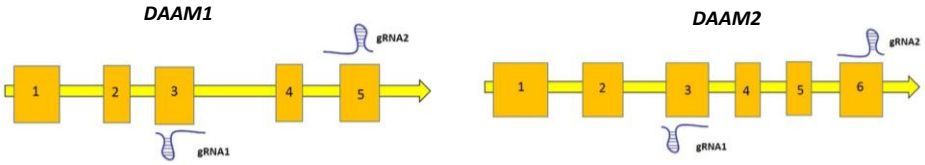

B

Clones	
A6	Daam1 KO
E1	Daam1 KO
A7	Daam1/2 KO
G1	Daam1/2 KO

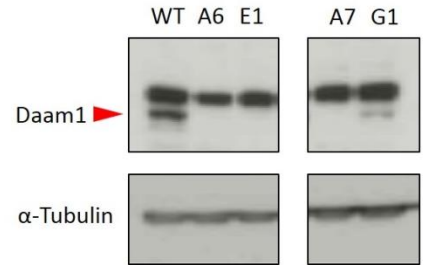

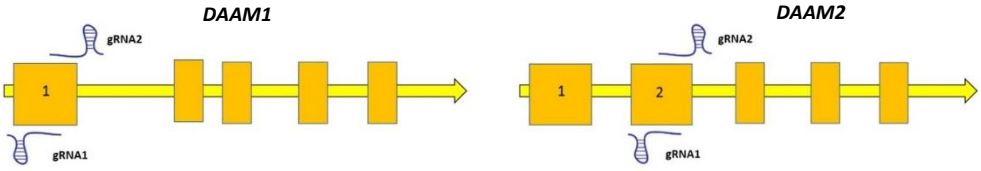

Figure 5.1 Daam KO HEK293T clones. **A)** *DAAM1* and *DAAM1/2* knockout HEK293T cells generated using CRISPR/Cas9 technology. The genotype of each clone is displayed in the table (from TIDE analysis) and the schematic below illustrates which exons are targeted by the different gRNAs. **B)** Additional DAAM KO clones with a representative western blot showing DAAM1 levels in the clones (right). These clones were generated by using a different CRISPR strategy targeting two gRNAs 200bp from each other against each gene. Such a large deletion allows PCR-based genotyping. The schematic illustrates which exons are targeted by the different gRNAs.

Because HEK293 cells are subject to large inter-clone variations in phenotype, pulse chase experiments were repeated with the additional *DAAM* KO clones created by deletion of larger genomic regions (**Figure 5.3**). When further clones were analysed, it was clear that there were large differences in terms of the dynamics of Frizzled internalisation between the mutant lines; in fact, only one *DAAM1* KO clone retained Frizzled surface labelling after a 2-hour chase, whereas the receptor was seen to be internalised over time in all other clones at a rate similar to that of WT cells.

Although all images shown here are representative of the relative cell populations, quantification will provide more solid basis to infer on each clone's behaviour.

Nevertheless, given the great variability of the dynamics of Frizzled internalisation between clones, I could not conclude that the endocytosis of Frizzled was altered in the absence of DAAM, although some clones did show a loss of internalisation upon loss of DAAM.

In order to examine the internalisation of Frizzled over a longer time period, mature levels of V5-tagged Frizzled5 were checked by western blot 2 days after transfection in both WT and mutant cells, before and after RNF43 overexpression.

This longer-term investigation demonstrated that the overexpression of RNF43 reduced Frizzled5 levels in both WT and *DAAM* KO cells in a comparable fashion; this effect was clone-independent and could be rescued by Bafilomycin treatment, which inhibits lysosomal protein degradation (**Figure 5.4**).

Surface levels of V5-Frizzled5 were also investigated by FACS indirect staining with PE-Texas Red®-conjugated antibody in *DAAM1/2* knockout cells 2 days post-transfection. Once again, it was possible to observe complete Frizzled internalisation in both WT and mutant cells upon RNF43 overexpression (**Figure 5.5**). Interestingly, it was also noticeable that without RNF43 overexpression *DAAM* KO cells seemed to display higher levels of Frizzled5 at the cell surface when compared to WT, not only as a proportion of the population but also in terms of Texas Red intensity.

However, despite an initial delay in some clones, Frizzled5 was cleared from the cell surface with comparable efficiency in WT and *DAAM* KO cells.

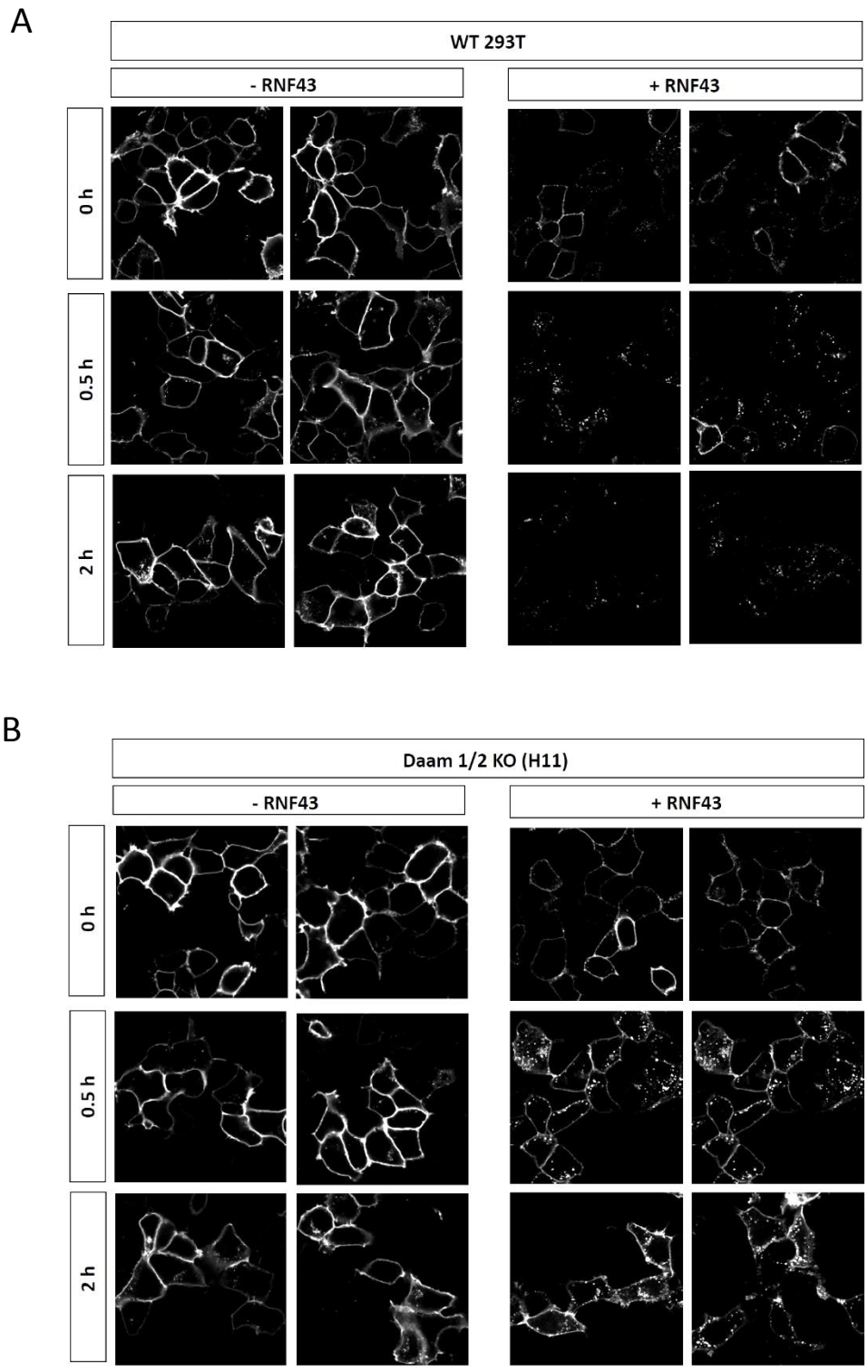
A
WT 293T
- RNF43
+ RNF43
0 h
0.5 h
2 h
B
Daam 1/2 KO (H11)
- RNF43
+ RNF43
0 h
0.5 h
2 h

C

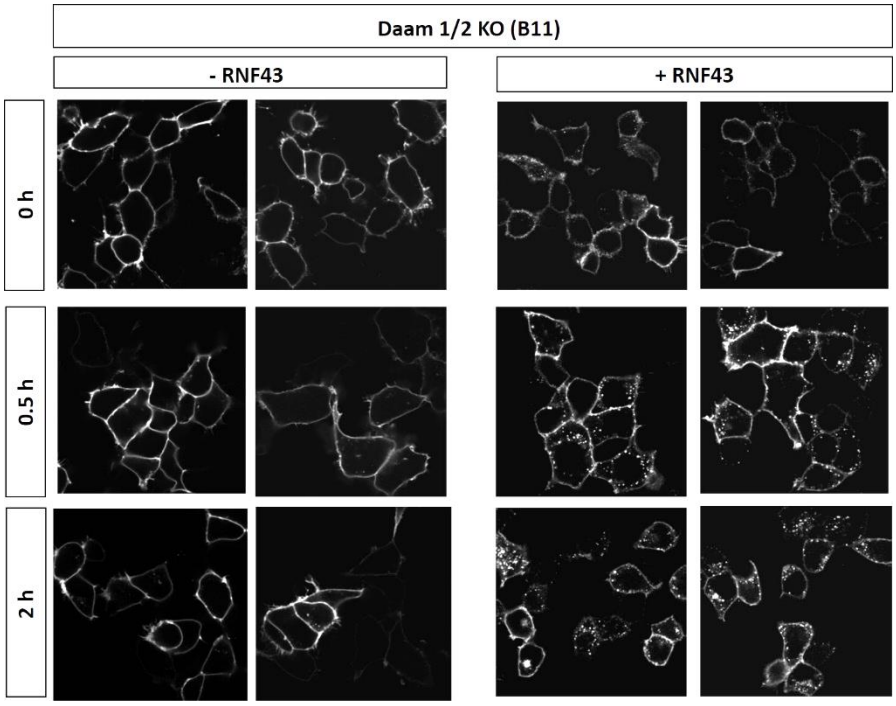

Figure 5.2 Dynamics of Frizzled internalisation in DAAM KO cells. Pulse chase experiments of SNAP-Frizzled5 comparing WT cells (panel A) and two *DAAM1/2* KO clones (panel B and C). Whereas *RNF43* overexpression causes a rapid internalisation of Frizzled5 in WT cells **(A)**, both *DAAM1/2* KO clones retain significant surface labelling, even after 2 hours **(B, C)**. The presence of intracellular puncta suggests that these cells are not completely deficient in the ability to internalise Frizzled, but internalisation is decreased compared to wildtype cells.

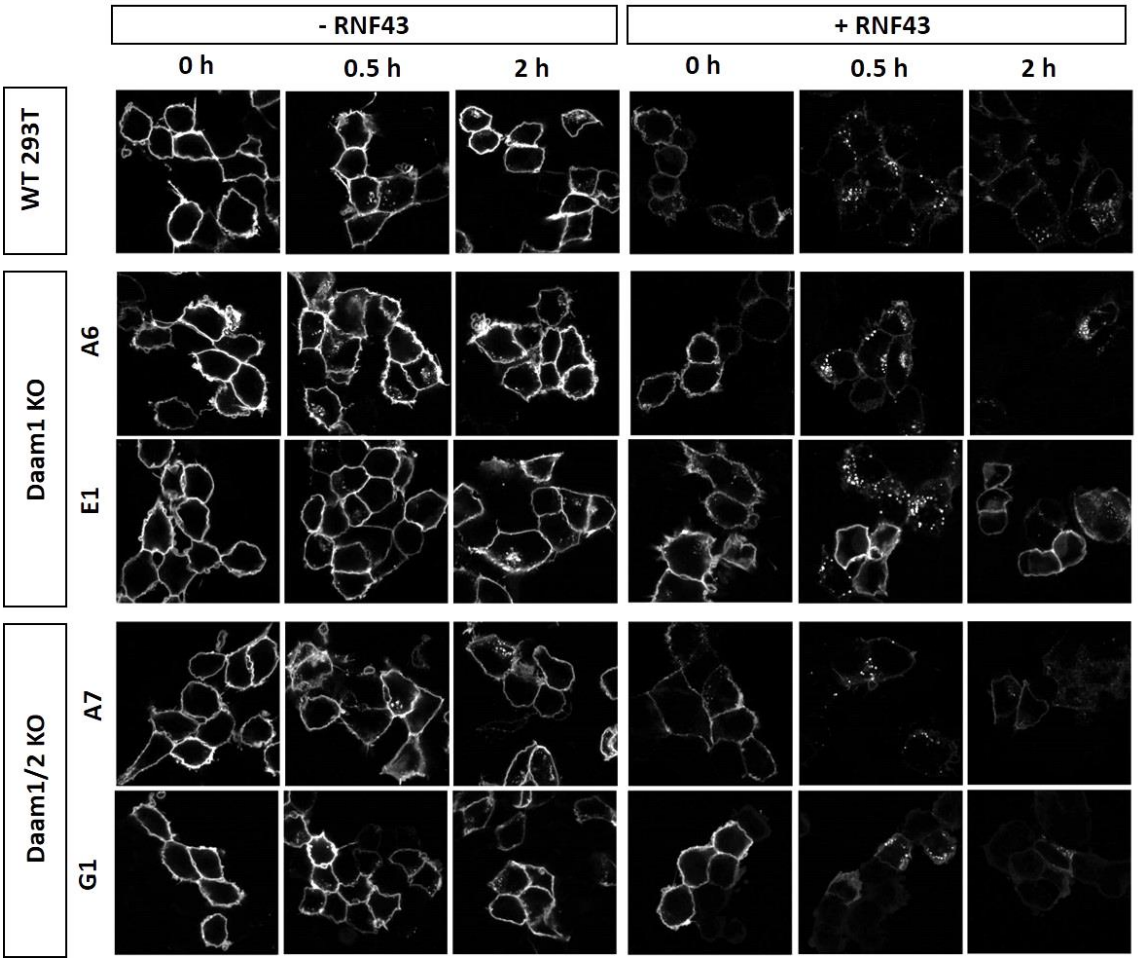

Figure 5.3 DAAM mutant clones display variable dynamics of Frizzled internalisation. Pulse chase experiments of SNAP-Frizzled5 with additional *DAAM* KO clones. While Frizzled labelling appears to be slightly higher in *DAAM* mutant clones when compared to WT cells at time 0 upon RNF43 overexpression, surface levels of the receptor decrease over time at a comparable rate in all samples, except for *DAAM1* KO clone E1 which retains Frizzled labelling even after 2 hours, as observed with the original *DAAM* KO H11 and B11 clones.

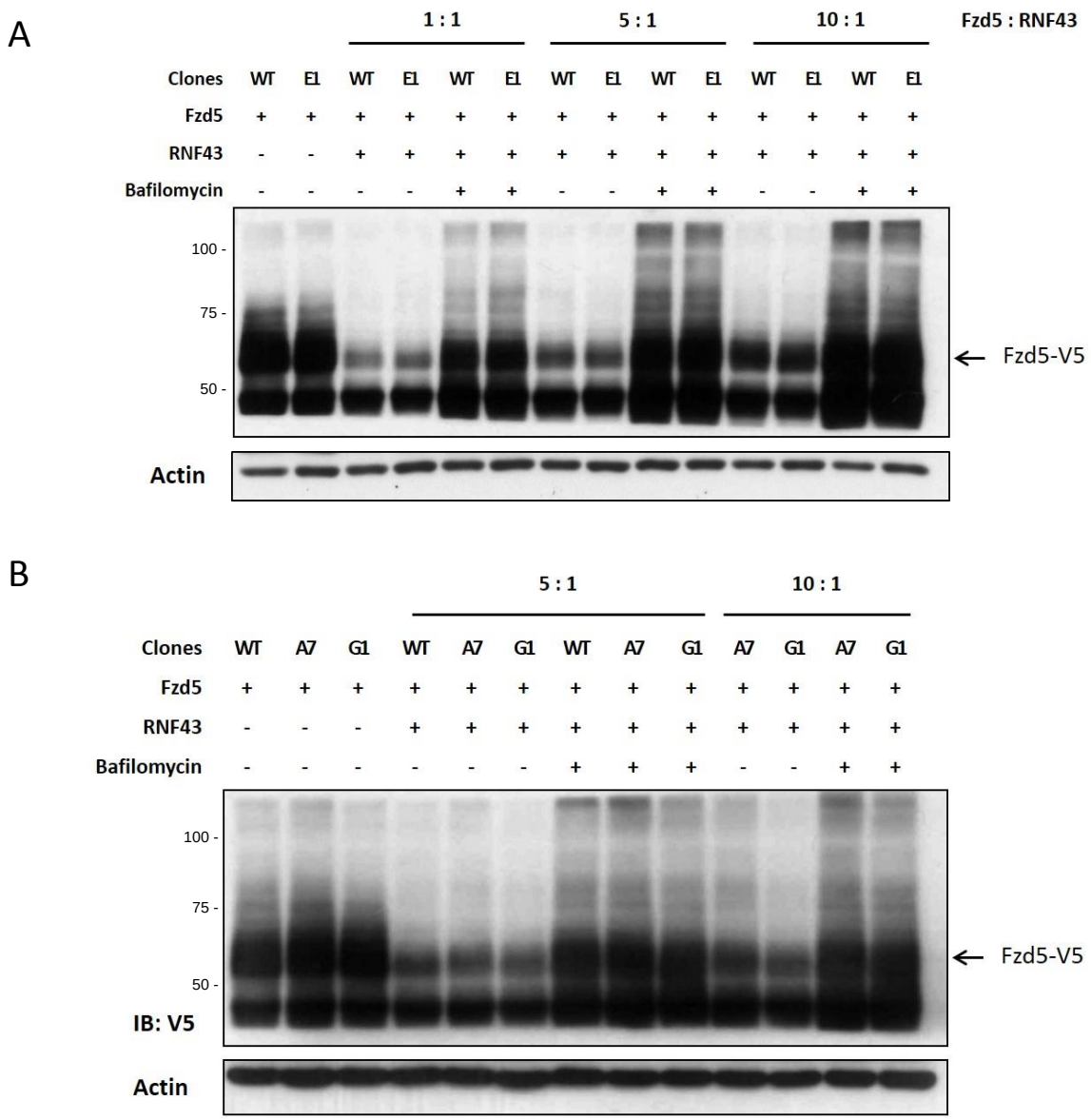

Figure 5.4 RNF43 overexpression reduces Frizzled5 levels in both WT and Daam KO cells. Western blot comparing mature FZD5 levels in WT and *DAAM* KO HEK293T 2 days post-transfection. Regardless of FZD5:RNF43 transfection ratio, RNF43 overexpression reduces Frizzled5 to comparable levels in both WT and *DAAM1* KO cells (E1 clone, **A**). Bafilomycin treatment can restore FZD5 to basal levels under all conditions by inhibiting lysosomal protein degradation. **B**) A similar decrease in Frizzled5 levels is seen in both WT and *DAAM1/2* double KO cells (A7 and G1 clones).

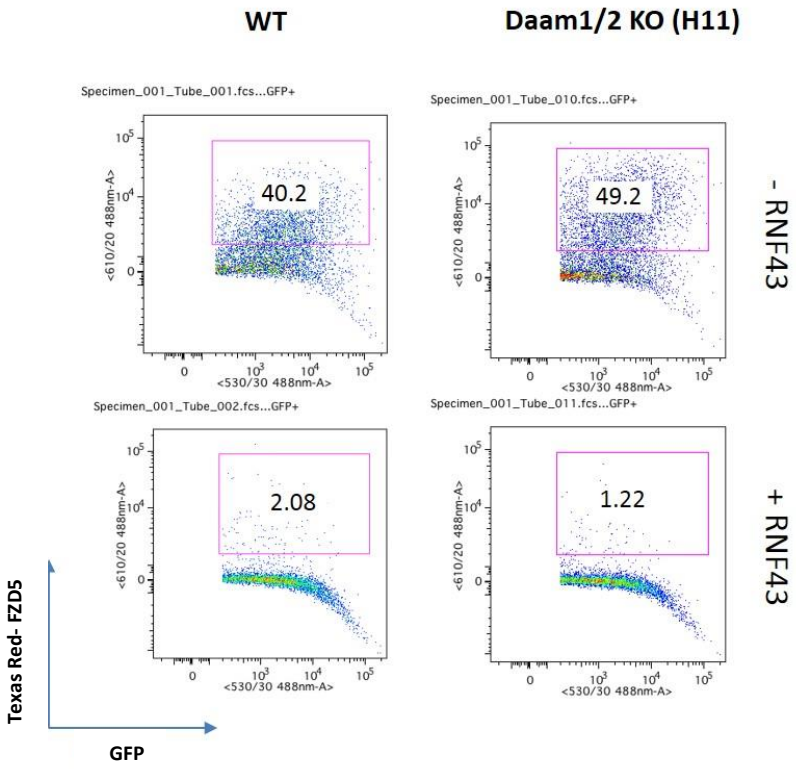

Figure 5.5 Frizzled5 surface expression is downregulated following RNF43 overexpression in both WT and DAAM KO cells. FACS analysis of V5-Frizzled5 surface levels revealed that RNF43 overexpression could induce receptor internalisation in both WT and *DAAM* KO cells (H11 clone) to a comparable level. Surface levels of V5-FZD5 were analysed by staining with a PE-Texas Red®-conjugated secondary antibody in GFP⁺-gated cells 2 days after transfection.

Given that Frizzled endocytosis did not seem to be significantly affected by the absence of DAAM, ubiquitination of Frizzled was investigated next.

Immunoprecipitation of V5-Frizzled5 followed by western blot against HA-ubiquitin showed that RNF43 overexpression was able to induce ubiquitination of Frizzled in both WT and *DAAM1* KO cells. Bafilomycin treatment increased the level of ubiquitination in both WT and *DAAM1* KO cells. Moreover, levels of receptor ubiquitination again appeared to be very similar between knockout and control, suggesting that Frizzled5 ubiquitination was unlikely to be impaired in the absence of DAAM (**Figure 5.6**).

However, before concluding that Frizzled surface levels are not regulated by DAAM in HEK293T cells, the same experiments should ideally be repeated by looking at the *global* endogenous population of Frizzled receptors.

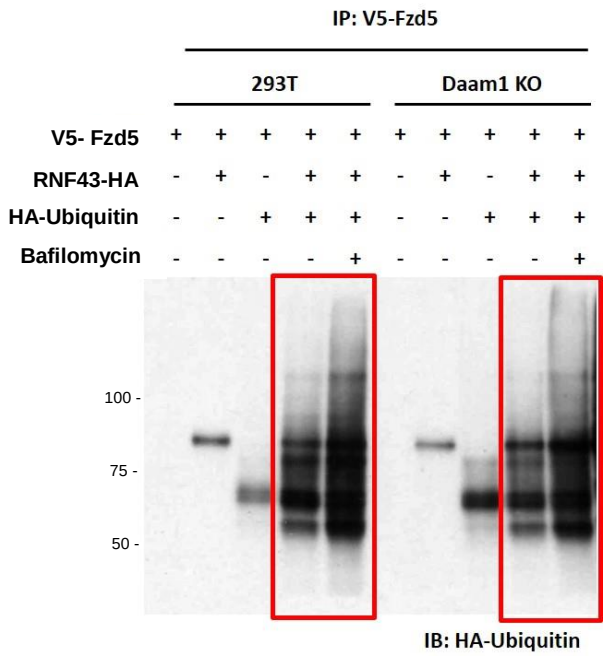

Figure 5.6 Frizzled5 ubiquitination levels are unchanged in DAAM KO cells. Ubiquitination assay showing that, in both WT and *DAAM1* KO cells, RNF43 overexpression leads to augmented Frizzled5 ubiquitination. No significant difference can be observed in FZD ubiquitination levels between WT and mutant cells (red rectangles). Bafilomycin treatment emphasises accumulation of the ubiquitinated receptor.

Finally, to check whether DAAM1 and RNF43 could physically interact with each other, co-immunoprecipitation experiments were performed on epitope-tagged proteins. I could not detect evidence of direct physical interaction, as only a faint band could be seen on the western blot after a long exposure.

However, when DVL2 was co-transfected with RNF43 and DAAM1, it was possible to detect an interaction between DAAM1 and RNF43 (**Figure 5.7**). The observation that DVL2 seems required to trigger DAAM1 binding to RNF43 is quite interesting and supports my initial hypothesis of a ternary complex regulating the RNF43-mediated downregulation of Frizzled.

This result raised various questions: what are the respective roles of DAAM and DVL? Do they cooperate to enhance RNF43 function? Does DAAM act as a cofactor for DVL, or are both equally important?

Given the inconclusive nature of the results presented in this section, it is clear that further investigation to elucidate the role of DAAM is needed and experiments to better characterise its *in vitro* function are ongoing.

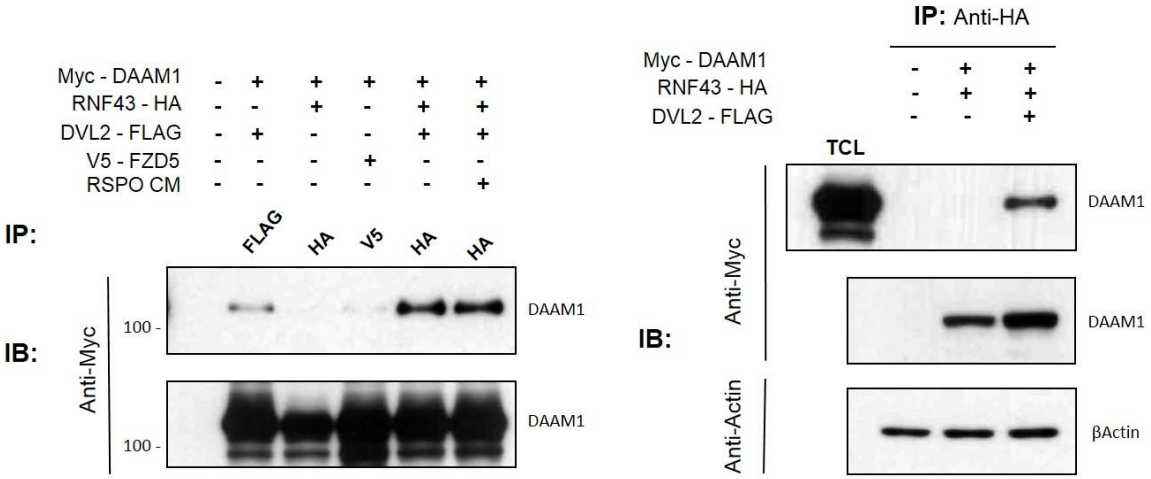

Figure 5.7 An interaction between RNF43 and DAAM1 is detectable in the presence of DVL2. Co-immunoprecipitation experiments demonstrate that Myc-DAAM1 can interact with DVL2-HA, but not with RNF43-FLAG or FZD5-V5. However, when DVL2 is co-transfected with RNF43-FLAG and Myc-DAAM1, it possible to observe a DAAM1 band in the FLAG pull-down (red rectangles). Of note, pre-treating cells with RSPO-conditioned medium does not have any effect (left).

5.2.2 Study of the *in vivo* role of *Daam* in the small intestine

The majority of the *in vivo* studies investigating *Daam1* and *Daam2* have been conducted on *Drosophila* and *Xenopus* and have highlighted the importance of these genes in the regulation of actin cytoskeleton organisation and in tissue morphogenesis (Prokop Andreas et al. 2011).

Mouse genetic studies have also confirmed a prominent role for *Daam1* in development, as *Daam1*-deficient mice exhibited embryonic and neonatal lethality due to several cardiac abnormalities (Li et al. 2011). More recently it has been shown using a conditional double knockout approach that both *Daam1* and *Daam2* are required for cardiomyocyte maturation (Ajima et al. 2015) but until now, no reports have attempted conditional depletion of both genes in the intestine.

Consultation of the Catalogue Of Somatic Mutations In Cancer (COSMIC) reveals a prevalence of point mutations in both *DAAM1* and *DAAM2* (especially missense) in human

tumours of the gut epithelium, at frequencies ranging from 2.21% to 3.82% in the intestine. By comparison, mutations in the well-known tumour suppressor *RNF43* are found in 5.77% of small intestinal tumours.

In light of the above, I decided to generate an intestine-specific *Daam1* and *Daam2* double knockout mouse model and to analyse whether *Daam* depletion could recapitulate the *Rnf43*&*Znrf3* KO phenotype.

In order to accelerate the time-consuming process of mouse line generation, a line with ubiquitous inducible expression of Cas9 (Rosa26-floxed STOP-Cas9 or Rosa-iCas9 for simplicity) was imported and crossed with a tamoxifen-inducible, intestine-specific Cre-expressing line, VillinCre-ERT2.

Thence, the first step was to rederive ESC from double heterozygous mice and to apply our CRISPR-concatemer strategy to them in order to obtain a gRNA-carrying Rosa-iCas9::VillinCre-ERT2 ESC line. Our concatemer constructs are based on the MSCV retroviral vector backbone and thus can be exploited to infect ESC and stably modify their genome by gRNA integration (**Figure 5.8**).

Cells in which the gRNA expression cassette against *Daam1* and *Daam2* had been integrated were used for blastocyst injection and successfully contributed to chimera generation with 12.5% efficiency (90-95% chimerism). Injection of WT Rosa-iCas9::VillinCre-ERT2 ESC was carried out in parallel to create matching controls.

As a pilot study, preliminary experiments were conducted on adult chimeras which were injected with 3 mg of tamoxifen and analysed after either one or two weeks from induction. These time points were chosen based on the fact that *Rnf43*&*Znrf3* KO mice already show intestinal adenoma formation after one week from tamoxifen treatment (Koo et al, 2012). However, at these stages it was not possible to identify any morphological alteration or difference in the epithelium thickness of my gRNA-carrying chimeras compared to the wildtype control from hematoxylin and eosin staining (**Figure 5.9**). Thus, the sections were stained for Ki67 to evaluate whether gRNA-carrying mice were characterised by an increased proliferative activity, but this was not the case as both WT and gRNA-carrying mice showed comparable Ki67 staining at the bottom of the crypts. It would therefore

appear that depletion of *Daam1* and *Daam2* does not lead to a clear phenotype in these mice.

Immunohistochemistry for DAAM1 and DAAM2 levels is necessary to demonstrate that gene knockout has occurred as required, and that both proteins are absent in the intestine of gRNA-carrying chimeras. Only once this is confirmed it can be definitively concluded that no phenotype is evident 2 weeks from *Daam1/2* depletion in the mouse intestine.

Moving forwards with this part of the study, rederived ESC were shown to be germ-line competent and so further experiments are now ongoing with the progeny of the chimeras. For instance, it could be possible that a longer time is needed for *Daam* depletion to generate a phenotype when compared to *RZ* KO mice and it is also possible that this CRISPR-based system takes longer to achieve conditional knockouts compared to conventional strategies based on floxed genes. This is plausible as, following tamoxifen injection, Cre recombinase must translocate to the nucleus in intestinal cells and excise the stop codon in front of Cas9 to trigger its expression before the genes of interest can then be targeted.

In conclusion, I have presented an alternative system that could potentially be very useful for the generation of conditional knockout mouse lines in a timely manner.

This strategy has been employed to allow the double knockout of *Daam1* and *Daam2* in mouse intestine; although no manifest phenotype could be observed in preliminary experiments, further studies are still required to validate the efficacy of the strategy.

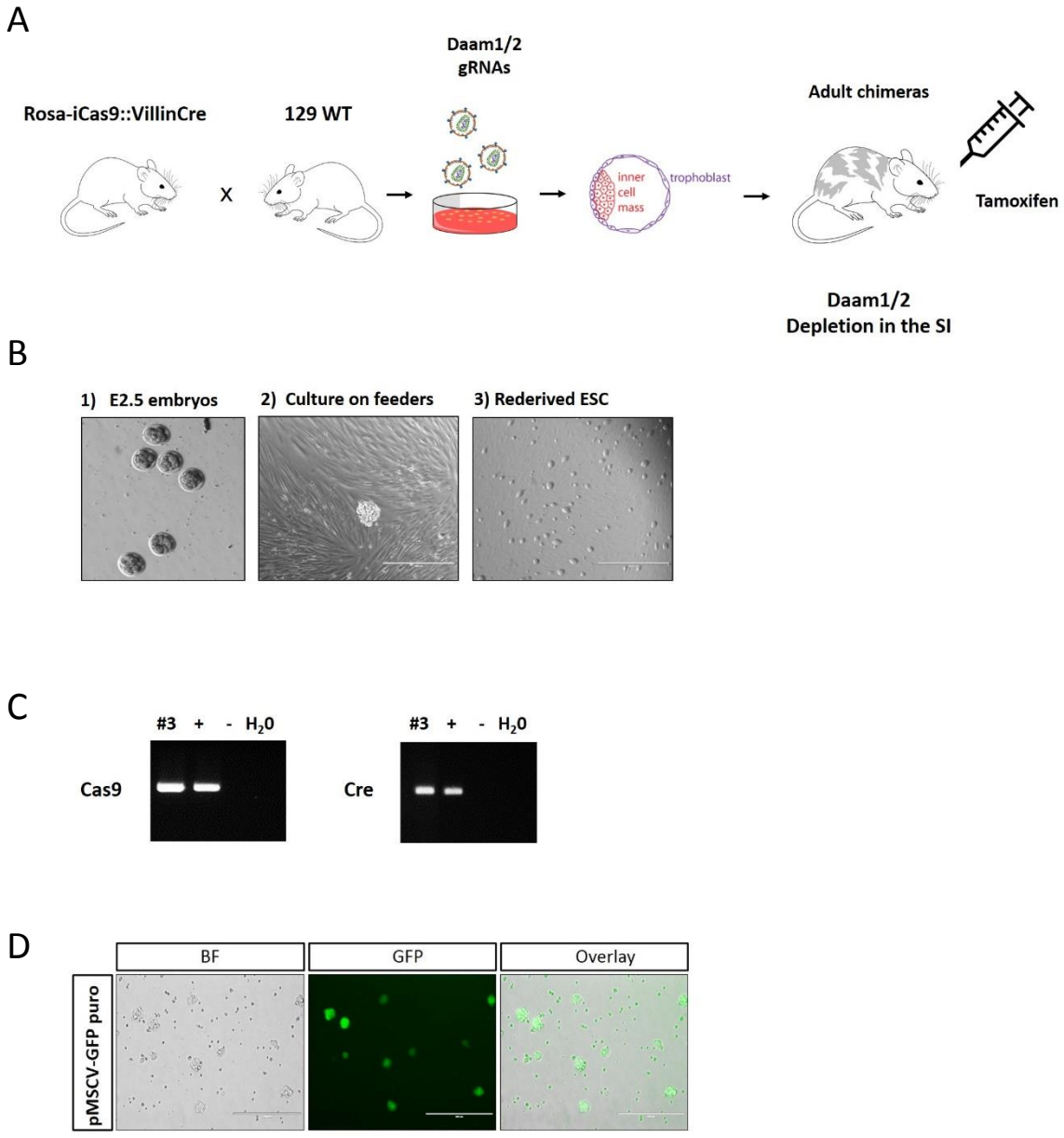

Figure 5.8 Daam1/2 conditional double knockout mouse generation. **A)** Schematic drawing illustrating the steps in conditional knockout mouse line generation. Double heterozygous Rosa-iCas9::VillinCreERT2 mice are crossed with WT 129 background mice to rederive ESC ready for viral infection of gRNAs against *Daam1* and *Daam2*. Infected ESC are then used to generate adult chimeras that can be injected with Tamoxifen to induce *Daam1/2* knockout in the mouse intestine. **B)** Representative pictures for the different steps in the ESC rederivation protocol: 1) culturing of E2.5 embryos; 2) attachment of the ICM (inner cell mass) to the feeder layer; 3) rederived ESC colonies growing on feeders. **C)** Genotyping PCR to confirm that clone #3 has inherited both alleles (Rosa-iCas9 and VillinCreERT2). **D)** Positive control for successful viral infection in rederived ESC (pMSCV-GFP).

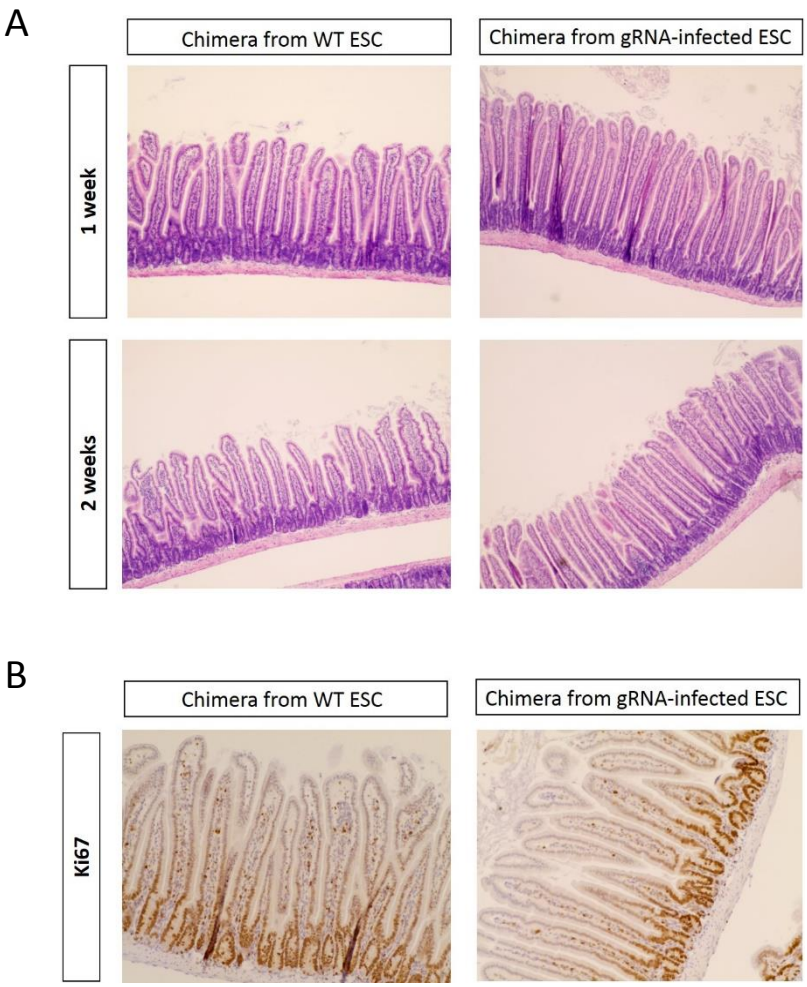

Figure 5.9 Cas9 induction does not result in any obvious phenotype in the small intestine of chimeric mice carrying gRNAs against Daam. **A)** H&E (hematoxylin and eosin) staining of mouse intestinal epithelium of RosaiCas9::VilCreERT2 chimeras obtained from injection of both WT and gRNA-infected ESC, 1 or 2 weeks after Tamoxifen administration. Cas9 induction does not seem to cause any morphological alteration in the epithelium of gRNA-carrying chimeras. **B)** Ki67 staining of mouse intestinal epithelium 2 weeks after Tamoxifen treatment does not show any increased proliferation in gRNA-carrying chimeras compared to wildtype chimeras.

5.3 Summary and conclusions

The CRISPR screen in intestinal organoids and subsequent growth factor withdrawal experiments highlighted DAAM as an interesting candidate for further study in order to characterise the mechanism of action of RNF43.

Thus, I started investigating the role of DAAM in RNF43-mediated downregulation of Frizzled through a series of *in vitro* assays aimed at examining Frizzled endocytosis and ubiquitination in *DAAM* knockout HEK293T cells compared to WT cells.

Pulse chase experiments suggested that upon RNF43 overexpression, Frizzled internalisation did not occur at the WT rate in *DAAM* KO clones as receptor surface labelling could be retained for up to 2 hours. However, with further analysis clone-to-clone variations in Frizzled endocytosis could be observed, and at least some of the mutant clones behaved similarly to the control. Further, complete removal of Frizzled from the cell surface could be achieved in the presence or absence of DAAM 2 days after transfection, as confirmed by both western blot and FACS experiments. In addition, no significant differences in Frizzled ubiquitination levels between *DAAM* KO and WT cells could be detected upon RNF43 overexpression.

Overall, it was surprising that the results of the cell-based assays did not support the phenotype and the hypothesised role of *Daam* observed in organoids; it is therefore planned to repeat all experiments by analysing endogenous receptors with a pan-Frizzled antibody in order to globally monitor all the Frizzleds expressed at the cell surface and not just Frizzled5. It cannot be excluded that different members of the Frizzled family may be subject to different mechanisms of regulation by RNF43.

One additional aspect worth pointing out is that my *in vitro* system in HEK293 cells is rather far from physiological conditions as it is based on overexpressed proteins. For instance, having large amounts of both Frizzled and RNF43 at non-physiological levels could increase their ability to interact by simple kinetics, potentially masking any effect of DAAM in promoting association at physiological levels.

On the other hand, it is also plausible that *Daam* has a context-dependent role, and that an immortalised cell line like HEK293 does not represent an appropriate system for the

study of its mechanism of action. If this is the case, checking Frizzled endocytosis and ubiquitination in mutant organoid lines will be essential.
Lastly, since HEK293 cells are of human origin and organoids are murine, potential specie-specific effects should be taken into account.

Based on recent reports demonstrating how the inhibitory activity of RNF43 relies on the presence of Dishevelled (Jiang et al. 2015; Tsukiyama et al. 2015), I postulated that DAAM could physically bridge RNF43 and DVL. Although this hypothesis was strengthened by my co-immunoprecipitation experiments showing that DVL2 overexpression seemed to induce DAAM1 binding to RNF43, additional experiments are necessary in order to generate evidence for the formation of a ternary complex. Biophysical methods for the study of endogenous protein complexes such as Proximity Ligation Assay (PLA) or Protein complementation assays (PCAs) will be key in the understanding of the interaction dynamics among RNF43, DVL2 and DAAM1.
For instance, the respective roles of each player are still unclear and further investigation is necessary; for example, DAAM and DVL could synergise in binding to RNF43, each with similar contributions to binding, or DVL could be the more important partner.
If it is true that DAAM has a secondary or partly redundant role compared to DVL, it could be worthwhile to perform the same *in vitro* experiments in a DVL mutant background to assess whether Frizzled internalisation and ubiquitination are affected under these circumstances.

In parallel to the *in vitro* studies, I also pursued the investigation of the role of *Daam in vivo* by adopting an alternative CRISPR-based strategy for generating a conditional *Daam1/2* knockout mouse line.
Preliminary experiments on adult chimeras injected with tamoxifen to induce Cas9 expression, and consequently gene knockout, have failed to highlight differences in morphology and proliferation activity in the intestine of gRNA-carrying mice compared to controls. However, proving that the system has worked and that both genes have been depleted in the intestinal epithelium is an absolute prerequisite for definitive conclusions.
In this regard, it is noteworthy to mention that the alternative strategy I employed relies on the concerted action between an inducible Cas9 and constitutively expressed gRNAs

and it might not be as efficient as expected in terms of knockout induction. We ignore, for example, the number of copies of retroviral DNA (the concatemer vector against *Daam1/2*) that got inserted into ESC genome following their infection and thus it is not possible to predict whether the gRNA dosage in each cell is sufficient for Cas9 activity.
In addition, this is the first time that our concatemer strategy has been applied *in vivo* and we are still in the process of assessing its efficiency and robustness. For this reason, all mouse experiments will be repeated with existing conditional *Daam* KO lines as a backup plan in case my system turns out to be unsuitable.

Taken together, the observations made so far have pointed out on one hand potentially conflicting data between two different in vitro systems, while on the other hand they have hinted promisingly at the formation of a ternary complex between RNF43, DVL and DAAM. A deeper analysis of these membrane-proximal events, combined with *in vivo* studies, is now ongoing and will hopefully clarify the mechanism of RNF43-mediated Frizzled downregulation as well as the role that DAAM fulfils.

Chapter 6

Investigation of other PA-RING family members

6.1 Aims of the chapter

In recent years, several reports describing the role of E3 ubiquitin ligases in the regulation of membrane signalling have seen ubiquitination move to centre stage as a critical regulatory modification, especially in terms of membrane receptor remodelling (MacGurn et al. 2012). For instance, E3 ligases like Nedd4 and Cbl were shown, respectively, to regulate the FGF and EGF signalling pathways (Persaud et al. 2011; Umebayashi 2008), in the same way that RNF43 and ZNRF3 modulate the WNT pathway, namely by the ubiquitination of the signalling receptor leading to its subsequent internalisation.

Bioinformatics studies have identified an additional 10 transmembrane E3 ubiquitin ligases in human that are closely related to RNF43 and ZNRF3 through sequence homology and domain organisation; these proteins have therefore been designated as members of the the same gene family, the PA-RING family, which remains mostly uncharacterised.

In light of this, it is possible that additional PA-RING ligases could have a similar function to RNF43 by targeting signalling receptors, or more generally, transmembrane proteins, for degradation. In addition, I thought that elucidating the mechanism of action of RNF43 could provide new insights into other PA-RING family members and generalities of their molecular behaviour.

Amongst all of the many unexplored aspects and possible questions, I specifically focused on the following:

1) Addressing the potential involvement of other PA-RING members in the regulation of the WNT pathway, and
2) Identifying molecular targets for some representative members of the family.

This chapter describes how PA-RING ligases were overexpressed in mouse intestinal organoids in parallel with RNF43 to address the first question, and how Surface Proteome Analysis was employed in order to address the second question and identify new targets for the selected E3 ligases.

Overall, the ultimate goal of this study is to unravel the biological function of some of the uncharacterised PA-RING family members and potentially link them to the regulation of transmembrane proteins.

6.2 Results

6.2.1 Overexpression screen of PA-RING members in intestinal organoids

Given their remarkable structural similarity to RNF43 and ZNRF3, it is reasonable to assume that there could be additional PA-RING family members involved in the regulation of the WNT pathway.

In order to test this hypothesis, mouse intestinal organoids were employed once again as a physiologically relevant model system to perform gain-of-function experiments of uncharacterised PA-RING E3 ligases. As already outlined previously, the WNT pathway

plays a pivotal role in the maintenance of intestinal organoids, and for this reason, they represent a particularly useful system to study genes that could potentially be involved in the regulation of WNT signalling.

Therefore, PA-RING family members were cloned into a retroviral vector suitable for Cre-induced overexpression and before being transduced into WT organoids carrying the Villin-CreERT2 transgene; of note, PA-RING genes were placed downstream of a floxed dsRed cassette, removal of which allowed their overexpression (**Figure 6.1 A**). Protein expression of the candidate genes was confirmed by western blot using HEK293 cells transfected with the same retroviral vectors in which the dsRed cassette had been removed prior to transfection by amplification in Cre-expressing *E. coli* (**Figure 6.1 B**).

Stably transduced organoids were selected with Puromycin before being induced with 4-hydroxytamoxifen (4-OHT) to trigger overexpression of my genes of interest. The pMSCV loxP-dsRed-loxP-eGFP vector was used in parallel as a control to test the correct functioning of the cassette in organoids; for instance, when 4-OHT is administered to Villin-CreERT2 organoids, the dsRed cassette is removed and organoids lose dsRed fluorescence to acquire GFP expression (**Figure 6.2 B**, panels **V**-**VIII**).

Growth and survival of PA-RING-expressing organoids were then tested under two different culture conditions: standard ENR medium and in EN medium lacking RSPO.

AS RSPO is a strong WNT pathway agonist, it is an essential component of the growth medium that allows survival of intestinal organoids; consequently, if a gene involved in WNT pathway activation is overexpressed it should render organoids viable in the absence of RSPO, and similarly, overexpression of a gene involved in WNT signalling inhibition should lead to organoid death, as is observed with overexpression of RNF43.

As summarised in **Table 6.1**, none of the candidates caused organoid death when overexpressed, such as in the case of RNF43-overexpressing cultures, suggesting that no other PA-RING members play a similar role to RNF43 in downregulation of the WNT pathway. On the other hand, none of the candidates promoted organoid survival under RSPO withdrawal when overexpressed, indicating that none of them is involved in WNT pathway activation either.

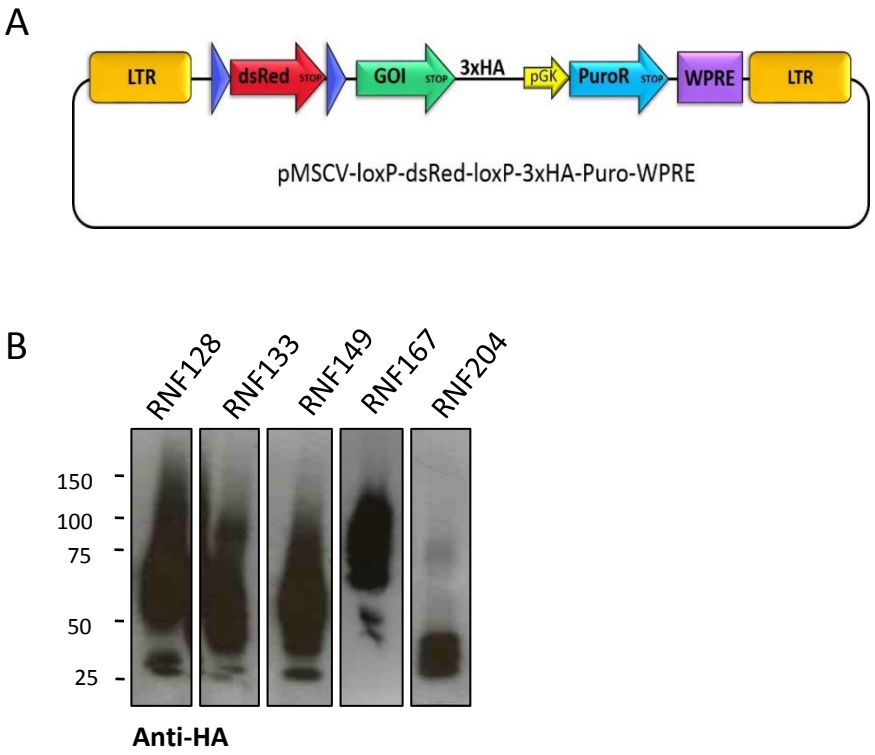

Figure 6.1 Retroviral construct for E3 overexpression in intestinal organoids.
A) Retroviral expression vector carrying the cDNA of my genes of interest (GOI) for their conditional overexpression in VillinCreERT2 organoids. The expression cassette is flanked by LTR (long terminal repeat) regions for genome integration and contains a floxed dsRed cassette upstream of the GOI. The Puro resistance cassette allows selection of stably transduced organoids and the WPRE sequence enhances expression of the construct. B) Confirmation by western blot of protein overexpression of PA-RING members in HEK293T cells.

Nevertheless, since I could not exclude any possible masking effects of paralog compensation, the same overexpression screen was conducted in Villin-CreERT2 organoids that lacked expression of both RNF43 and ZNRF3 (RZ KO). As a reminder, this organoid line displays the phenotype of survival in the absence of RSPO because WNT receptor levels are not downregulated.

As a result, while the overexpression of RNF43 led to rapid organoid death in both ENR and EN medium due to WNT pathway downregulation, the overexpression of other PA-RING family members did not affect organoid growth or survival (**Figure 6.3**). This indicated that

none of the PA-RING ligases behaved similarly to RNF43 by being able to revert the RZ KO phenotype when overexpressed.

Taken together, these data indicate that no E3 ligases in the PA-RING family, other than RNF43 and ZNRF3, are likely to be involved in modulation of the WNT pathway. Further, none of the candidates when overexpressed led to either organoid death under standard culture conditions or increased survival under growth factor withdrawal, suggesting that there are no members of the family acting either to inhibit or to promote WNT pathway activity, respectively.

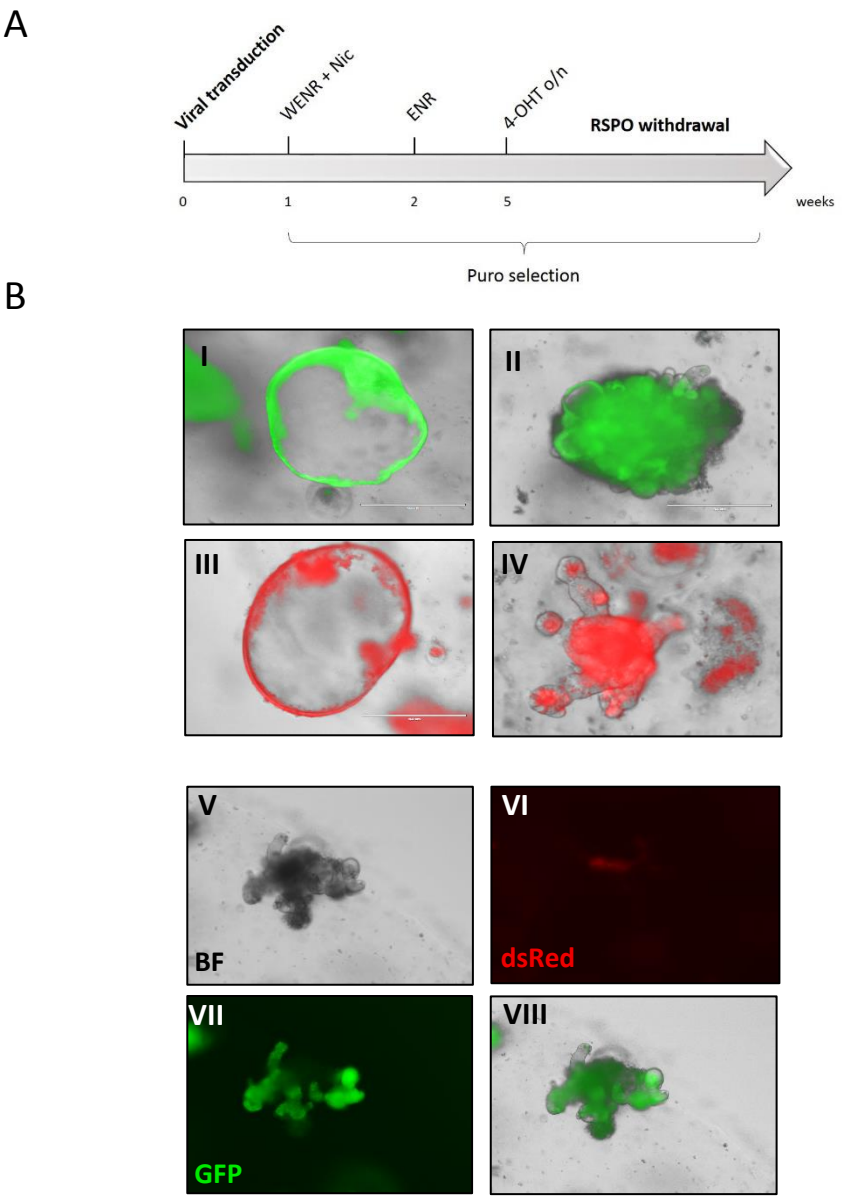

Figure 6.2 Viral transduction of intestinal organoids for E3 overexpression screening. **A)** Timeline of the overexpression screen of PA-RING members in intestinal organoids. *Continued on next page.* **B)** Organoids successfully transduced with pMSCV-eGFP display green fluorescence in WENR+Nic medium 3 days after infection (**I**) and in ENR medium 2 weeks after infection (**II**). Organoids successfully transduced with pMSCV-dsRed display red fluorescence in WENR+Nic medium 3 days after infection (**III**) and after 2 weeks in ENR medium (**IV**). Scale bar = 400µm. Panels **V-VIII** show an organoid transduced with loxP-dsRed-loxP-eGFP that has lost red fluorescence and has started expressing GFP 4 days after 4-OHT treatment. Scale bar = 400µm.

Table 6.1 Gain-of-function experiment using overexpression of PA-RING members in VillinCreERT2 intestinal organoids.

E3	Media condition	
	ENR	EN
GFP		
dsRed-GFP		
RNF43		
RNF148		
RNF150		
RNF167		
RNF215		
RNF128		
RNF133		
RNF149		
RNF13		
RNF204		

Survival
Death

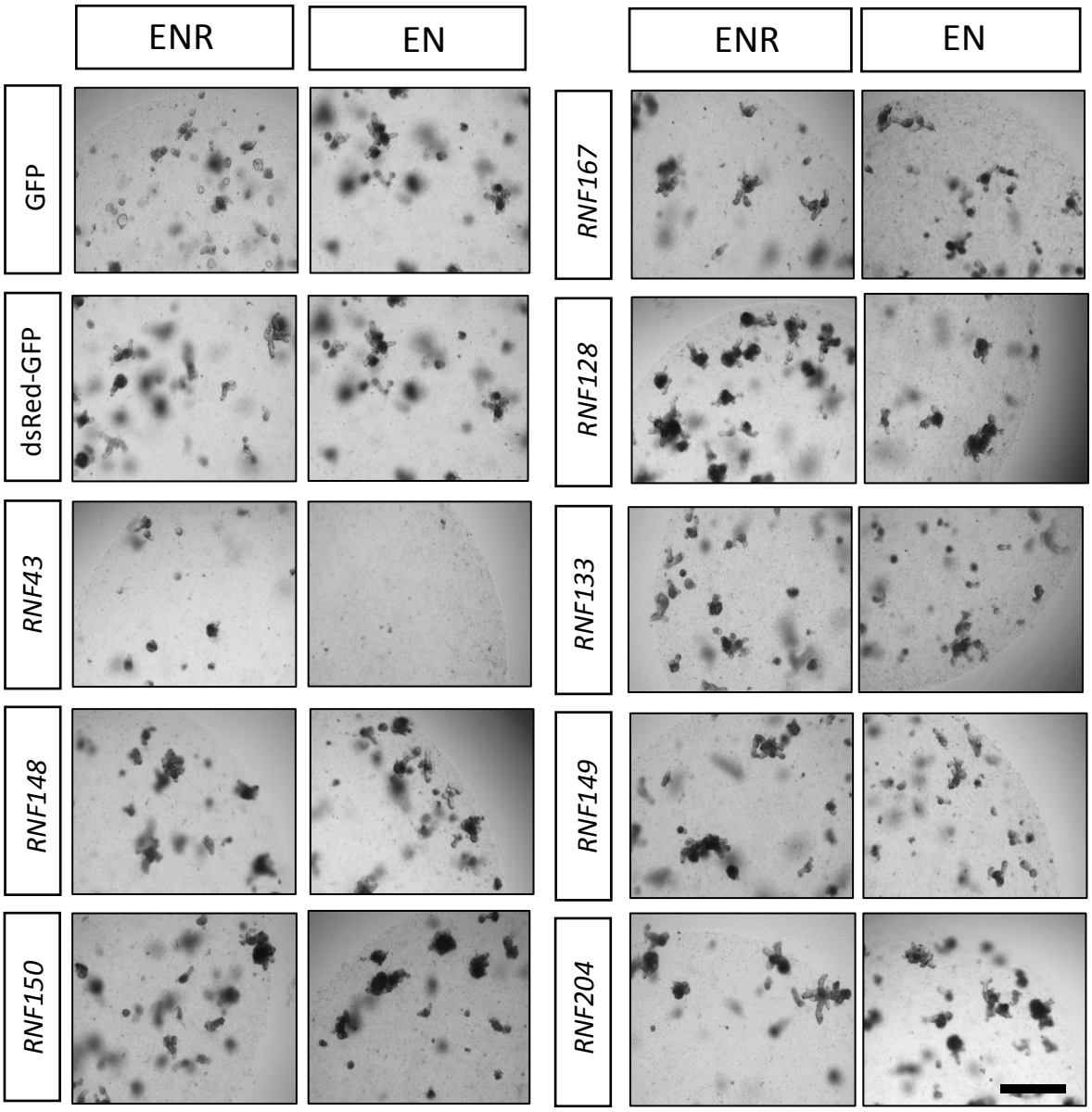

Figure 6.3 Gain-of-function experiment using overexpression of PA-RING members in RZ KO VillinCreERT2 intestinal organoids. Overexpression of PA-RING E3 ligases in RZ KO organoids after 4-OHT treatment, carried out in both ENR and EN media. While overexpression of RNF43 resulted in complete organoid death after passage 2 in both ENR and EN media, overexpression of other PA-RING family members did not affect organoid survival and cultures could be propagated over the course of 4 passages, suggesting that no other members of the family are likely to have a similar role to RNF43 and ZNRF3. Scale bar = 400 µm.

6.2.2 Identification of novel targets of PA-RING proteins by Surface Proteome Analysis

Overexpression experiments with additional PA-RING family members in intestinal organoids suggested that there are no additional members likely to interact with Frizzled receptors and to work in WNT pathway regulation. Hence, I next asked whether these members were involved in the regulation of some other signalling pathway or more generally in targeting transmembrane proteins for degradation. By address this question and investigating the molecular targets of some representative members of the family, it was hoped to gain more insight into PA-RING proteins and their biological function.

Accordingly, one member of each unexplored branch of the PA-RING family phylogenetic tree was selected for further characterisation through a proteomic approach. Based on their expression levels in various tissues, *RNF13*, *RNF128* and *RNF150* were selected because of their broad expression pattern (**Figure 6.4**). Stable HEK293 cell lines were generated for their inducible overexpression by exploiting the T-REx™ system based on dox-dependent Tet Repressor release from the Tet operator, as described in **Figure 6.5 A**. Single clones were screened by western blot for their capacity to express my HA-tagged genes of interest upon doxycycline treatment and their homogeneous expression was confirmed by immunocytochemistry (**Figure 6.5 B, C**). For completeness, my initial plan was to generate also RNF215-overexpressing cell lines but a series of technical difficulties hampered the study of the E3 ligase, which is the most closely related to *RNF43* and *ZNRF3*. Thus, two clones for each candidate gene were chosen to undergo Surface Proteome Analysis or SPA, a novel mass spectrometry-based technique developed by Dr. Koo to identify the targets of RNF43 (Koo et al, 2012). Briefly, the technique relies upon comparative mass spectrometry between membrane fractions of E3 ligase-overexpressing cells (dox-treated samples) and control cells (non-treated samples); this method should highlight those proteins whose levels are significantly reduced in dox-treated samples and who are therefore candidate targets for the E3 ligase of interest (**Figure 6.6**).

After treating cells with doxycycline overnight, surface proteins were labelled with biotin and subsequently pulled down by NeutrAvidin affinity to obtain membrane fractions that were then used in mass spectrometry.

A

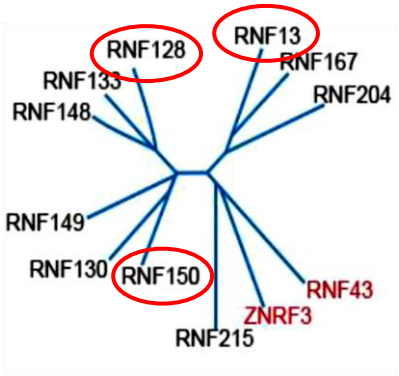

B

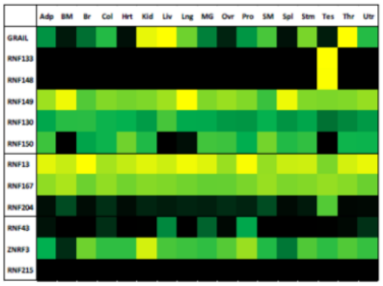

C

	Molecular weight	Expression in the mouse intestine
RNF43	86 kDa	Medium
RNF13	43 kDa	High
RNF128	46 kDa	High
RNF150	48 kDa	Low

D

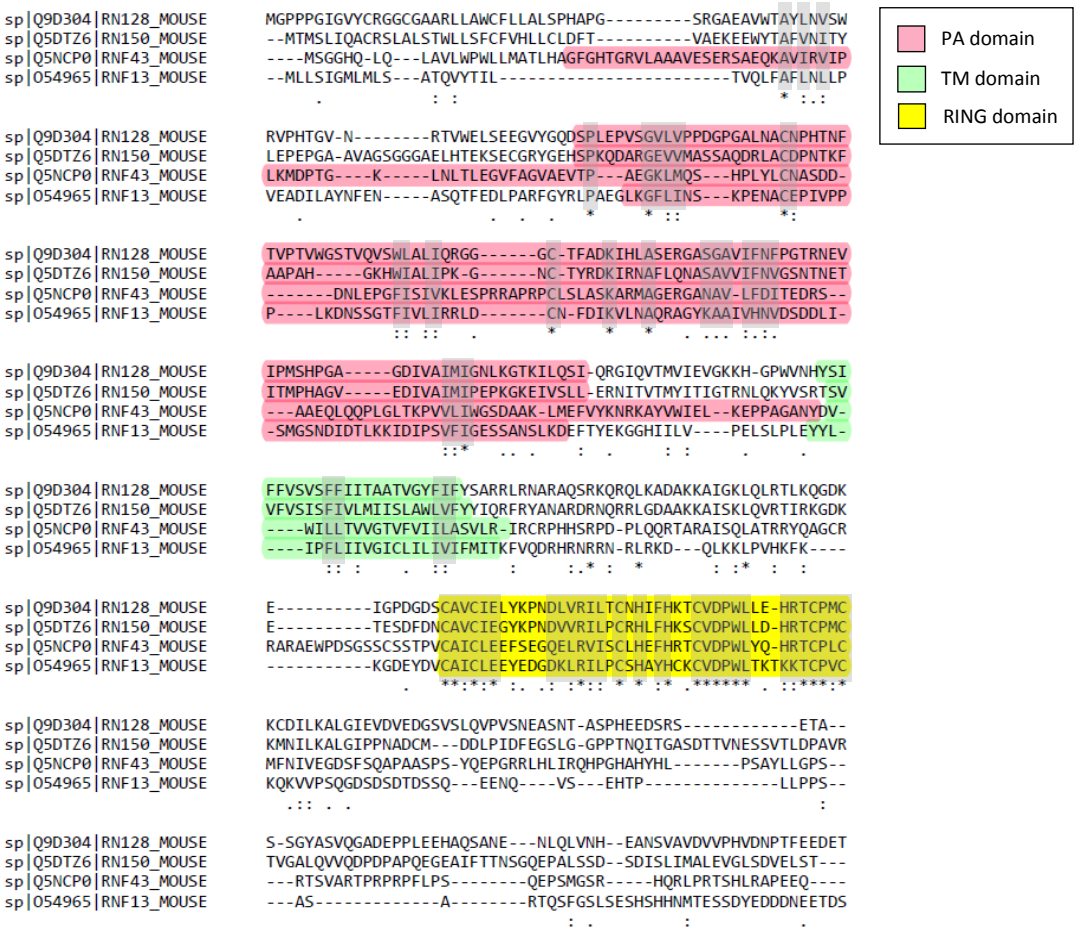

Figure 6.4 PA-RING protein comparison. **A)** RNF13, RNF128 and RNF150 were the selected PA-RING members for inducible cell line generation and proteomic analysis. *Continues on next page.*

Figure 6.4 PA-RING protein comparison. **B)** Expression profile of PA-RING family members in various tissues based on microarray data. The selected members have a broad expression profile. Black, no/low levels of expression; green, middle level of expression; yellow, high level of expression. **C)** Summary table of the selected members compared to RNF43. **D)** Partial sequence alignment between *Rnf43* and the selected members displaying domain conservation (ClustalW2). It is possible to notice a higher similarity between *Rnf128* and *Rnf150*.

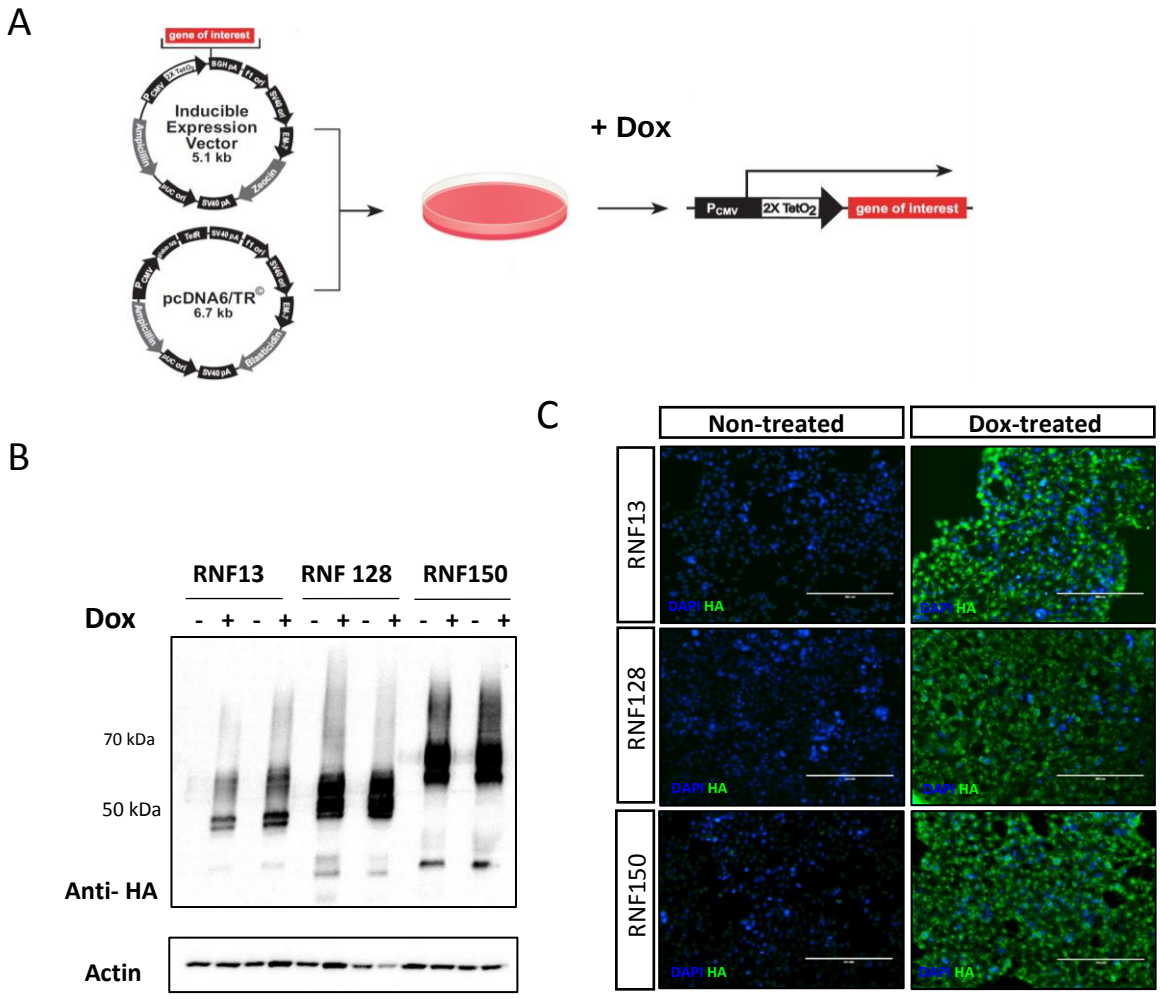

Figure 6.5 Generation and validation of doxycycline-inducible E3 ligase-overexpressing cell lines. **A)** T-REx™-293 cells were transfected with dox-inducible vectors containing the cDNA of the selected PA-RING family members, downstream of the Tet operator. Addition of doxycycline prevents the Tet repressor from binding to the operator and triggers the expression of my genes of interest (Tet-Off system). **B-C)** Western blot analysis and immunocytochemistry confirmed strong and homogeneous overexpression of each gene of interest after overnight doxycycline treatment. Scale bar= 200 µm.

When analysing the data, common contaminant species, such as nuclear and mitochondrial proteins, were filtered out and protein hits with a 10-fold difference between dox- and dox+ samples were shortlisted; then, gene ontology annotations (GO) were employed to narrow down the list of putative targets to those proteins containing a transmembrane domain, which were localised at the plasma membrane and involved in signalling transduction. The identification of known targets in my lists that are already described in the literature validates the reliability of my approach; for example, CD81 has been previously reported in the literature to be targeted by RNF128 (Lineberry et al. 2008) and was also present as a hit in my analysis.

The results of the identification process are summarised in **Tables 6.2-6.4**, which list the putative targets of each PA-RING ligase identified by SPA divided into two columns: proteins that are significantly downregulated and proteins that are absent in dox-treated samples compared to controls.

A point worth highlighting is that some common trends can be observed by looking at the data: for example, the overexpression of each individual E3 ligase affects different classes of adhesion molecules as well as membrane transporters and G-protein coupled receptors (GPCRs). In particular, overexpression of the T cell anergy mediator RN128 seems to markedly reduce the abundance of tight junction proteins, such as ZO-1 and Occludin, and some GPCRs, together with G protein subunits and GPCR-associated proteins; overexpression of RNF150 instead seems to lead to a specific depletion of adherens junction proteins at the membrane.

On the other hand, it is possible to notice a certain overlap between RNF128 and RNF150 as they share some putative targets, such as CD44 antigen, G-protein subunits and the G-protein associated Rhodopsin kinase; this is in accordance with the fact that these two E3 ligases are closer to each other in terms of phylogenetic distance when compared to *RNF13* and display a higher sequence similarity (**Figure 6.4 A, D**).

In conclusion, this recently described proteomics method allowed us to shortlist candidates that may potentially be novel molecular targets of the selected PA-RING family members. As could be expected considering the limited information about PA-RING

members, none of the hits had ever been associated with any of these E3 ligases before, not even to the best-characterised member, RNF128.

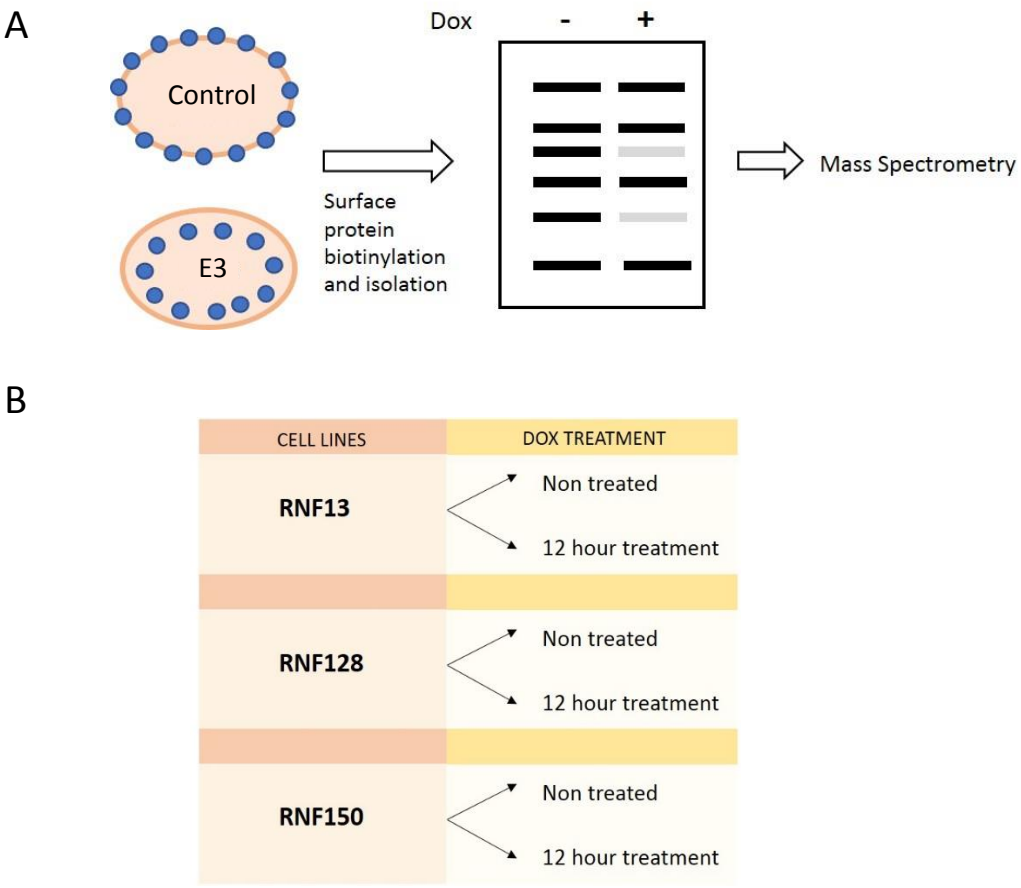

Figure 6.6 Surface Proteome Analysis (SPA). **A)** SPA is the technique that led to the identification of Frizzled as a target of RNF43 (Koo et al, 2012). Cells overexpressing the E3 ligase of interest (+ dox) and control cells (- dox) are both subjected to biotin labelling of surface proteins, which are then pulled down and analysed by mass spectrometry. The comparison between dox-treated and non-treated samples will reveal those proteins whose levels are significantly reduced upon overexpression of the E3 ligase of interest, and which could therefore be its putative targets. **B)** Sample overview: 3 different cell lines were employed, each of which was left untreated or treated with 1 µg/µl doxycycline for 12 hours and then subjected to biotin labelling and pull-down.

Table 6.2 Proteins downregulated by RNF13 overexpression.

RNF13 OE			
Absent proteins		**Downregulated proteins**	
Name	**GO annotations**	**Name**	**GO annotations**
Embigin	neuromuscular junction formation	Integrin beta-5	cell-matrix adhesion
Nectin-3	adherens junctions	Neuroplastin	cell adhesion molecule at synapses
Limbic system-associated membrane protein	cell-cell junctions	Sodium-coupled neutral amino acid transporter 1	transporter activity
Junctional adhesion molecule B	tight junctions	Folate transporter 1	transporter activity
Junctional protein associated with coronary artery disease	adherens junctions		
Pleckstrin homology domain-containing family A member 7	endosome fusion		
Utrophin	cell-matrix adhesion		
Ephrin type-A receptor 1	signalling receptor		
Adhesion G-protein coupled receptor G2	G-protein coupled receptor activity		
5-Hydroxytryptamine receptor 3A	ion channel		

Table 6.3 Proteins downregulated by RNF128 overexpression

RNF128 OE			
Absent proteins		**Downregulated proteins**	
Name	**GO annotations**	**Name**	**GO annotations**
Multidrug resistance protein 1	transporter activity	Tight junction protein ZO-1	tight junctions
Merlin	adherens junctions	Occludin	tight junctions
CD63 antigen	tetraspanin	CD44 antigen	cell-matrix adhesion
V-type proton ATPase subunit H	ion transport		
Raftlin	B cell receptor signalling pathway		
Tyrosine-protein kinase Fyn	signalling receptor		
Flotillin-1/2	caveolae formation		
Olfactory receptor 4A15	G-protein coupled receptor		
Olfactory receptor 6P1	G-protein coupled receptor		
Rhodopsin kinase	G-protein coupled receptor activity		
Guanine nucleotide-binding protein G(I)/G(S)/G(T) subunit beta-1	G-protein coupled receptor signalling		
Guanine nucleotide-binding protein G(i) subunit alpha-1	G-protein coupled receptor signalling		
Cingulin	tight junctions		

Table 6.4 Proteins affected by RNF150 overexpression.

RNF150 OE	
Absent proteins	
Name	**GO annotations**
HLA class I histocompatibility antigen, alpha chain G	antigen presentation
Retinoic acid-induced protein 3	G-protein coupled receptor activity
K-cadherin	adherens junctions
Catenin delta-1	adherens junctions
CD81 antigen	signalling receptor
Guanine nucleotide-binding protein G(I)/G(S)/G(T) subunit beta-2	G-protein coupled receptor signalling
Lipolysis-stimulated lipoprotein receptor	transporter activity
Excitatory amino acid transporter 1	transporter activity
Platelet-derived growth factor receptor alpha	signalling receptor
Rhodopsin kinase	G-protein coupled receptor activity
Sodiumbicarbonate cotransporter 3	transporter activity
Piezo-type mechanosensitive ion channel component 1	ion channel
CD44 antigen	cell-matrix adhesion

6.2.3 In vitro validation of shortlisted targets

The analysis of the surface proteome revealed significantly reduced levels of several protein classes upon overexpression of individual PA-RING ligases. This allowed us to draw up a shortlist of putative targets that may be specifically ubiquitinated by the E3 ligase of interest. However, despite being an extremely useful technique, SPA has some limitations: firstly, it does not guarantee that the observed downregulation occurs at the protein level and secondly, it does not allow us to establish any direct link between the overexpressed E3 ligase and the downregulated protein species. For this reason, I next focused on validating some of the putative targets identified with SPA *in vitro*.

Therefore, I first checked the expression levels of all the shortlisted candidates (**Tables 6.2-6.4**) by RT-qPCR in dox-treated cells compared to untreated cells; this allowed me to further narrow down the list of putative targets by discarding those hits that were already downregulated at the mRNA level (**Figure 6.7**).

Next, I tested antibodies for western blot against the selected hits using both total cell lysates and membrane fractions. In some cases the analysis of protein abundance in the total cell lysate perfectly matched that in the membrane fraction, e.g. Occludin was found to be almost absent in RNF128-overepressing cells in both sample types. However, in some other cases only one sample type showed a reduction in the candidate protein, e.g. overexpression of RNF150 could be linked to a reduction in K-cadherin levels only in the membrane eluate (**Figure 6.8**). This could indicate either that K-cadherin is being internalised or that in the whole cell lysate its intracellular fraction can mask the effect of RNF150 at the plasma membrane.

For the remaining candidates, the investigation of their protein levels has been mainly hindered by a lack of suitable antibodies.

To conclude, it was possible to confirm by western blot the downregulation upon E3 overexpression of two of the putative targets identified by SPA; their mRNA levels were not found to be downregulated in dox-treated samples, as opposed to their protein levels, which were. Most importantly, this is the first time that RNF128 has been associated with the regulation of tight junctions and has been hypothesised to play a role in a process other

than T cell anergy. Even though this study does not provide evidence for a direct interaction between the E3 ligase and its putative target, and additional experimental evidence is required, its informative value in identifying candidates for future work is great.

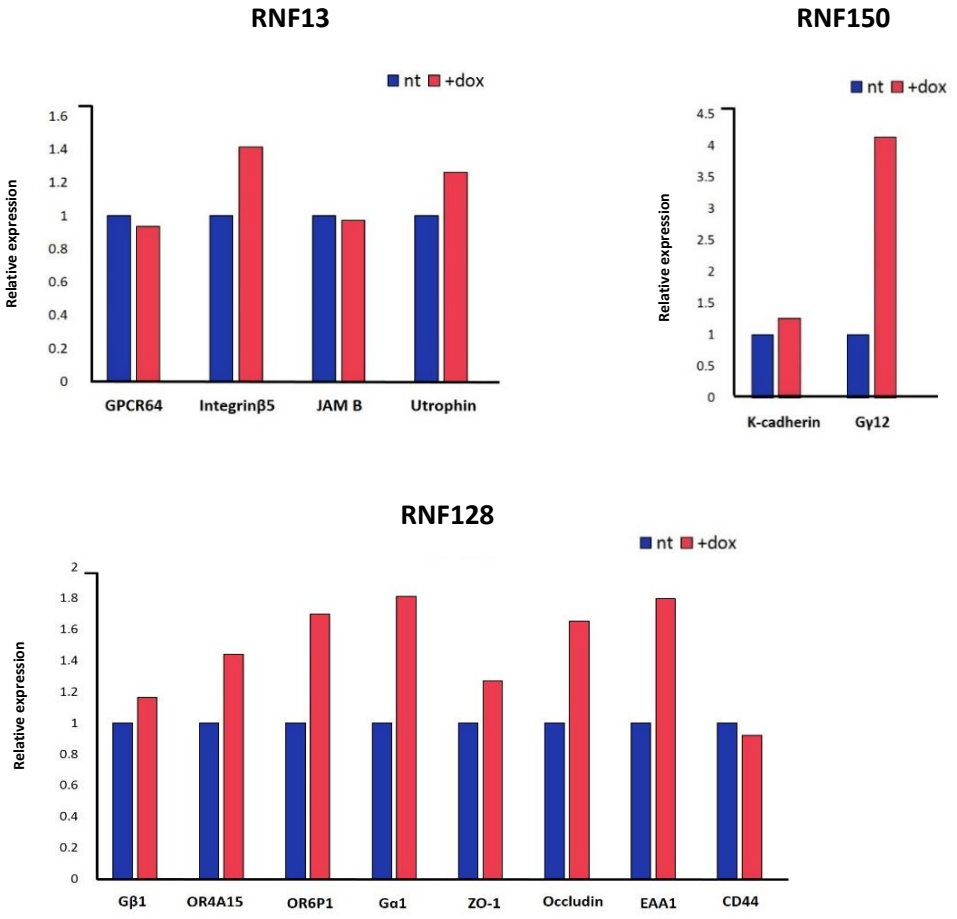

Figure 6.7 mRNA levels of putative targets upon overexpression of PA-RING E3 ligases. RT-qPCR analysis allowed the selection of those candidates that were not downregulated at the mRNA level in dox-treated samples (red bars) for future work; these genes are more likely to encode direct targets for the PA-RING E3 ligases.

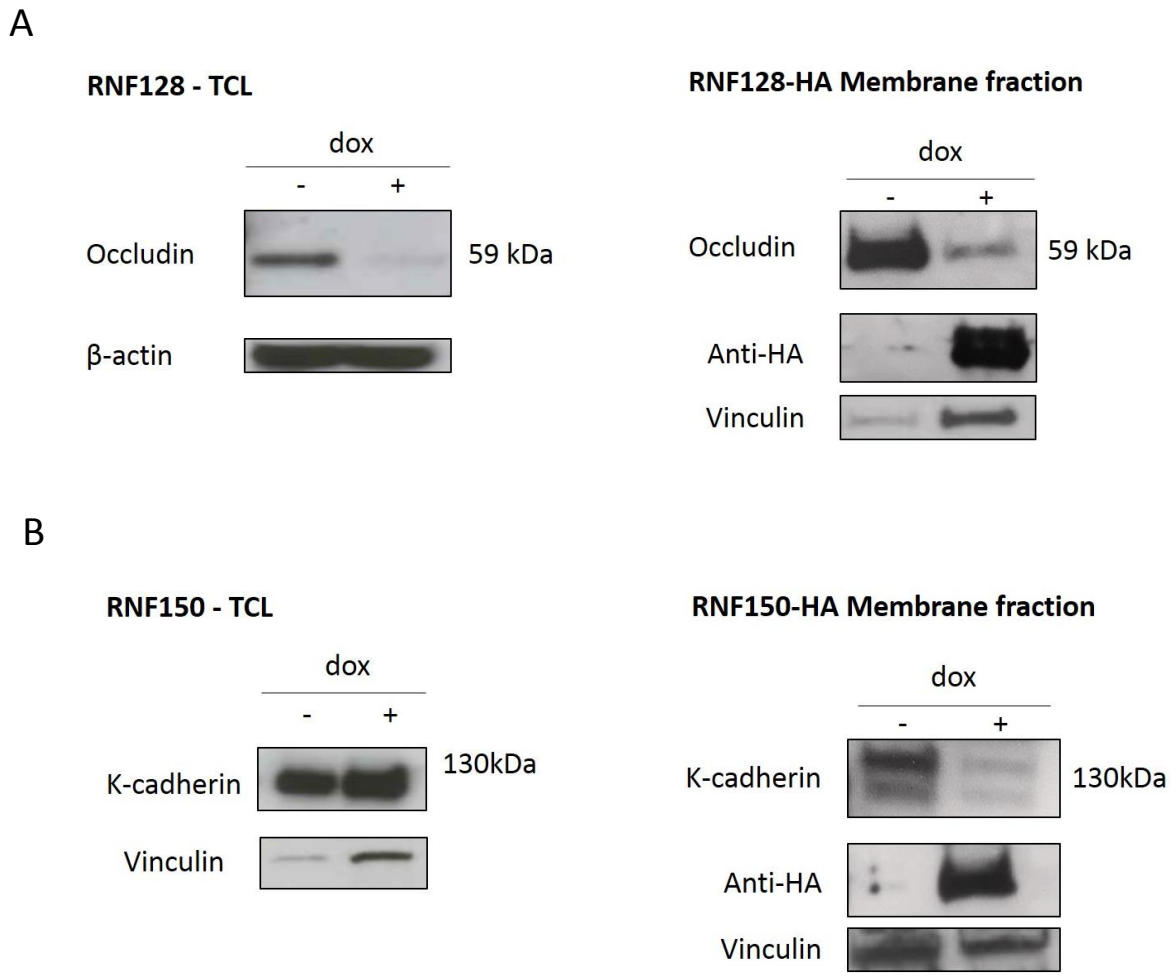

Figure 6.8 Overexpression of RNF128 and RNF150 leads to the downregulation of Occludin and K-cadherin, respectively. **A)** Reduction in the levels of the tight junction protein Occludin upon RNF128-HA overexpression (+dox) in both total cell lysate (TCL) and the membrane fraction. **B)** Reduction in the levels of K-cadherin upon RNF150-HA overexpression (+dox) could be observed only in the membrane fraction.

6.4 Summary and conclusions

This chapter has illustrated the approaches undertaken in order to investigate additional members of the PA-RING family of E3 ubiquitin ligases and deepen our understanding of its less well-characterised members. In particular, I was interested in unravelling a potential involvement of additional E3 ligases in WNT pathway regulation as well as identifying new molecular targets for selected members.

To address the former, an overexpression screen of all PA-RING members was conducted in mouse intestinal organoids with different genetic backgrounds and in differing culture conditions (standard and RSPO-depleted). These experiments brought us to the conclusion that no PA-RING members are likely to be involved in WNT pathway modulation other than RNF43 and ZNRF3, not even their close homolog RNF215. However, a complementary knockout screen of the PA-RING members that are expressed in the mouse intestine would be required to have a definitive answer and to be able to conclude that none of them is linked to WNT signalling.

Some further data not presented in this chapter is that withdrawal of the other key components of organoid culture medium, Noggin and EGF, also did not result in any phenotype in E3 ligase-overexpressing organoids; this suggests that PA-RING family members are also not likely to be involved in the regulation of either the BMP or EGF signalling pathways.

To look further into the roles of PA-RING members, I then decided to pursue a proteomics approach aimed at identifying their targets from among membrane proteins; the method I employed allowed the identification of several different classes of proteins that were markedly downregulated upon overexpression of RNF13, RNF150 or RNF128. For example, I observed a pronounced decrease in the levels of tight junction proteins, GPCRs and related proteins upon RNF128 overexpression. Furthermore, RNF150 showed some similarities to RNF128 but also differences in that its overexpression mainly caused depletion of adherens junction proteins like K-cadherin and Catenin delta-1.

Among the putative targets highlighted by the surface proteome analysis, it was possible to confirm downregulation of the tight junction protein Occludin and the adherens junction protein K-cadherin upon overexpression of RNF128 and RNF150, respectively.
Thus, this technique was instrumental for the identification of potential molecular targets for some of these members of the family, although only co-immunoprecipitation experiments will enable us to establish a direct link between a particular E3 ligase and its putative target.

Not surprisingly, none of the potential candidates has ever been associated with any member of the family; also in case of RNF128, one of the most well characterised PA-RING proteins, no reports exist in the literature associating it with tight junction regulation. In this regard, my work might open RNF128 to investigation in the context of a novel role or it could also contribute to a better definition of its known role as a mediator of T cell anergy. Interestingly, it has been reported that only activated T-lymphocytes express Occludin in order to enable their aggregation (Alexander et al. 1998). Therefore, targeting Occludin directly for degradation might be an additional way through which RNF128 mediates T cell unresponsiveness and anergy.

Overall, my work suggests new putative targets and potentially suggests novel roles for some representative members of the PA-RING family and this may be considered a valid starting point for further investigation.

Chapter 7

Discussion, conclusions and future perspectives

7.1 Summary and main findings

During the course of my PhD studies I have investigated the details of the mechanism of action of RNF43 by developing a new intestinal organoid-based screening platform that has allowed the identification of novel genes with a functional connection to RNF43 activity. Following identification of these genes, I then focused on *Daam* and tried to further characterise its role in the RNF43-mediated clearance of Frizzled.

Since the detailed study of the molecular mechanism of RNF43 activity could also serve as a paradigm for its paralogous genes, I also directed my attention to the investigation of other PA-RING family members by first evaluating their potential involvement in the WNT

signalling pathway and by then identifying some of their putative targets through a proteomics approach.

Below, I have summarised the main findings and achievements of my work, which will be further discussed in the next sections of this chapter to provide future perspectives and possible ways to develop this study.

Thus, the main findings presented in this thesis are:

- Establishment of a robust screening platform for genetic studies in intestinal organoids by exploiting novel CRISPR/Cas9 techniques.
- Identification of DAAM1, SEC16A, UBL4A AND SLC12A2 as potential interactors in the context of the RNF43-mediated downregulation of Frizzled and WNT pathway modulation.
- The recapitulation of the Rnf43&Znrf3 knockout phenotype by *Daam* knockout in intestinal organoids based on their survival in RSPO-depleted medium and continued sensitivity to the complete depletion of WNT ligands.
- Frizzled5 internalisation seems to be impaired/delayed in *DAAM* KO HEK293T clones. However, there are no significant differences between WT and *DAAM* KO cells in Frizzled5 endocytosis and ubiquitination levels.
- Interestingly, co-immunoprecipitation studies suggest that DAAM may participate in a ternary complex with DVL and RNF43.

- No other PA-RING family members are likely to be involved in WNT pathway regulation, based on an overexpression screen in intestinal organoids followed by RSPO withdrawal experiments.
- The expression of different classes of adhesion molecules and G protein-coupled receptors are significantly affected by the overexpression of selected PA-RING members, as assessed using a mass spectrometry-based approach. In particular, the overexpression of *RNF128* and *RNF150* can strongly downregulate Occludin and K-cadherin levels, respectively.

In summary, I believe that my work overall addressed all of the predetermined aims by providing interesting experimental observations, and in addition has provided insightful starting points for future lines of research.

7.2 Discussion

7.2.1 Establishment of new genetic tools for organoid manipulation

A number of different genetic tools applied to organoid culture have been presented in this thesis with the intent to study regulatory mechanisms of the WNT pathway in the murine intestine.

Firstly, the application of the PiggyBac transposon system to intestinal organoids allowed establishing a solid platform with inducible overexpression of RNF43, which subsequently resulted instrumental to functionally test mass-spectrometry hits after RNF43 pull-down. To this purpose, our CRISPR concatemer vector for simultaneous multiple gene knockout was indispensable to tackle the possible issue of genetic compensation while carrying out knockout screens (Andersson-Rolf et al. 2016). Furthermore, by coupling this concatemer strategy with electroporation as a delivery method it was possible to sensibly increase the success of loss-of-function studies in organoids (Merenda et al, 2017. *In press*).

Interestingly, the potential of the CRISPR concatemer strategy is now also being explored *in vivo* in combination with an inducible-Cas9 mouse line, with the aim to simplify the generation of conditional knockout models.

Another example of genetic modification tool applied to intestinal organoids is represented by the overexpression screening of all PA-RING members that was enabled by the inducible MSCV retroviral system; this could be efficiently delivered to organoid cultures by retroviral transduction, as previously described by Koo et al., 2012.

In the matter of conditional gene manipulation, it is worth mentioning one more strategy that has been recently developed by our group in order to efficiently achieve conditional and reversible gene knockouts in diploid cells (Andersson-Rolf et al. 2017).
It is based on an invertible drug selection intronic cassette, named FLIP cassette, which exists in two different configurations. In its non-mutagenic orientation, the cassette expresses a resistance gene to select for correct Cas9-assisted targeting into the exon of one allele as well as simultaneous enrichment of cells in which the second allele has been inactivated by non-homologous end joining (NHEJ).
Upon Cre recombination, the cassette is then inverted to a mutagenic configuration that activates a cryptic splice acceptor while disrupting the initial splicing acceptor; this, together with the introduction of polyadenylation signal, results in gene disruption. Thorough testing of the FLIP cassette in different cell lines and intestinal organoids proved the wide applicability of this strategy.

For instance, the overall advantage of the genetic tools reported in this dissertation is their versatility. For example, it could be possible to apply an analogous approach to the one employed for RNF43 to the investigation of other regulators of the WNT pathway as well as to the study of other signalling pathways that are key for the maintenance of intestinal stem cells.

7.2.2 Investigation of the molecular mechanisms of RNF43-mediated downregulation of Frizzled

The WNT pathway regulator RNF43 (Koo et al. 2012; Hao et al. 2012) is an E3 ubiquitin ligase that has attracted increasing attention because of its crucial role as a tumour suppressor in the intestine, consistent with its mutation rate in various types of malignancies. Despite that, the molecular details of its mechanism of action and its molecular partners have not been fully explored. For this reason, I decided to establish an organoid-based screening platform for the identification of genes with a functional connection to RNF43. This system has been an extremely advantageous tool for the study

of the molecular mechanism of RNF43 activity, and *Daam1* was among the first of the RNF43-linked candidates to be identified. Furthermore, *Daam* knockout organoids could mimic the RZ KO phenotype, suggesting that DAAM might be involved in membrane-proximal events of WNT/β-catenin pathway modulation.

Generally, DAAM1 has always been associated with the "non-canonical" WNT PCP pathway as an interactor of Dishevelled able to induce actin cytoskeleton rearrangements (Oishi et al. 2003; Komiya & Habas 2008). Up to now, only one report has linked its homologue, *Daam2*, to canonical WNT/β-catenin signalling during chick spinal cord development, by showing that the *Daam2* loss-of-function phenotype could be rescued by activation of β-catenin (Lee & Deneen 2012). Aside from that report, this is the first time that *DAAM1* has been linked to the regulation of the canonical WNT/β-catenin pathway, RNF43 activity and maintenance of intestinal homeostasis.

These observations appear to be particularly interesting in light of two recent reports demonstrating that Dishevelled is an important partner of RNF43 in the downregulation of Frizzled (Jiang et al. 2015; Tsukiyama et al. 2015). However, neither of these two studies managed to fully clarify the exact mechanism(s) by which DVL and RNF43 cooperate and some important questions remained unanswered, for example, whether DVL and RNF43 could interact directly with one other or not, or whether direct interaction was essential for downregulation of the WNT/β-catenin pathway.

Within this wider context, the novelty of my work was to introduce a new player into this picture, DAAM, which could potentially represent the key to understand RNF43-mediated Frizzled clearance. For instance, it was interesting to observe how DVL2 overexpression was able to promote the interaction between DAAM1 and RNF43, suggesting the formation of a ternary complex, which enables RNF43 to promote Frizzled internalisation.

Among multiple possibilities, such complex might be important for RNF43 activation, for example, and DAAM-DVL could function as a docking platform for an effector required for post-translational modifications to RNF43, such as phosphorylation.

Furthermore, it might be also possible that, depending on where in the cell DVL and DAAM interact with each other, different signalling events are affected. For instance, if their

interaction takes place in the cytoplasm, this leads to a reorganisation of the actin cytoskeleton, whereas if the two proteins contact each other at the plasma membrane in proximity to RNF43, this could result in the downregulation of Frizzled surface levels.
Nevertheless, in order to support the existence of a ternary complex among RNF43, DVL2 and DAAM1, biophysical approaches for the study of protein complexes will be required; techniques like the Proximity Ligation Assay (PLA) or Protein complementation assays (PCAs) might be instrumental to elucidate the dynamics of interaction among my players (Soderberg et al. 2006; Shyu et al. 2008). Details of possible follow-up experiments will be discussed in the final paragraph within the context of the future perspectives of my work.

Additional *in vitro* assays were employed to characterise the role of DAAM in Frizzled endocytosis and ubiquitination but, surprisingly, their outcome was unclear and did not explain the phenotype observed in organoids; in fact, Frizzled5 endocytosis and ubiquitination did not seem to be impaired in the absence of DAAM in HEK293T cells. Although these experiments will be repeated by analysing other members of the Frizzled family, discrepancies between the two systems could be due to a context-dependency of DAAM activity, which may be specific to the intestinal epithelium. Therefore, it is worth noting that HEK293T cells do not depend on WNT signalling for their survival and, assuming that DAAM plays a role in regulating both canonical and non-canonical WNT pathways, it could be possible that its levels are subject to different regulation in HEK293T cells compared to organoids. For this reason, studying Frizzled downregulation in the absence of DAAM in a physiologically relevant system might ultimately be necessary, as the organoid experiments conducted so far still constitute an indirect evidence for DAAM role in Frizzled internalisation.
In addition, it is worth pointing out that HEK293 is a transformed cell line with highly aberrant karyotype (Lin et al. 2014) and as a consequence it could display completely different levels of *DAAM* compared to organoids, which could trigger unknown feedback mechanisms.
Alternatively, DAAM could have a secondary role compared to DVL, or their functions could be slightly redundant and DVL alone might be sufficient to promote maximal RNF43

activity. Determining the potential hierarchy between these two players will be essential to get a clearer picture of DAAM's role.

In addition to *in vitro* experiments, *in vivo* loss-of-function studies will be conclusive in assessing DAAM's contribution to the maintenance of homeostasis in the intestine. To date, there are no reports addressing the role of *Daam1* and/or *Daam2* in the intestine, although somatic mutations in both genes have been observed in human tumours of the gut (COSMIC database); previous studies have focused mainly on their role in development and cardiomyogenesis (Li et al. 2011; Ajima et al. 2015).

I performed an alternative CRISPR-based strategy to generate an intestine-specific, conditional *Daam1/2* knockout mouse line, as this strategy was predicted to be faster than the conventional Cre-Lox system. However, whilst advantageous in terms of speed, this is still a novel approach whose efficiency remains to be fully tested; for this reason, the preliminary data presented here using this system are currently inconclusive as a more detailed characterisation of the line needs to be undertaken.

Therefore, I believe that the major contribution of my work to the investigation of the mechanism of action of RNF43 has been the identification of a potential new player by exploiting novel genetic tools for *in vitro* and *in vivo* studies.

7.2.3 Characterisation of other PA-RING members

In parallel to the characterisation of the molecular mechanism of RNF43 activity, I also focused on the investigation of additional members of the PA-RING family. This evolutionarily conserved family comprises genes that are so closely related to each other that it is reasonable to assume that they might share common functions. As both RNF43 and its homologue ZNRF3 are such important modulators of the WNT pathway, my first hypothesis was that some other members of the family could play a similar role in the regulation of the same signalling cascade. In particular, those genes closer to R&Z in the phylogenetic classification, such as *RNF215*, were hypothesised as the most likely to act on Frizzled receptors or on other effectors of the WNT pathway. However, overexpression of

each family member in intestinal organoids could not phenocopy the effect of RNF43 overexpression, suggesting that no additional PA-RING proteins are likely to be involved in downregulation of the WNT pathway. This was found to be true even in the absence of RNF43&ZNRF3, indicating that there was no redundancy with these two known tumour suppressors.

Hence, it could be plausible that RNF43 has a context-specific role in the intestinal epithelium working as a dedicated E3 ligase for the intestinal stem cell compartment, where the WNT pathway plays such a pivotal role in the maintenance of tissue homeostasis (Koo&Clevers, 2014).

In accordance with this, it is worth pointing out that no reports have appeared so far in the literature linking any PA-RING family member to the WNT pathway, and that no WNT receptor or co-receptor emerged from the surface proteome analysis (SPA) that I conducted on selected members of the family with the intent of identifying their molecular targets. Nevertheless, these data would need to be complemented by a knockout screening in intestinal organoids of those family members expressed in the murine intestine before being able to definitively conclude that no PA-RING family members, other than RNF43 and ZNRF3, are involved in WNT pathway regulation.

The above-mentioned proteomic approach did, however, provide interesting insights in terms of putative targets for RNF13, RNF150 and RNF128; in fact, upon their overexpression, it was possible to observe significant downregulation of different classes of adhesion molecules, membrane transporters and G-protein coupled receptors. Interestingly, none of the molecules identified by this mass spectrometry-based approach had been formerly associated with any of the selected PA-RING family members, highlighting the value and potential of this strategy.

In this regard, I believe that one of the most exciting observations concerns RNF128, the E3 ubiquitin ligase that mediates T-cell anergy by targeting the T-cell receptor and its co-stimulatory molecules for degradation (Lineberry et al. 2008; Su et al. 2009; Nurieva et al. 2010). My work has now linked this protein to tight junction regulation for the first time; this could either suggest a novel role for RNF128 or contribute to provide additional details on the mechanisms through which RNF128 promotes the establishment and maintenance

of immune cell anergy. This latter hypothesis has some support from previous data showing that Occludin is expressed by T-cells only when they are in their activated state and so need adhesion molecules for cell-cell interactions and aggregation (Alexander et al. 1998). In light of this, it is reasonable to hypothesise that RNF128 could further promote T-lymphocyte unresponsiveness by degradation of those tight junction proteins upregulated during the immune response. Although proteomic data were confirmed by western blot and this strategy has been previously reported in the literature as a robust and useful technique (Koo et al. 2012), additional *in vitro* approaches, such as co-immunoprecipitation experiments and ubiquitination assays, will be required in order to consolidate a role for RNF128 in the degradation of Occludin.

In addition to this, it could also be worthwhile to speculate on possible implications of the selected PA-RING E3 ligases in cancer biology and cell-cell signalling, as overexpression of all three members was shown to significantly affect adhesion molecules, signalling receptors and membrane transporters. For instance, when cells lose the ability to respond to exogenous signals, they may become cancer cells and when these cells lose adhesion molecules, cancer progression is favoured (Behrens, 1993; Knights et al. 2012).
Thus, it cannot be excluded that the PA-RING family might also include some proto-oncogenes that, when activated, can facilitate epithelial-mesenchymal transition (Lamouille et al. 2014).

In conclusion, after my initial hypothesis that multiple PA-RING family members could regulate the WNT pathway had been discarded, mass spectrometry experiments on plasma membrane fractions provided an insightful starting point for the identification of novel, putative targets of PA-RING proteins.

7.3 Concluding remarks and future work

The aim of my PhD thesis was to expand our current knowledge of the mechanism of action of RNF43 and, more broadly, to analyse other members of the PA-RING family in terms of putative roles and molecular targets. I believe that my work has made interesting contributions to both of these topics, as well as developing some novel approaches for their study.

In term of future directions, I would prioritise the following aspects:

- Understanding interaction dynamics among RNF43, DVL2 and DAAM1.

Further experiments will be required in order to demonstrate the existence of a ternary complex among these three components under physiological conditions; for example, techniques such as the Proximity Ligation Assay (PLA) or Protein complementation assays (PCAs) allow the study of endogenous protein complexes (Soderberg et al. 2006).
As further examples of relevant techniques, Bimolecular fluorescence complementation assays (BiFC) or FRET (Fluorescence Resonance Energy Transfer) could be pursued in order to visualise protein-protein interactions in living cells, and a combination of both approaches has been successfully applied to the study of ternary protein complexes (Shyu et al. 2008).

- Mapping regions in both DAAM and RNF43 that are responsible for reciprocal binding, providing the ternary complex model is confirmed.

Deletion mutants of DAAM1 will be essential to pinpoint one or more functional domains of this protein that are required for interaction with RNF43. Furthermore, the same approach can be utilised to map regions in RNF43 responsible for DAAM1 binding.

- Assessing whether overexpression of *Daam* in intestinal organoids has an analogous effect to RNF43 overexpression.

- Determine whether all domains of RNF43 are important for its mechanism of action.

Since it has already been shown that the extracellular PA domain of RNF43 could be interacting with the extracellular portion of Frizzled (Tsukiyama et al. 2015), it might be interesting to assess Frizzled endocytosis and ubiquitination in WT and *DAAM* mutant cells upon the overexpression of both WT and ΔPA RNF43.

- Focus on the role of SEC16 in the regulation and mechanism of action of RNF43.

From amongst the other candidates identified in the CRISPR screen, SEC16 seems to be one of the most promising given its role in the secretory pathway from the ER to Golgi (Sprangers & Rabouille 2015); this candidate could be involved in RNF43 maturation and targeting to the plasma membrane. Interestingly, preliminary data seem to point to a concurrence of RNF43 and *SEC16* mutations in human gastric cancer samples (unpublished).

In terms of other PA-RING family members, my work may represent a useful starting point for in-depth analysis of additional members of the family, especially for those less well-characterised members, such as RNF150. I believe it could be particularly interesting to further study the mechanism of action of RNF128 and its interaction with Occludin in the context of establishment of T cell anergy. For example, in addition to *in vitro* experiments aimed at confirming a direct link between the two proteins, such as co-immunoprecipitation and ubiquitination assays, it would be worthwhile to check whether RNF128 knockout mice display higher levels of Occludin on T lymphocytes after immune stimulation compared to wildtype controls.

All of the possible future experiments suggested here, in combination with the ongoing studies that have been mentioned in the discussion sections of previous chapters, will hopefully help us to clarify the details of RNF43-mediated downregulation of Frizzled and potentially suggest a conserved mechanism of action for PA-RING E3 ubiquitin ligases.

Appendix A

Supplementary information

Materials

S2.1.1 Devices, consumables and chemicals

Table S1. List of devices, software and consumables

Devices / Software / Consumable	Supplier
2720 Thermo Cycler (PCR-Machine)	Applied Biosystems
48-well clear TC treated Microplates	Corning
60x15mm Centre Well IVF Tissue Culture Dish	BD Falcon
AMAXA Human Nucleofector	LONZA
Amersham Hyperfilm ECL	GE Healthcare Life Sciences
BD FACS-Diva Software	BD Biosciences
BD LSRFortessa™ cell analyser	BD Biosciences
Confocal Microscope	LEICA
Electroporation Cuvettes	BioRad
Electroporation Cuvettes 2mm gap	NepaGene
EVOS Stand Alone Digital Imaging System	Scientific Instrument Company Inc.
FlowJo | Single Cell Analysis Software	FLOWJO, LLC
Gene Pulser X-Cell	BioRad
LEICA Application Suite	LEICA

Low binding 15ml tubes	Sigma
MicroAmp® Fast Optical 96-Well Plate	Applied Biosystems
Mini Trans-Blot® Cell	Biorad
Nanodrop ND1000	Labtech
Nanodrop software ND1000 V3.3.1	Labtech
NEPA21 Super Electroporator	NepaGene
Protein LoBind tubes low binding	Thermo Fisher
Standard filter pipette tips	Starlabs
StepOne™ Real-Time PCR machine	Applied Biosystems
Trans-Blot® Turbo™ Mini PVDF Transfer Packs	Biorad
Trans-Blot® Turbo™ Transfer	Biorad

Table S2. List of chemicals

Chemical	Supplier
0.1% Gelatine	Sigma-Aldrich Co. LLC
2-Mercaptoethanol	Sigma-Aldrich Co. LLC
4-OHT (4-Hydroxytamoxifen)	Sigma-Aldrich Co. LLC
B27 (50x)	Life Technologies
BlastAssist medium	Origio
Blasticidin	Sigma-Aldrich Co. LLC
Carbenicillin	Sigma-Aldrich Co. LLC
Chiron	Stewart lab
DMEM Hams F12 Medium	Sigma-Aldrich Co. LLC
DMEM, High Glucose, GlutaMAX™, Pyruvate	Life Technologies
DMEM/F-12, no glutamine	Life Technologies
DMSO	Sigma-Aldrich Co. LLC
Doxycycline	Invitrogen
DTT	Thermo Scientific
Dulbecco's phosphate buffered saline	Sigma-Aldrich Co. LLC
EGF	Life Technologies
FBS (GIBCO)	Life Technologies
G-418	Invitrogen
Glasgow's MEM (GMEM)	Life Technologies

HEPES	Life Technologies
IWP-2	Cell Guidance Systems
L-glutamine (200nM)	Life Technologies
Low-melt agarose	BioRad
MEM NEAA (100x)	Life Technologies
Murine LIF	Hyvonen lab
N2 (200x)	Millipore
Neurobasal Medium	Life Technologies
PDO3	Stewart lab
Penicillin Streptomycin	Sigma-Aldrich Co. LLC
Polybrene	Sigma-Aldrich Co. LLC
Puromycin	Sigma-Aldrich Co. LLC
Sodium Pyruvate (100mM)	Life Technologies
Synthemax II	Coning
Trypan blue	Life Technologies
TypLE express	Invitogen
Trypsin-EDTA 0.25%	Life Technologies
TeSR-E8 media	Stem Cell Technologies
UltraPure DNase/RNase-Free Distilled Water	Life Technologies
Y-27632	Sigma-Aldrich Co. LLC
Zeocin	Invitrogen

S2.1.2 Kits and enzymes

Table S3. List of kits

Kit	Supplier
BCA Protein Assay Reagent	Thermo Scientific
Dual-Luciferase® Reporter Assay System	Promega
GoTaq G2 Flexi DNA Polymerase	Promega
Hot start LongAmp™ Taq 2X Master Mix	New England Biolabs
In-Fusion® HD Cloning Kit	Clontech Laboratories, Inc.
Lipofectamin2000	Life Technologies

Mighty Cloning Kit	Takara
MinElute PCR Purification Kit	Qiagen
Phusion® High-Fidelity PCR Kit	NEB
Pierce Cell Surface Protein Isolation Kit	Thermo Scientific
Pierce ECL Western Blotting Substrate	Thermo Scientific
CloneJET PCR Cloning Kit	Thermo Scientific
QIAGEN Plasmid Midi Kit	Qiagen
QIAprep Spin Miniprep Kit	Qiagen
QIAquick Gel Extraction Kit	Qiagen
RNeasy Micro kit	Qiagen
RNeasy Mini kit	Qiagen

Table S4. List of enzymes

Enzymes	Supplier
Acc65I	NEB
AloI	Thermo Scientific
BamHI	NEB
BglII	NEB
DpnI	NEB
EcoRI	NEB
EcoRV	NEB
Fast Digest BbsI	NEB
NcoI	NEB
NotI	NEB
PlasmidSafe™ ATP-Dependent DNase	Cambio
SalI	NEB
SapI	NEB
T4 DNA ligase	NEB
T4 Polynucleotide Kinase	NEB

S2.1.3 Plasmids

Table S5. List of plasmids

Plasmid	Supplier
pCMV-GFP	Addgene
Empty gRNA vector	Addgene
Human codon optimized Cas9	Addgene
gRNA_GFP-T1	Addgene
pcDNA4TO	Thermo Scientific
pJet1.2	Thermo Scientific
pMSCV-loxp-dsRed-loxp-3xHA-Puro-WPRE	Addgene

S2.1.4 Cloning and genotyping primers

Table S6. List of cloning primers for PiggyBac vectors

Primers	Sequence
hRNF43-2F2H_InfL	CAAAGAATTCCTCGAGGTTGAAGTGCATTGCTGCAGCTGGTA
hRNF43-2F2H_InfR	GCTTATCGAGCGGCCGTTTAAACGGGCCCTCTAGACTCGATCA
hCas9-infL	CTTGACATGCTCCCCGGAAGCGGAGCTACTAACTTCAGCCTGCTGAAGCA GGCTGGAGACGTGGAGGAGAACCCTGGACCTATGGACAAGAAGTACTC CATTGGGCTCG
hCas9-infR	GCTTATCGAGCGGCCTCACACCTTCCTCTTCTTCTTGGGGTCA
Hygro-infL	CACGATGATAATATGGCCACAACCATGAAAAAGCCTGAACTCACCGCG
Hygro-infR	TTAATAGATCATCAATTTCTCGACTATTCCTTTGCCCTCGGACGAG

Table S7. List of oligos for concatemer cloning

Gene	Forward primer	Reverse primer
Sh3bp4	CACCGGTCCCCTCCGACTTGCACCGAGT	TAAAACTCGGTGCAAGTCGGAGGGGACC
	ACCGGCATTCAGAAAGGGGTTCGTTG	AAAACAACGAACCCCTTTCTGAATGC
Macc1	CCGGTTGATTTTTTGAGCGTTTCG	AAACCGAAACGCTCAAAAAATCAA
	ACACCGGTGATGTCTGAGTCGGGTAATGTT	CTAAAACATTACCCGACTCAGACATCACCG
Emerin	CACCGGCAAGTGAGGTCCCCGGCTGGGT	TAAAACCCAGCCGGGGACCTCACTTGCC
	ACCGGATACATGTCTGAGTCCACGGG	AAAACCCGTGGACTCAGACATGTATC
	CCGGCACTGCGGCCAGCTCAGTAT	AAACATACTGAGCTGGCCGCAGTG
Adam17	CACCGGCATATACCGGAACACGTCGTGT	TAAAACACGACGTGTTCCGGTATATGCC
	ACCGGCGTCCTGGCACCCCGACCTCG	AAAACGAGGTCGGGGTGCCAGGACGC
	CCGGGAATCAAGCTTCTCAAGTCG	AAACCGACTTGAGAAGCTTGATTC
Zmynd19	CACCGGACTTTAAATTGGGCATCGTGGT	TAAAACCACGATGCCCAATTTAAAGTCC
	ACCGGAAATTGGGCATCGTGCGGCTG	AAAACAGCCGCACGATGCCCAATTTC
	CCGGTGGGCATCGTGCGGCTCGGC	AAACGCCGAGCCGCACGATGCCCA
Tmed10	CACCGGAGACTGGTCGGTGATCTCGTGT	TAAAACACGAGATCACCGACCAGTCTCC
	ACCGGGAGACACTTGCGAGAGTTCAG	AAAACTGAACTCTCGCAAGTGTCTCC
	CCGGAGACACTTGCGAGAGTTCAC	AAACGTGAACTCTCGCAAGTGTCT
Bag6	CACCGGTCTTGTCGTCTTGTAGGACCGT	TAAAACGGTCCTACAAGACGACAAGACC
	ACCGGATGAGTGATCTGGTGGGCGAG	AAAACTCGCCCACCAGATCACTCATC
	CCGGTGGGAAATCCGGATGACCCG	AAACCGGGTCATCCGGATTTCCCA
Daam1	CACCGGACAGGGGGCATGGGCAGCGCGT	TAAAACGCGCTGCCCATGCCCCCTGTCC
	ACCGGTAAAAGCACTGGGCGTTATCG	AAAACGATAACGCCCAGTGCTTTTAC
Daam2	CCGGACCTTCCCGAGATCGACCTC	AAACGAGGTCGATCTCGGGAAGGT
	ACACCGGTCGAAGCTTAGGCCGCTACCGTT	CTAAAACGGTAGCGGCCTAAGCTTCGACCG
Ap2m1	CACCGGAGATGTTGGACCGCTTAACAGT	TAAAACTGTTAAGCGGTCCAACATCTCC
	ACCGGAGGGGGAGGTGCTTATCTCCG	AAAACGGAGATAAGCACCTCCCCCTC
	CCGGGAGAAGGCATCAAGTATCGC	AAACGCGATACTTGATGCCTTCTC
PLD1	CACCGGGCTGTGGACGTAGATGAGCTGT	TAAAACAGCTCATCTACGTCCACAGCCC
	ACCGGGCTGTGGACGTAGATGAGCTG	AAAACAGCTCATCTACGTCCACAGCC
PLD2	CCGGGAGTTCAGATAGTCCCCATA	AAACTATGGGGACTATCTGAACTC
	ACACCGGTAGGGAGGGTATATCCTCGGGTT	CTAAAACCCGAGGATATACCCTCCCTACCG
BRI3BP	CACCGGCACTCCCTGCACGAACCGCTGT	TAAAACAGCGGTTCGTGCAGGGAGTGCC
	ACCGGAGCTGCTCGTCGCGCGCCGGG	AAAACCCGGCGCGCGACGAGCAGCTC

TMEM109	CCGGGCGCACACAGCACTCCGTTA	AAACTAACGGAGTGCTGTGTGCGC
	ACACCGGCTTCAGAGATCGGCCAATCTGTT	CTAAAACAGATTGGCCGATCTCTGAAGCCG
Sdcbp	CACCGGCAGAACAAATGCTTGGCTGGGT	TAAAACCCAGCCAAGCATTTGTTCTGCC
	ACCGGCAGGTAACGATGCTGGAATTG	AAAACAATTCCAGCATCGTTACCTGC
Sdcbp2	CCGGAGGTGGATCTCTCGCACGCC	AAACGGCGTGCGAGAGATCCACCT
	ACACCGGTCTCTGCACGCAGTATACCCGTT	CTAAAACGGGTATACTGCGTGCAGAGACCG
Zyg11a	CACCGGCCCTCGAGGATCCATATGAGGT	TAAAACCTCATATGGATCCTCGAGGGCC
	ACCGGCGAGCGGGCGTTTTTCGTTAG	AAAACTAACGAAAAACGCCCGCTCGC
Zer1	CCGGAACCTGGGCCGCATGATTGA	AAACTCAATCATGCGGCCCAGGTT
	ACACCGGTGCGAGTGAGCCGAGTACTGGTT	CTAAAACCAGTACTCGGCTCACTCGCACCG
Vangl1	CACCGGAAGAGGCCGAACACGAACGCGT	TAAAACGCGTTCGTGTTCGGCCTCTTCC
	ACCGGCAGGTGGTCCGCTCCACCGAG	AAAACTCGGTGGAGCGGACCACCTGC
Vangl2	CCGGTGACCTCACGCGCATCGCCA	AAACTGGCGATGCGCGTGAGGTCA
	ACACCGGTGTGCGCATCTTGGACGCCCGTT	CTAAAACGGGCGTCCAAGATGCGCACACCG
Dvl1	CACCGGCCTCATCGCGGTTTCGACGTGT	TAAAACACGTCGAAACCGCGATGAGGCC
Dvl2	ACCGGCCGAGCGTGATGCGCTCCGCG	AAAACGCGGAGCGCATCACGCTCGGC
Dvl3	CCGGCCTTTGTGGTTCCATTGAGT	AAACACTCAATGGAACCACAAAGG
UBR2	CACCGGGTCCCACCTGACGCGTGATCGT	TAAAACGATCACGCGTCAGGTGGGACCC
	ACCGGTATGGAGGATGATCACGAGCG	AAAACGCTCGTGATCATCCTCCATAC
UBR3	CCGGCGCCCGCACGGTTATCCGGC	AAACGCCGGATAACCGTGCGGGCG
	ACACCGGCGCGGGGTCGTAGGCCCGCAGTT	CTAAAACTGCGGGCCTACGACCCCGCGCCG
SORT1	CACCGGCCGGTCCGGTCGGGGTGAGCGT	TAAAACGCTCACCCCGACCGGACCGGCC
SORL1	ACCGGCTTCTCCATCCCATTCCGGGG	AAAACCCCGGAATGGGATGGAGAAGC
SORCS2	CCGGCTGGCCCTACTGCGCCGGAC	AAACGTCCGGCGCAGTAGGGCCAG
WDR26	CACCGGGCCTGCCTGTCGGCGCAGAAGT	TAAAACTTCTGCGCCGACAGGCAGGCCC
	ACCGGGTCCCCTTCGGCGACGTCCGG	AAAACCGGACGTCGCCGAAGGGGACC
	CCGGACGTAGTGAACTGCCAATTG	AAACCAATTGGCAGTTCACTACGT
UBL4A	CACCGGGGAATGTAGCCTACAGGTGGGT	TAAAACCCACCTGTAGGCTACATTCCCC
	ACCGGCATTCAGCTTATCCGAGACCG	AAAACGGTCTCGGATAAGCTGAATGC
	CCGGCCACCTGTAGGCTACATTCC	AAACGGAATGTAGCCTACAGGTGG

SEC16A	CACCGGTGGGGTGATGTTCCGGGGACG T	TAAAACGTCCCCGGAACATCACCCCACC
	ACCGGAAAGCAAACGGATCCGTTACG	AAAACGTAACGGATCCGTTTGCTTTC
SEC16B	CCGGGGTACTTCGGCGAGCATCAT	AAACATGATGCTCGCCGAAGTACC
	ACACCGGAATTGAGGCTATCCAGCGGA GTT	CTAAAACTCCGCTGGATAGCCTCAATTCCG
RAB10	CACCGGCCACTCCCGAGTCCCCGATCGT	TAAAACGATCGGGGACTCGGGAGTGGCC
RAB8A	ACCGGTGTTCGAAACCGCTCCTGGCG	AAAACGCCAGGAGCGGTTTCGAACAC
RAB15	CCGGCGAGGAGTGGAACTCGTTGT	AAACACAACGAGTTCCACTCCTCG
PTGFRN	CACCGGTGCAATGTCAGCGACTATGAGT	TAAAACTCATAGTCGCTGACATTGCACC
	ACCGGCCACAGTGGGGACGTACGCCG	AAAACGGCGTACGTCCCCACTGTGGC
Igsf8	CCGGCACCTGCCGGGCGTAGCACC	AAACGGTGCTACGCCCGGCAGGTG
	ACACCGGCCACAGAGTACGCAGCATGA GTT	CTAAAACTCATGCTGCGTACTCTGTGGCCG
SPTLC1	CACCGGGATGAACCGCCGAGTCACACG T	TAAAACGTGTGACTCGGCGGTTCATCCC
	ACCGGCTCAACTACAACATCGTGTCG	AAAACGACACGATGTTGTAGTTGAGC
	CCGGTGTGACTCGGCGGTTCATCG	AAACCGATGAACCGCCGAGTCACA
Armc8	CACCGGCCTCCGAGAGGACGCTCATGG T	TAAAACCATGAGCGTCCTCTCGGAGGCC
	ACCGGGAGAGGACGCTCATGCGGATG	AAAACATCCGCATGAGCGTCCTCTCC
	CCGGCAACCTCATCGTTCTAGGAG	AAACCTCCTAGAACGATGAGGTTG
Lman2	CACCGGGTGGCTGCGGATATCACCGAG T	TAAAACTCGGTGATATCCGCAGCCACCC
	ACCGGGCCCTGGTACGAGGCGGTCTG	AAAACAGACCGCCTCGTACCAGGGCC
	CCGGCCCTGGTACGAGGCGGTCTC	AAACGAGACCGCCTCGTACCAGGG
Ap2a2	CACCGGGACCCATAAACGTAGGATTGG T	TAAAACCAATCCTACGTTTATGGGTCCC
	ACCGGGAGATGGCGGAGGCCTTCGCG	AAAACGCGAAGGCCTCCGCCATCTCC
Ap2a1	CCGGGCACCCCCGGCTCCCGTAGG	AAACCCTACGGGAGCCGGGGGTGC
	ACACCGGCCGTGTTCATCTCCGACATCG TT	CTAAAACGATGTCGGAGATGAACACGGCC G
Slc12a2	CACCGGCCGGGTCCACGAAGTTCACGG T	TAAAACCGTGAACTTCGTGGACCCGGCC
Slc12a8	ACCGGGAGGGCCTCTCGGGTACAGAG	AAAACTCTGTACCCGAGAGGCCCTCC
Slc12a9	CCGGTGGCCCCCGCTCGTGTTGAT	AAACATCAACACGAGCGGGGGCCA
TMEM59	CACCGGCTGTTGACTATGGCGCTGGCGT	TAAAACGCCAGCGCCATAGTCAACAGCC
	ACCGGGAGACACAGCGTCCTGTCACG	AAAACGTGACAGGACGCTGTGTCTCC
	CCGGTTTTATCTTCAAGCCGATGA	AAACTCATCGGCTTGAAGATAAAA

Table S8. List of primers for Daam1 cloning

Primers	Sequence
HA_Daam1_Fwd	TAGTCCAGTGTGGTGGAATTATGTACCCATACGATGTTCCAGATTACGCTGC CCCAAGAAAGAGAGGTGGACGAGGTATTTCATTCATCTTTTGCTGTTT
HA_Daam1_Rev	GGTTTAAACGGGCCCTCTAGTTAGAAATTAAGTTTTGTGATTGGTCTCTCTCT GCTGCTGTCA
Daam1_HA_Fwd	TAGTCCAGTGTGGTGGAATTATGGCCCCAAGAAAGAGAGGTGGACG
Daam1_HA_Rev	GGTTTAAACGGGCCCTCTAGTTAAGCGTAATCTGGAACATCGTATGGGTAGA AATTAAGTTTTGTGATTGGTCTCTCTCTGCTGCTGTCAGTCATCTGGT
Myc_Daam1_Fwd	TAGTCCAGTGTGGTGGAATTATGGAGCAAAAGCTCATTAGCGAAGAGGACT TGGCCCCAAGAAAGAGAGGTGGACGAGGTATTTCATTCATCTTTTGCTGTTT CCG
Myc_Daam1_Rev	GGTTTAAACGGGCCCTCTAGTTAGAAATTAAGTTTTGTGATTGGTCTCTCTCT GCTGCTGTCAGTCA

Table S9. List of genotyping primers

Gene	Forward primer	Reverse primer
Cas9	ACCCCACCATCTACCACCTGAGAAA	GGTGTTCACTCTCAGGATGTCGCTC
Cre	GCCTGCATTACCGGTCGATGCAACGA	GTGGCAGATGGCGCGGCAACACCATT
hDaam1	CTTTCTTGAGTTGGTCTGGCCTTTT	AGGAAGGGCAACTTAAGATGCAGTA
hDaam2	CTGTGTTCTCTCCTCTTGTCCAGAT	GAAACTCCAAGGAGCAGAAGAGAGA

S2.1.5 RT-qPCR primers

Table S11. List of primers for RT-qPCR

Gene	Forward	Reverse
hDaam1	ACCAGATTCATCGACTTGGATGG	CGGCCTTGAGAGTTGTTCATTA
hDaam2	CCTGAGGCCATTAGTACCATAGC	GACTTCGGTCTAGCTCGTTCA
mDaam1	CTCTGAGTCTCGGATACACACC	GCACGGCCACCTTTGTTTT
mDaam2	ACCACCTCTCCCCTTTGATAG	AGTGGGGCTTCATTGCTGG
Cadherin-4	CCATCAACAGCGAGACTGG	TGACTGTGTACTGCTGAACTTTCTC
Occludin	AGGAACCGAGAGCCAGGT	TGAGCAATGCCCTTTAGCTT
ZO-1	CATGAAGATGGGATTTCTTCG	GCCAGCTACAAATATTCCAACA
OR4A15	TGAAACTTGCTTGCACCAAT	TGAAGAAGGTGACAGCACAAA
OR6P1	TTTTTCCTTGGCCATCTCTC	AGAGCCGAGGAATGGTGAC
GPCR64	AGAGTAAAGATTCGACCAATGGA	CAGGTCACACTGAAGCTTTCC
Integrin beta-5	GGGAGTTTGCAAAGTTTCAGAG	TGTGCGTGGAGATAGGCTTT
Junctional adhesion molecule B	TGGCCTTGGTGTATGCTATG	CTCTTCTGGAAGGAGGTTTCTTT
Utrophin	CAGAGGTCCTGCCTGAGAAG	CGCAGAACAGATTCCAGAGAC
G subunit gamma-12	GAGGAGGAGGAGGAGAGGTC	TTTCAGGTTTTAAGTGGAATGAATC
G subunit beta-1	CTGGCAGGACACACAGGTT	CAGAGCTGGTGACGATCTGA
G(i) subunit alpha-1	AAGTACAATTGTGAAGCAGATGAAA	TGGTGTTACTGTAGACCACTGCTT
EAA transporter 1	CGGACAAATTATTACAATCAGCA	ATTCCAGCTGCCCCAATACT
CD44	CAAGCAGGAAGAAGGATGGAT	AACCTGTGTTTGGATTTGCAG

S2.1.6 Primary/Secondary Antibodies

Table S12. List of antibodies

Antibody	Dilution	Company
Mouse anti- β-actin	1:5000	Abcam
Mouse anti- HA Epitope	1:1000	BioLegend
Mouse anti- p53 (7F5)	1:500	Cell Signaling
Mouse anti- αTubulin	1:5000	Abcam
Rabbit anti- Cadherin-4	1:1000	Abcam
Rabbit anti- Flag	1:1000	Cell Signaling
Rabbit anti- HA-probe Antibody	1:1000	Santa Cruz
Rabbit anti- Occludin	1:50000	Abcam
Rabbit anti- Vinculin	1:3000	Abcam
Anti-mouse IgG, HRP-linked	1:5000	Cell Signaling
Anti-rabbit IgG, HRP-linked	1:5000	Cell Signaling

Methods

Table S13. PCR programs

Gene amplification	
Pre-PCR	
98 º C	30 sec
58 º C	30 sec
72 º C	3 min
x 3 cycles	
98 º C	15 sec
60 º C	30 sec
72 º C	60 sec/Kb
x 27 cycles	
98 º C	15 sec
68 º C	30 sec
72 º C	60 sec/Kb
Final extension	
72 º C	3 min
4º C	∞
Genotyping	
x 3 cycles	
94 º C	5 min
58º C	1 min
72 º C	1 min 30 sec
x 27 cycles	
98 º C	30 sec
68 º C	40 sec
72 º C	50 sec
Final extension	
72 º C	5 min
4º C	∞

Table S14. **Cell medium composition**

Medium	Reagent	Final concentration
Serum-LIF 2i medium	GMEM basal medium (1x)	1x
	FBS (GIBCO)	10%
	L-glutamine (200nM)	1% (2nM)
	Sodium Pyruvate (100mM)	1% (1mM)
	MEM NEEA (100x)	1% (1x)
	2-mercaptoethanol (50mM)	0.1% (50uM)
	Murine LIF (1000x)	20 ng/ml
	CHIRON	3 µM
	PD03	1µM
2i-LIF medium	DMEM Hams F12 (1x)	0.5x
	Neurobasal (1x)	0.5x
	L-glutamine (200nM)	1% (2nM)
	2-mercaptoethanol (50mM)	0.1% (50uM)
	N2 (200x)	0.5% (1x)
	B27 (50x)	1% (0.5x)
	Murine LIF (1000x)	20 ng/ml
	CHIRON	3 µM
	PD03	1µM
WNT-LIF medium	DMEM Hams F12 (1x)	0.5x
	Neurobasal (1x)	0.5x
	L-glutamine (200nM)	1% (2nM)
	2-mercaptoethanol (50mM)	0.1% (50uM)
	N2 (200x)	0.5% (1x)
	B27 (50x)	1% (0.5x)
	Murine LIF (1000x)	0.1% (1x)
	WNT-CM 100%	10%
HEK293 medium	DMEM High Glucose basal medium	1x
	FBS (GIBCO)	10%
	Penicillin Streptomycin (100x)	1% (1x)
Platinum-E cell medium	DMEM High Glucose basal medium	1x
	FBS (GIBCO)	10%
	Penicillin Streptomycin (100x)	1% (1x)
	Puromycin 10mg/ml (10000x)	1x

	Blasticidin 10mg/ml (1000x)	1x
T-REx™-293 cell medium	DMEM High Glucose basal medium	1x
	FBS (GIBCO)	10%
	Penicillin Streptomycin (100x)	1% (1x)
	Blasticidin 10mg/ml (1000x)	1x

Table S15. Organoid medium composition

Medium	Reagent	Final concentration
DMEM +++	DMEM/F12	1x
	L-glutamine (200mM)	20mM
	HEPES 1M	10mM
	Penicillin Streptomycin (100x)	1% (1x)
ENR medium	DMEM +++	
	B27 50x	2%
	N2 100x	1%
	EGF 100 µg/ml (2000x)	50 ng/ml
	Noggin 100 µg/ml	100 ng/ml
	R-spondin 1 - CM 100%	5%
	N-Acetylcysteine 500mM (400x)	125mM
WENR+Nic medium	DMEM +++ 100%	50%
	WNT-CM 100%	50%
	Nicotinamide 1M (1000x)	10mM
	B27 50x	2%
	N2 100x	1%
	EGF 100 µg/ml (2000x)	50 ng/ml
	Noggin 100 µg/ml	100 ng/ml
	R-spondin 1 - CM 100%	5%
	N-Acetylcysteine 500mM (400x)	125mM
Transduction medium	DMEM +++ 100%	50%
	WNT-CM 100%	50%
	Nicotinamide 1M (1000x)	10mM
	Polybrene 8mg/ml (1000x)	8 µg/ml
	Y-27632 10mM (1000x)	10 µM
EN+CHIR+Y- medium	DMEM ++	
	B27 50x	2%

	N2 100x	1%
	EGF 100 µg/ml (2000x)	50 ng/ml
	Noggin 100 µg/ml	100 ng/ml
	N-Acetylcysteine 500mM (400x)	125 mM
	CHIRON	4 µM
	Y-27632 (1000x)	1x

Table S16. Cell lysis buffer composition (for DNA extraction)

Chemical	Final concentration	Supplier
NP-40 (10%)	4.5%	Sigma-Aldrich Co. LLC
Tween (20%)	2.25%	Sigma-Aldrich Co. LLC
5X Go-Taq buffer	1x	Promega
Proteinase K (20 mg/ml)	0.2 mg/ml	Promega
Distilled water		

Table S17. Cell lysis buffer composition (for protein extraction)

Chemical	Final concentration	Supplier
2-Mercaptoethanol	0,1%	Sigma-Aldrich Co. LLC
EDTA	1mM	Sigma-Aldrich Co. LLC
EGTA	1mM	Sigma-Aldrich Co. LLC
Glycerol	10%	Sigma-Aldrich Co. LLC
KCl	10mM	Sigma-Aldrich Co. LLC
NaF	50mM	Sigma-Aldrich Co. LLC
Protease inhibitor cocktail	1 tablet/5ml	Roche
TrisHcl pH 7.4	50mM	Sigma-Aldrich Co. LLC
Triton-X100	1%	Sigma-Aldrich Co. LLC
Distilled water		

Table S18. Western Blot buffer composition

Chemical	Final concentration	Supplier
10x Running Buffer pH 8.3		
Glycine	1,92M	Sigma-Aldrich Co. LLC
SDS	10%	Sigma-Aldrich Co. LLC
Tris Base	0,25M	Sigma-Aldrich Co. LLC
Distilled water		
10x Wash Buffer		
Trizma base	0,2M	Sigma-Aldrich Co. LLC
NaCl	1,37M	Sigma-Aldrich Co. LLC
Tween 20	0,1%	Sigma-Aldrich Co. LLC
Distilled water		
Blocking solution		
Wash buffer 10x	1x	
Skim milk	5%	Sigma-Aldrich Co. LLC

Appendix B

Publications

1. Andersson-Rolf A, **Merenda A**, Mustata RC, Li T, Dietmann S, Koo BK. **Simultaneous paralogue knockout using a CRISPR-concatemer in mouse small intestinal organoids. Dev Biol. 2016** Oct 27. pii: S0012-1606(16)30479-1. doi: 10.1016/j.ydbio.2016.10.016.

2. Andersson-Rolf A*, Mustata RC*, **Merenda A***, Kim J, Perera S, Grego T, Andrews K, Fink J, Skarnes WC and Koo BK. **One-step generation of conditional and reversible gene knockouts. Nat Methods 2017.** *Nat Meth*, 14(3), pp.287–289. Available at: http://dx.doi.org/10.1038/nmeth.4156.
   ***Authors contributed equally to the work.*

3. **Merenda A**, Andersson-Rolf A, Mustata RC, Li T, Kim H, Koo BK. **A protocol for multiple gene knockout in mouse small intestinal organoids using a CRISPR-concatemer. Jove** (in press).

References

1. van Amerongen, R., Bowman, A.N. & Nusse, R., 2012. Developmental stage and time dictate the fate of Wnt/beta-catenin-responsive stem cells in the mammary gland. *Cell stem cell*, 11(3), pp.387–400.
2. van Amerongen, R., Mikels, A. & Nusse, R., 2008. Alternative wnt signaling is initiated by distinct receptors. *Science signaling*, 1(35), p.re9.
3. Anandasabapathy, N. et al., 2003. GRAIL: An E3 ubiquitin ligase that inhibits cytokine gene transcription is expressed in anergic CD4+ T cells. *Immunity*, 18(4), pp.535–547.
4. Andersson-Rolf, A. et al., 2016. Simultaneous paralogue knockout using a CRISPR-concatemer in mouse small intestinal organoids. *Developmental Biology*, (October), pp.1–7. Available at: http://linkinghub.elsevier.com/retrieve/pii/S0012160616304791.
5. Anon, 2014. Identification and functional analysis of a testis-specific E3 ubiquitin ligase gene Rnf148 in mouse . , 45(1), p.2014.
6. Assie, G. et al., 2014. Integrated genomic characterization of adrenocortical carcinoma. *Nature genetics*, 46(6), pp.607–612.
7. Aubert, J. et al., 2002. Functional gene screening in embryonic stem cells implicates Wnt antagonism in neural differentiation. *Nature biotechnology*, 20(12), pp.1240–1245.
8. Babon J, Leila N. Varghese, and N.A.N., 2014. Inhibition of IL-6 family cytokines by SOCS3. *Semin Immunol*, 26(1), pp.13–19.
9. Baker, S.J. & Reddy, E.P., 2000. Cloning of murine G1RP, a novel gene related to Drosophila melanogaster g1. *Gene*, 248(1–2), pp.33–40.
10. Barker, N. et al., 2007. Identification of stem cells in small intestine and colon by marker gene Lgr5. *Nature*, 449(7165), pp.1003–1007. Available at:

http://www.ncbi.nlm.nih.gov/pubmed/17934449.

11. Barker, N., 2014. Adult intestinal stem cells: critical drivers of epithelial homeostasis and regeneration. Nat Rev Mol Cell Biol, 15(1), pp.19–33. Available at: http://dx.doi.org/10.1038/nrm3721.
12. Bassett, A.R., Kong, L. & Liu, J.L., 2015. A Genome-Wide CRISPR Library for High-Throughput Genetic Screening in Drosophila Cells. *Journal of Genetics and Genomics*, 42(6), pp.301–309. Available at: http://dx.doi.org/10.1016/j.jgg.2015.03.011.
13. Behrens J. The role of cell adhesion molecules in cancer invasion and metastasis. Breast Cancer Res Treat [Internet]. 1993;24(3):175–84. Available from: http://dx.doi.org/10.1007/BF01833258
14. Behrens, J. et al., 1998. Functional interaction of an axin homolog, conductin, with beta-catenin, APC, and GSK3beta. *Science (New York, N.Y.)*, 280(5363), pp.596–599.
15. ten Berge, D. et al., 2011. Embryonic stem cells require Wnt proteins to prevent differentiation to epiblast stem cells. *Nature cell biology*, 13(9), pp.1070–1075.
16. Bhat, J.M., Pan, J. & Hutter, H., 2015. PLR-1, a putative E3 ubiquitin ligase, controls cell polarity and axonal extensions in C. elegans. *Developmental Biology*, 398(1), pp.44–56. Available at: http://dx.doi.org/10.1016/j.ydbio.2014.11.008.
17. Bilic, J. et al., 2007. Wnt induces LRP6 signalosomes and promotes dishevelled-dependent LRP6 phosphorylation. *Science (New York, N.Y.)*, 316(5831), pp.1619–1622.
18. Bishop, K.A. et al., 2016. CRISPR/Cas9-Mediated Insertion of loxP Sites in the Mouse Dock7 Gene Provides an Effective Alternative to Use of Targeted Embryonic Stem Cells. *G3: Genes|Genomes|Genetics*, 6(7), pp.2051–2061. Available at: http://www.ncbi.nlm.nih.gov/pmc/articles/PMC4938658/.
19. Bocock, J.P. et al., 2009. The PA-TM-RING protein RING finger protein 13 is an endosomal integral membrane E3 ubiquitin ligase whose RING finger domain is released to the cytoplasm by proteolysis. *FEBS Journal*, 276(7), pp.1860–1877.
20. Borchers, A.G.M. et al., 2002. The E3 ubiquitin ligase GREUL1 anteriorizes

ectoderm during Xenopus development. *Developmental biology*, 251(2), pp.395–408.

21. Bouchard, M.L. & Côté, S., 1993. The Drosophila melanogaster developmental gene g1 encodes a variant zinc-finger-motif protein. *Gene*, 125(2), pp.205–209.
22. Carroll, D., 2011. Genome Engineering With Zinc-Finger Nucleases L. M. Wahl, ed. *Genetics*, 188(4), p.773 LP-782. Available at: http://www.genetics.org/content/188/4/773.abstract.
23. Chen, S. et al., 2015. Genome-wide CRISPR screen in a mouse model of tumor growth and metastasis. *Cell*, 160(6), pp.1246–1260.
24. Cheng, H. et al., 2015. Enhanced metastasis in RNF13 knockout mice is mediated by a reduction in GM-CSF levels. *Protein & Cell*. Available at: http://link.springer.com/10.1007/s13238-015-0188-7.
25. Cho, S.W. et al., 2013. Targeted genome engineering in human cells with the Cas9 RNA-guided endonuclease. *Nat Biotech*, 31(3), pp.230–232. Available at: http://dx.doi.org/10.1038/nbt.2507.
26. Clague, M.J., Heride, C. & Urbe, S., 2015. The demographics of the ubiquitin system. *Trends in cell biology*, 25(7), pp.417–426.
27. Clevers, H., 2013. The intestinal crypt, a prototype stem cell compartment. *Cell*, 154(2), pp.274–284. Available at: http://dx.doi.org/10.1016/j.cell.2013.07.004.
28. Clevers, H., Loh, K.M. & Nusse, R., 2014. Stem cell signaling. An integral program for tissue renewal and regeneration: Wnt signaling and stem cell control. *Science (New York, N.Y.)*, 346(6205), p.1248012.
29. Crosnier, C., Stamataki, D. & Lewis, J., 2006. Organizing cell renewal in the intestine: stem cells, signals and combinatorial control. *Nature reviews. Genetics*, 7(5), pp.349–59. Available at: http://www.ncbi.nlm.nih.gov/pubmed/16619050.
30. De, A., 2011. Wnt/Ca2+ signaling pathway: a brief overview. *Acta biochimica et biophysica Sinica*, 43(10), pp.745–756.
31. van Dijk, J.R., Yamazaki, Y. & Palmer, R.H., 2014. Tumour-associated mutations of PA-TM-RING ubiquitin ligases RNF167/RNF13 identify the PA domain as a determinant for endosomal localization. *Biochemical Journal*, 459(1), pp.27–36.

Available at: http://www.biochemj.org/bj/459/bj4590027.htm.

32. Dijksterhuis, J.P., Petersen, J. & Schulte, G., 2014. WNT/Frizzled signalling: receptor-ligand selectivity with focus on FZD-G protein signalling and its physiological relevance: IUPHAR Review 3. *British journal of pharmacology*, 171(5), pp.1195–1209.
33. Dow, L.E. et al., 2015. Inducible in vivo genome editing with CRISPR-Cas9. *Nat Biotech*, 33(4), pp.390–394. Available at: http://dx.doi.org/10.1038/nbt.3155.
34. Drost, J. et al., 2015. Sequential cancer mutations in cultured human intestinal stem cells. *Nature*, 521(7550), pp.43–47.
35. van Es, J.H. et al., 2012. A critical role for the Wnt effector Tcf4 in adult intestinal homeostatic self-renewal. *Molecular and cellular biology*, 32(10), pp.1918–1927.
36. van Es, J.H., van Gijn, M.E., et al., 2005. Notch/gamma-secretase inhibition turns proliferative cells in intestinal crypts and adenomas into goblet cells. *Nature*, 435(7044), pp.959–963.
37. van Es, J.H., Jay, P., et al., 2005. Wnt signalling induces maturation of Paneth cells in intestinal crypts. *Nat Cell Biol*, 7(4), pp.381–386. Available at: http://dx.doi.org/10.1038/ncb1240.
38. Farin, H.F., Van Es, J.H. & Clevers, H., 2012. Redundant sources of Wnt regulate intestinal stem cells and promote formation of paneth cells. *Gastroenterology*, 143(6), p.1518–1529.e7. Available at: http://dx.doi.org/10.1053/j.gastro.2012.08.031.
39. Finkbeiner, S.R. et al., 2012. Stem cell-derived human intestinal organoids as an infection model for rotaviruses. *mBio*, 3(4), pp.e00159-12.
40. Flanagan, D.J. et al., 2015. Frizzled7 Functions as a Wnt Receptor in Intestinal Epithelial Lgr5(+) Stem Cells. *Stem Cell Reports*, 4(5), pp.759–767. Available at: http://www.ncbi.nlm.nih.gov/pmc/articles/PMC4437483/.
41. Friedel, R.H. et al., 2011. Generating conditional knockout mice. *Methods in molecular biology (Clifton, N.J.)*, 693, pp.205–231.
42. Fujii, M. et al., 2015. Efficient genetic engineering of human intestinal organoids using electroporation. *Nature protocols*, 10(10), pp.1474–1485.

43. Gao, C. & Chen, Y.-G., 2010. Dishevelled: The hub of Wnt signaling. *Cellular signalling*, 22(5), pp.717–727.
44. Giancotti, F.G., 2014. Deregulation of cell signaling in cancer. *FEBS Letters*, 588(16), pp.2558–2570. Available at: http://dx.doi.org/10.1016/j.febslet.2014.02.005.
45. Giannakis, M. et al., 2014. RNF43 is frequently mutated in colorectal and endometrial cancers. *Nature genetics*, 46(12), pp.1264–1266.
46. Gilbert, L.A. et al., 2013. CRISPR-mediated modular RNA-guided regulation of transcription in eukaryotes. *Cell*, 154(2), pp.442–451.
47. Guais, A. et al., 2006. h-Goliath, paralog of GRAIL, is a new E3 ligase protein, expressed in human leukocytes. *Gene*, 374(1–2), pp.112–120.
48. Guo, G. et al., 2011. A PiggyBac-based recessive screening method to identify pluripotency regulators. *PloS one*, 6(4), p.e18189.
49. Hao, H.-X. et al., 2012. ZNRF3 promotes Wnt receptor turnover in an R-spondin-sensitive manner. *Nature*, 485(7397), pp.195–200. Available at: http://dx.doi.org/10.1038/nature11019.
50. Hao, H.-X., Jiang, X. & Cong, F., 2016. Control of Wnt Receptor Turnover by R-spondin-ZNRF3/RNF43 Signaling Module and Its Dysregulation in Cancer. *Cancers*, 8(6).
51. Haramis, A.-P.G. et al., 2004. De Novo Crypt Formation and Juvenile Polyposis on BMP Inhibition in Mouse Intestine. *Science*, 303(5664), p.1684 LP-1686. Available at: http://science.sciencemag.org/content/303/5664/1684.abstract.
52. He, T.C. et al., 1998. Identification of c-MYC as a target of the APC pathway. *Science (New York, N.Y.)*, 281(5382), pp.1509–1512.
53. Ho, H.-Y.H. et al., 2012. Wnt5a-Ror-Dishevelled signaling constitutes a core developmental pathway that controls tissue morphogenesis. *Proceedings of the National Academy of Sciences of the United States of America*, 109(11), pp.4044–4051.
54. Huch, M. & Koo, B.-K., 2015. Modeling mouse and human development using organoid cultures. *Development*, 142(18), p.3113 LP-3125. Available at:

http://dev.biologists.org/content/142/18/3113.abstract.

55. Hwang, W.Y. et al., 2013. Efficient genome editing in zebrafish using a CRISPR-Cas system. *Nat Biotech*, 31(3), pp.227–229. Available at: http://dx.doi.org/10.1038/nbt.2501.
56. Ireland, H. et al., 2004. Inducible Cre-mediated control of gene expression in the murine gastrointestinal tract: effect of loss of beta-catenin. *Gastroenterology*, 126(5), pp.1236–1246.
57. Jia, L. & Sun, Y., 2011. SCF E3 ubiquitin ligases as anticancer targets. *Current cancer drug targets*, 11(3), pp.347–356.
58. Jiang, X. et al., 2015. Dishevelled promotes Wnt receptor degradation through recruitment of ZNRF3/RNF43 E3 ubiquitin ligases. *Molecular cell*, 58(3), pp.522–533.
59. Jiao, Y. et al., 2014. Whole-exome sequencing of pancreatic neoplasms with acinar differentiation. *The Journal of pathology*, 232(4), pp.428–435.
60. Jinek, M. et al., 2012. A programmable dual-RNA-guided DNA endonuclease in adaptive bacterial immunity. *Science (New York, N.Y.)*, 337(6096), pp.816–821.
61. Kabadi, A.M. et al., 2014. Multiplex CRISPR/Cas9-based genome engineering from a single lentiviral vector. *Nucleic Acids Research*, 42(19), pp.1–11.
62. Kabiri, Z. et al., 2014. Stroma provides an intestinal stem cell niche in the absence of epithelial Wnts. *Development (Cambridge, England)*, 141(11), pp.2206–15. Available at: http://dev.biologists.org/content/141/11/2206.long.
63. Kang, E., Yousefi, M. & Gruenheid, S., 2016. R-spondins are expressed by the intestinal stroma and are differentially regulated during Citrobacter rodentium- and dssinduced colitis in mice. *PLoS ONE*, 11(4), pp.1–13.
64. Karkera, J. et al., 2014. Abstract B03: Identification of R-spondin fusions in NSCLC. *Clinical Cancer Research*, 20(2 Supplement), p.B03 LP-B03. Available at: http://clincancerres.aacrjournals.org/content/20/2_Supplement/B03.abstract.
65. Knights, A.J. et al., 2012. Holding Tight: Cell Junctions and Cancer Spread. Trends in cancer research, 8, pp.61–69. Available at: http://www.ncbi.nlm.nih.gov/pmc/articles/PMC3582402/.

66. Koike-Yusa, H. et al., 2014. Genome-wide recessive genetic screening in mammalian cells with a lentiviral CRISPR-guide RNA library. *Nat Biotech*, 32(3), pp.267–273. Available at: http://dx.doi.org/10.1038/nbt.2800.
67. Koo, B.-K., Stange, D.E., et al., 2012. Controlled gene expression in primary Lgr5 organoid cultures. *Nat Meth*, 9(1), pp.81–83. Available at: http://dx.doi.org/10.1038/nmeth.1802.
68. Koo, B.-K. et al., 2005. Mind bomb-2 is an E3 ligase for Notch ligand. *The Journal of biological chemistry*, 280(23), pp.22335–22342.
69. Koo, B.-K. et al., 2015. Porcupine inhibitor suppresses paracrine Wnt-driven growth of Rnf43;Znrf3-mutant neoplasia. *Proceedings of the National Academy of Sciences of the United States of America*, 112(24), pp.7548–7550.
70. Koo, B.-K. et al., 2016. Rapid, one-step generation of biallelic conditional gene knockouts. *bioRxiv*. Available at: http://biorxiv.org/content/early/2016/06/01/056549.abstract.
71. Koo, B.-K., Spit, M., et al., 2012. Tumour suppressor RNF43 is a stem-cell E3 ligase that induces endocytosis of Wnt receptors. *Nature*, 488(7413), pp.665–669. Available at: http://dx.doi.org/10.1038/nature11308.
72. Koo, B.-K., Sasselli, V. & Clevers, H., 2013. Retroviral gene expression control in primary organoid cultures. *Current protocols in stem cell biology*, 27, p.Unit 5A.6.
73. Koo, B.K. et al., 2007. An obligatory role of mind bomb-1 in Notch signaling of mammalian development. *PLoS ONE*, 2(11).
74. Koo, B.K. & Clevers, H., 2014. Stem cells marked by the r-spondin receptor LGR5. *Gastroenterology*, 147(2), pp.289–302. Available at: http://dx.doi.org/10.1053/j.gastro.2014.05.007.
75. Koo, B.-K. & Huch, M. Organoids: A new in vitro model system for biomedical science and disease modelling and promising source for cell-based transplantation. *Developmental Biology* **420** (2), 197–198.
76. Korinek, V. et al., 1998. Depletion of epithelial stem-cell compartments in the small intestine of mice lacking Tcf-4. *Nature genetics*, 19(4), pp.379–383.
77. Kosinski, C. et al., 2007. Gene expression patterns of human colon tops and basal

crypts and BMP antagonists as intestinal stem cell niche factors. *Proceedings of the National Academy of Sciences* , 104(39), pp.15418–15423. Available at: http://www.pnas.org/content/104/39/15418.abstract.

78. Lamouille, S., Xu, J. & Derynck, R., 2014. Molecular mechanisms of epithelial–mesenchymal transition. Nature reviews. Molecular cell biology, 15(3), pp.178–196. Available at: http://www.ncbi.nlm.nih.gov/pmc/articles/PMC4240281/.
79. de Lau, W. et al., 2011. Lgr5 homologues associate with Wnt receptors and mediate R-spondin signalling. *Nature*, 476(7360), pp.293–297.
80. de Lau, W. et al., 2014. The R-spondin/Lgr5/Rnf43 module: regulator of Wnt signal strength. *Genes & development*, 28(4), pp.305–316.
81. Lau, W. De et al., 2014. The R-spondin / Lgr5 / Rnf43 module : regulator of Wnt signal strength The R-spondin / Lgr5 / Rnf43 module : regulator of Wnt signal strength. , pp.305–316.
82. Leon L. Su, Hideyuki Iwai, Jack T. Lin, and C.G.F., 2009. The Transmembrane E3 Ligase GRAIL Ubiquitinates and Degrades CD83 on CD4 T Cells. *J Immunol.*, 29(6), pp.997–1003.
83. Lim, X. et al., 2016. Axin2 marks quiescent hair follicle bulge stem cells that are maintained by autocrine Wnt/beta-catenin signaling. *Proceedings of the National Academy of Sciences of the United States of America*, 113(11), pp.E1498-505.
84. Lin, Q. et al., 2010. HECT E3 ubiquitin ligase Nedd4-1 ubiquitinates ACK and regulates epidermal growth factor (EGF)-induced degradation of EGF receptor and ACK. *Molecular and cellular biology*, 30(6), pp.1541–1554.
85. Lineberry, N.B. et al., 2008. Cutting edge: The transmembrane E3 ligase GRAIL ubiquitinates the costimulatory molecule CD40 ligand during the induction of T cell anergy. *Journal of immunology (Baltimore, Md. : 1950)*, 181(3), pp.1622–1626.
86. Liu, Y.Q. et al., 2013. Identification of a novel human testicular interstitial gene , RNF148 , and its expression regulated by histone deacetylases. , 12(3), pp.4060–4069.
87. Lussier, M.P. et al., 2012. Ubiquitin ligase RNF167 regulates AMPA receptor-mediated synaptic transmission. *Proceedings of the National Academy of Sciences*

of the United States of America, 109(47), pp.19426–31. Available at: http://www.pubmedcentral.nih.gov/articlerender.fcgi?artid=3511152&tool=pmcentrez&rendertype=abstract.

88. Macdonald, B.T., Semenov, M. V & He, X., 2007. SnapShot: Wnt/beta-catenin signaling. *Cell*, 131(6), p.1204.
89. MacGurn, J. a., Hsu, P.-C. & Emr, S.D., 2012. Ubiquitin and Membrane Protein Turnover: From Cradle to Grave. *Annual Review of Biochemistry*, 81(1), pp.231–259.
90. Mahon, P. & Bateman, a, 2000. The PA domain: a protease-associated domain. *Protein science : a publication of the Protein Society*, 9(10), pp.1930–1934.
91. Mali, P. et al., 2013. RNA-Guided Human Genome Engineering via Cas9. *Science*, 339(6121), p.823 LP-826. Available at: http://science.sciencemag.org/content/339/6121/823.abstract.
92. Matano, M. et al., 2015. Modeling colorectal cancer using CRISPR-Cas9-mediated engineering of human intestinal organoids. *Nat Med*, 21(3), pp.256–262. Available at: http://dx.doi.org/10.1038/nm.3802.
93. Meng, Q., 2010. Three-dimensional culture of hepatocytes for prediction of drug-induced hepatotoxicity. *Expert opinion on drug metabolism & toxicology*, 6(6), pp.733–746.
94. Metzger, M.B., Hristova, V. a. & Weissman, a. M., 2012. HECT and RING finger families of E3 ubiquitin ligases at a glance. *Journal of Cell Science*, 125(3), pp.531–537.
95. Miyoshi, H. & Stappenbeck, T.S., 2013. In vitro expansion and genetic modification of gastrointestinal stem cells as organoids. *Nature protocols*, 8(12), pp.2471–2482. Available at: http://www.ncbi.nlm.nih.gov/pmc/articles/PMC3969856/.
96. Moffat, L.L. et al., 2014. The conserved transmembrane RING finger protein PLR-1 downregulates Wnt signaling by reducing Frizzled, Ror and Ryk cell-surface levels in C. elegans. *Development (Cambridge, England)*, 141(3), pp.617–28. Available at: http://www.ncbi.nlm.nih.gov/pubmed/24401370.
97. Molenaar, M. et al., 1996. XTcf-3 transcription factor mediates beta-catenin-

induced axis formation in Xenopus embryos. *Cell*, 86(3), pp.391–399.

98. Mueller, D.L., 2004. E3 ubiquitin ligases as T cell anergy factors. *Nature immunology*, 5(9), pp.883–890.
99. Mussolino, C. et al., 2011. A novel TALE nuclease scaffold enables high genome editing activity in combination with low toxicity. *Nucleic acids research*, 39(21), pp.9283–9293.
100. Nian, H. et al., 2008. Mouse RING finger protein Rnf133 is a testis-specific endoplasmic reticulum-associated E3 ubiquitin ligase. *Cell research*, 18(7), pp.800–802.
101. Niehrs, C., 2012. The complex world of WNT receptor signalling. *Nature reviews. Molecular cell biology*, 13(12), pp.767–779.
102. Nozaki, K. et al., 2016. Co-culture with intestinal epithelial organoids allows efficient expansion and motility analysis of intraepithelial lymphocytes. *Journal of Gastroenterology*, 51(3), pp.206–213. Available at: http://dx.doi.org/10.1007/s00535-016-1170-8.
103. Nurieva, R.I. et al., 2010. The E3 ubiquitin ligase GRAIL regulates T cell tolerance and regulatory T cell function by mediating T cell receptor-CD3 degradation. *Immunity*, 32(5), pp.670–680. Available at: http://dx.doi.org/10.1016/j.immuni.2010.05.002.
104. Ogawa, K. et al., 2004. A novel mechanism for regulating clonal propagation of mouse ES cells. *Genes to cells : devoted to molecular & cellular mechanisms*, 9(5), pp.471–477.
105. Ogawa, K. et al., 2006. Synergistic action of Wnt and LIF in maintaining pluripotency of mouse ES cells. *Biochemical and biophysical research communications*, 343(1), pp.159–166.
106. Oishi, I. et al., 2003. The receptor tyrosine kinase Ror2 is involved in non-canonical Wnt5a/JNK signalling pathway. *Genes to cells : devoted to molecular & cellular mechanisms*, 8(7), pp.645–654.
107. Ong, C.K. et al., 2012. Exome sequencing of liver fluke-associated cholangiocarcinoma. *Nature genetics*, 44(6), pp.690–693.

108. Ootani, A. et al., 2009. Sustained in vitro intestinal epithelial culture within a Wnt-dependent stem cell niche. *Nat Med*, 15(6), pp.701–706. Available at: http://dx.doi.org/10.1038/nm.1951.

109. Pellegrinet, L. et al., 2012. NIH Public Access. , 140(4), pp.1230–1240.

110. Persaud, A. et al., 2011. Nedd4-1 binds and ubiquitylates activated FGFR1 to control its endocytosis and function. *The EMBO journal*, 30(16), pp.3259–3273. Available at: http://dx.doi.org/10.1038/emboj.2011.234.

111. Platt, R.J. et al., 2014. CRISPR-Cas9 knockin mice for genome editing and cancer modeling. *Cell*, 159(2), pp.440–455. Available at: http://dx.doi.org/10.1016/j.cell.2014.09.014.

112. Port, F. et al., 2014. Optimized CRISPR/Cas tools for efficient germline and somatic genome engineering in *Drosophila*. *Proceedings of the National Academy of Sciences of the United States of America*, 111(29), pp.E2967-2976. Available at: http://www.pubmedcentral.nih.gov/articlerender.fcgi?artid=4115528&tool=pmcentrez&rendertype=abstract.

113. Press, D., 2015. EGLN2 and RNF150 genetic variants are associated with chronic obstructive pulmonary disease risk in the Chinese population. , pp.145–151.

114. Ran, F.A. et al., 2013. Double nicking by RNA-guided CRISPR Cas9 for enhanced genome editing specificity. *Cell*, 154(6), pp.1380–1389.

115. Ran, F.A. et al., 2013. Genome engineering using the CRISPR-Cas9 system. *Nature protocols*, 8(11), pp.2281–308. Available at: http://www.ncbi.nlm.nih.gov/pubmed/24157548%5Cnhttp://www.pubmedcentral.nih.gov/articlerender.fcgi?artid=3969860&tool=pmcentrez&rendertype=abstract%5Cnhttp://www.ncbi.nlm.nih.gov/pubmed/24157548%5Cnhttp://www.nature.com/nprot/journal/v8/n11/abs/nprot.2013.143.h.

116. Reya, T. & Clevers, H., 2005. Wnt signalling in stem cells and cancer. *Nature*, 434(7035), pp.843–850.

117. Ritsma, L. et al., 2014. Intestinal crypt homeostasis revealed at single-stem-cell level by in vivo live imaging. *Nature*, 507(7492), pp.362–5. Available at: http://dx.doi.org/10.1038/nature12972.

118. Ryland, G.L. et al., 2013. RNF43 is a tumour suppressor gene mutated in mucinous tumours of the ovary. *The Journal of pathology*, 229(3), pp.469–476.

119. Sakuma, T. et al., 2014. Multiplex genome engineering in human cells using all-in-one CRISPR/Cas9 vector system. *Scientific reports*, 4(5), p.5400. Available at: http://www.pubmedcentral.nih.gov/articlerender.fcgi?artid=4066266&tool=pmcentrez&rendertype=abstract.

120. Sampaziotis, F. et al., 2015. Cholangiocytes derived from human induced pluripotent stem cells for disease modeling and drug validation. *Nature biotechnology*, 33(8), pp.845–852.

121. Sanjana, N.E., Shalem, O. & Zhang, F., 2014. Improved vectors and genome-wide libraries for CRISPR screening. *Nature methods*, 11(8), pp.783–784. Available at: http://www.ncbi.nlm.nih.gov/pmc/articles/PMC4486245/.

122. Sansom, O.J. et al., 2004. Loss of Apc in vivo immediately perturbs Wnt signaling, differentiation, and migration. *Genes & Development*, 18(12), pp.1385–1390. Available at: http://www.ncbi.nlm.nih.gov/pmc/articles/PMC423189/.

123. Sansom, O.J. et al., 2007. Myc deletion rescues Apc deficiency in the small intestine. *Nature*, 446(7136), pp.676–679.

124. Sato, A. et al., 2010. Wnt5a regulates distinct signalling pathways by binding to Frizzled2. *The EMBO journal*, 29(1), pp.41–54.

125. Sato, N. et al., 2004. Maintenance of pluripotency in human and mouse embryonic stem cells through activation of Wnt signaling by a pharmacological GSK-3-specific inhibitor. *Nature medicine*, 10(1), pp.55–63.

126. Sato, T. et al., 2011. Paneth cells constitute the niche for Lgr5 stem cells in intestinal crypts. *Nature*, 469(7330), pp.415–418.

127. Sato, T. et al., 2009. Single Lgr5 stem cells build crypt–villus structures in vitro without a mesenchymal niche. *Nature*, 459(7244), pp.262–265. Available at: http://dx.doi.org/10.1038/nature07935.

128. Sato, T. & Clevers, H., 2013. Growing Self-Organizing Mini-Guts from a Single Intestinal Stem Cell: Mechanism and Applications. *Science*, 340(6137), p.1190 LP-1194. Available at:

http://science.sciencemag.org/content/340/6137/1190.abstract.

129. Schick, J.A. et al., 2016. CRISPR-Cas9 enables conditional mutagenesis of challenging loci. *Scientific reports*, 6, p.32326.

130. Schwank, G. et al., 2016. Functional Repair of CFTR by CRISPR/Cas9 in Intestinal Stem Cell Organoids of Cystic Fibrosis Patients. *Cell Stem Cell*, 13(6), pp.653–658. Available at: http://dx.doi.org/10.1016/j.stem.2013.11.002.

131. Sekine, S. et al., 2016. Frequent PTPRK-RSPO3 fusions and RNF43 mutations in colorectal traditional serrated adenoma. *The Journal of pathology*, 239(2), pp.133–138.

132. Semenov, M. V et al., 2007. SnapShot: Noncanonical Wnt Signaling Pathways. *Cell*, 131(7), p.1378.

133. Seroogy, C.M. et al., 2004. The gene related to anergy in lymphocytes, an E3 ubiquitin ligase, is necessary for anergy induction in CD4 T cells. *Journal of immunology (Baltimore, Md. : 1950)*, 173(1), pp.79–85.

134. Seshagiri, S. et al., 2012. Recurrent R-spondin fusions in colon cancer. *Nature*, 488(7413), pp.660–664. Available at: http://dx.doi.org/10.1038/nature11282.

135. Shinmura, K. et al., 2014. RSPO fusion transcripts in colorectal cancer in Japanese population. *Molecular biology reports*, 41(8), pp.5375–5384.

136. Shyu YJ, Suarez CD, Hu C-D. Visualization of ternary complexes in living cells by using a BiFC-based FRET assay. Nat Protoc [Internet]. Nature Publishing Group; 2008 Oct;3(11):1693–702. Available from: http://dx.doi.org/10.1038/nprot.2008.157

137. Simons, B.D. & Clevers, H., 2011. Strategies for homeostatic stem cell self-renewal in adult tissues. Cell, 145(6), pp.851–862. Available at: http://dx.doi.org/10.1016/j.cell.2011.05.033.

138. Simons, M. & Mlodzik, M., 2008. Planar cell polarity signaling: from fly development to human disease. *Annual review of genetics*, 42, pp.517–540.

139. Slusarski, D.C., Corces, V.G. & Moon, R.T., 1997. Interaction of Wnt and a Frizzled homologue triggers G-protein-linked phosphatidylinositol signalling. *Nature*, 390(6658), pp.410–413.

140. Snippert, H.J. et al., 2010. Intestinal crypt homeostasis results from neutral competition between symmetrically dividing Lgr5 stem cells. *Cell*, 143(1), pp.134–144. Available at: http://dx.doi.org/10.1016/j.cell.2010.09.016.

141. Soderberg O, Gullberg M, Jarvius M, Ridderstrale K, Leuchowius K-J, Jarvius J, et al. Direct observation of individual endogenous protein complexes in situ by proximity ligation. Nat Meth [Internet]. 2006 Dec;3(12):995–1000. Available from: http://dx.doi.org/10.1038/nmeth947

142. Spence, J.R. et al., 2011. Directed differentiation of human pluripotent stem cells into intestinal tissue in vitro. *Nature*, 470(7332), pp.105–109.

143. Stanger, B.Z. et al., 2005. Direct regulation of intestinal fate by Notch. *Proc Natl Acad Sci U S A*, 102(35), pp.12443–12448. Available at: http://www.ncbi.nlm.nih.gov/pmc/articles/PMC1194941/pdf/pnas-0505690102.pdf.

144. Strikoudis, A., Guillamot, M. & Aifantis, I., 2014. Regulation of stem cell function by protein ubiquitylation. *EMBO Reports*, 15(4), pp.365–382.

145. Tamiya, T. et al., 2011. Suppressors of cytokine signaling (SOCS) proteins and JAK/STAT pathways: Regulation of T-cell inflammation by SOCS1 and SOCS3. *Arteriosclerosis, Thrombosis, and Vascular Biology*, 31(5), pp.980–985.

146. Tetsu, O. & McCormick, F., 1999. Beta-catenin regulates expression of cyclin D1 in colon carcinoma cells. *Nature*, 398(6726), pp.422–426.

147. Toyooka, Y. et al., 2008. Identification and characterization of subpopulations in undifferentiated ES cell culture. *Development (Cambridge, England)*, 135(5), pp.909–918.

148. Tranque, P. et al., 1996. Identification and characterization of a RING zinc finger gene (C-RZF) expressed in chicken embryo cells. *Proceedings of the National Academy of Sciences of the United States of America*, 93(7), pp.3105–3109.

149. Trott, J. & Martinez Arias, A., 2013. Single cell lineage analysis of mouse embryonic stem cells at the exit from pluripotency. *Biology open*, 2(10), pp.1049–1056.

150. Tsukiyama, T. et al., 2015. Molecular Role of RNF43 in Canonical and Noncanonical

Wnt Signaling. *Molecular and Cellular Biology*, 35(11), pp.2007–2023. Available at: http://www.ncbi.nlm.nih.gov/pmc/articles/PMC4420922/.

151. Turner, D.A. et al., 2014. An interplay between extracellular signalling and the dynamics of the exit from pluripotency drives cell fate decisions in mouse ES cells. *Biology Open*, 3(7), p.614 LP-626. Available at: http://bio.biologists.org/content/3/7/614.abstract.
152. Turner, J.R., 2009. Intestinal mucosal barrier function in health and disease. *Nat Rev Immunol*, 9(11), pp.799–809. Available at: http://dx.doi.org/10.1038/nri2653.
153. Umebayashi K, S.H. and Y.T., 2008. Ubc4/5 and c-Cbl Continue to Ubiquitinate EGF Receptor after Internalization to Facilitate Polyubiquitination and Degradation. *Molecular biology of the cell*, 19(1), pp.3454–3462.
154. Valenta, T. et al., 2016. Wnt Ligands Secreted by Subepithelial Mesenchymal Cells Are Essential for the Survival of Intestinal Stem Cells and Gut Homeostasis. *Cell Reports*, 15(5), pp.911–918.
155. VanDussen, K.L. et al., 2012a. Notch signaling modulates proliferation and differentiation of intestinal crypt base columnar stem cells. *Development (Cambridge, England)*, 139(3), pp.488–497. Available at: http://www.ncbi.nlm.nih.gov/pmc/articles/PMC3252352/.
156. VanDussen, K.L. et al., 2012b. Notch signaling modulates proliferation and differentiation of intestinal crypt base columnar stem cells. *Development (Cambridge, England)*, 139(3), pp.488–497.
157. Vilella, A.J. et al., 2009. EnsemblCompara GeneTrees: Complete, duplication-aware phylogenetic trees in vertebrates. *Genome Research*, 19(2), pp.327–335.
158. Wang, H. et al., 2013. One-step generation of mice carrying mutations in multiple genes by CRISPR/Cas-mediated genome engineering. *Cell*, 153(4), pp.910–918.
159. Wang, K. et al., 2014. Whole-genome sequencing and comprehensive molecular profiling identify new driver mutations in gastric cancer. *Nature genetics*, 46(6), pp.573–582.
160. Wang, W. et al., 2016. Delivery of Cas9 Protein into Mouse Zygotes through a Series of Electroporation Dramatically Increases the Efficiency of Model Creation.

Journal of genetics and genomics = Yi chuan xue bao, 43(5), pp.319–327.

161. Wang, X.W. et al., 2014. RING Finger Proteins Are Involved in the Progression of Barrett Esophagus to Esophageal Adenocarcinoma : A Preliminary Study. , 8(5), pp.487–494.
162. van de Wetering, M. et al., 2015. Prospective derivation of a living organoid biobank of colorectal cancer patients. *Cell*, 161(4), pp.933–945.
163. van de Wetering, M. et al., 2002. The beta-catenin/TCF-4 complex imposes a crypt progenitor phenotype on colorectal cancer cells. *Cell*, 111(2), pp.241–250.
164. Wray, J. et al., 2011. Inhibition of glycogen synthase kinase-3 alleviates Tcf3 repression of the pluripotency network and increases embryonic stem cell resistance to differentiation. *Nature cell biology*, 13(7), pp.838–845.
165. Wu, J. et al., 2011. Whole-exome sequencing of neoplastic cysts of the pancreas reveals recurrent mutations in components of ubiquitin-dependent pathways. *Proceedings of the National Academy of Sciences of the United States of America*, 108(52), pp.21188–21193.
166. Wyman, C. & Kanaar, R., 2006. DNA double-strand break repair: all's well that ends well. *Annual review of genetics*, 40, pp.363–383.
167. Yamazaki, Y. et al., 2013. Goliath family E3 ligases regulate the recycling endosome pathway via VAMP3 ubiquitylation. *The EMBO journal*, 32(4), pp.524–37. Available at: http://www.pubmedcentral.nih.gov/articlerender.fcgi?artid=3579141&tool=pmcentrez&rendertype=abstract.
168. Yanagawa, S. et al., 2002. Casein kinase I phosphorylates the Armadillo protein and induces its degradation in Drosophila. *The EMBO journal*, 21(7), pp.1733–1742.
169. Yang, Q. et al., 2001. Requirement of Math1 for Secretory Cell Lineage Commitment in the Mouse Intestine. *Science*, 294(5549), p.2155 LP-2158. Available at: http://science.sciencemag.org/content/294/5549/2155.abstract.
170. Yin, L. et al., 2015. Multiplex Conditional Mutagenesis Using Transgenic Expression of Cas9 and sgRNAs. *Genetics*, 200(June), pp.431–441. Available at:

http://www.genetics.org/cgi/doi/10.1534/genetics.115.176917.

171. Yin, X. et al., 2014. Niche-independent high-purity cultures of Lgr5+ intestinal stem cells and their progeny. *Nat Meth*, 11(1), pp.106–112. Available at: http://dx.doi.org/10.1038/nmeth.2737.

172. Yu, Z. et al., 2013. Highly efficient genome modifications mediated by CRISPR/Cas9 in Drosophila. *Genetics*, 195(1), pp.289–291.

173. Yui, S. et al., 2012. Functional engraftment of colon epithelium expanded in vitro from a single adult Lgr5+ stem cell. *Nat Med*, 18(4), pp.618–623. Available at: http://dx.doi.org/10.1038/nm.2695.

174. Zaravinos, A. et al., 2011. Identification of common differentially expressed genes in urinary bladder cancer. *PLoS ONE*, 6(4).

175. Zasloff, M., 2002. Antimicrobial peptides of multicellular organisms. *Nature*, 415(6870), pp.389–395. Available at: http://dx.doi.org/10.1038/415389a.

176. Zebisch, M. et al., 2013. Structural and molecular basis of ZNRF3/RNF43 transmembrane ubiquitin ligase inhibition by the Wnt agonist R-spondin. *Nature communications*, 4, p.2787.

177. Zetche, B., Volz, S.E. & Zhang, F., 2015. A Split Cas9 Architecture for Inducible Genome Editing and Transcription Modulation. *Nature biotechnology*, 33(2), pp.139–142. Available at: http://www.ncbi.nlm.nih.gov/pmc/articles/PMC4503468/.

178. Zhang, Q. et al., 2013. E3 ubiquitin ligase RNF13 involves spatial learning and assembly of the SNARE complex. *Cellular and Molecular Life Sciences*, 70(1), pp.153–165.

179. Zhang, Y.-G. et al., 2014. Salmonella-infected crypt-derived intestinal organoid culture system for host-bacterial interactions. *Physiological reports*, 2(9).